The Plasma Membrane Lipid Asymmetry of *Leishmania donovani* and its Relevance for Phagocytosis

Dissertation

zur Erlangung des akademischen Grades
doctor rerum naturalium
(Dr. rer. nat.)
im Fach Biophysik

eingereicht an der
Mathematisch Naturwissenschaftlichen Fakultät I
der Humboldt Universität zu Berlin

von

Diplom Biophysiker Adrien Weingärtner

Präsident der Humboldt-Universität zu Berlin

Prof. Dr. Jan-Hendrik Olbertz

Dekan der Mathematisch Naturwissenschaftlichen Fakultät I

Prof. Dr. Andreas Herrmann

Gutachter: 1. Prof. Dr. Andreas Herrmann

2. Prof. Dr. Thomas Günther-Pomorski

3. PD Dr. Joachim Clos

Tag der mündlichen Prüfung: 07.06.2011

Für meine Familie

Zusammenfassung

In großen Teilen der Welt verursachen Parasiten der Spezies *Leishmania* schwerwiegende Infektionen beim Menschen. Nach ihrer Übertragung auf einen Wirbeltierwirt durch Sandmücken dringen die extrazellulären Einzeller in Phagozyten ein und legen damit den Grundstein für eine lang andauernde Infektion. Spezielle auf der Oberfläche exponierte Phospholipide stehen unter Verdacht, die Fresszellen zur Aufnahme der Parasiten zu stimulieren. Bisher sind Mechanismen, welche die Phospholipidverteilung in der Plasmamembran dieser Parasiten kontrollieren, kaum erforscht.

In der vorliegenden Arbeit wurde ein lipidtransportierender Proteinkomplex identifiziert, der einen wesentlichen Beitrag zur asymmetrischen Verteilung der Lipide in der Plasmamembran von *Leishmania donovani* leistet. Die Zerstörung des Komplexes führte zum Verlust des einwärts gerichteten Lipidtransports und zur Anreicherung von Phosphatidylethanolamin (PE) auf der Zelloberfläche des Parasiten. Diese veränderte Lipidasymmetrie hatte jedoch keinen Einfluss auf die Phagozytose durch Makrophagen. Darüber hinaus brachte die Untersuchung des Insektenstadiums (Promastigote) verschiedener *Leishmania* Spezies zu Tage, dass die Menge an Phosphatidylserin (PS) unterhalb des Detektionslimits modernster Nachweisverfahren liegt, sie jedoch nach wie vor phagozytiert werden.

Des Weiteren konnte gezeigt werden, dass der Parasit über einen Scramblase-Mechanismus verfügt, der durch intrazelluläres Kalzium stimulierbar ist. Die Scramblase-Aktivität ist, im Gegensatz zu dem zuvor beschriebenen einwärts gerichteten Lipidtransport, energieunabhängig und ermöglicht die bidirektionale Translokation von fluoreszenzmarkiertem Phosphatidylcholin (PC), PE, PS und Sphingomyelin (SM). Dementsprechend konnte nach Kalziumstimulierung endogenes PE auch in der äußeren Lipidschicht der Plasmamembran detektiert werden, wobei deren Barrierefunktion nicht beeinträchtigt wurde.

Diese Ergebnisse geben neue Einblicke in die dynamische Regulation der Lipidverteilung über die Plasmamembran des Parasiten und verdeutlichen, dass die Exposition von PS und PE nicht essentiell für das Eindringen der Leishmanien in die Wirtszellen ist.

Schlagworte: *Leishmania*, Lipidasymmetrie, Typ 4 P-Typ ATPase, Scrambling, Phosphatidylserin

Abstract

The protozoan parasite *Leishmania* causes severe infections in humans throughout the world. Following the transmission via sand flies to its mammalian host the extracellular parasite has to gain entry into phagocytic cells to initiate a successful infection. Specific surface exposed phospholipids have been implicated in *Leishmania* macrophage-interaction, but the mechanisms controlling and regulating the plasma membrane lipid distribution remains to be elucidated.

In the present work a lipid transporting protein complex was identified in *Leishmania donovani* which plays an essential role in maintaining an asymmetric lipid distribution across the plasma membrane. Loss of the protein complex abolishes the inward-directed lipid transport and thus e.g. to an increased cell surface exposure of phosphatidylethanolamine (PE). In spite of this altered lipid asymmetry the uptake by macrophages is unaffected. Moreover, *Leishmania* promastigotes of different species lack detectable amounts of phosphatidylserine (PS) although being infective.

Furthermore, a scramblase activity following a cytosolic calcium signal was demonstrated. This scramblase mechanism facilitated, in contrast to the previous described inward directed lipid transport, the bidirectional movement of fluorescent lipid analogues of PC, PE, PS and SM in an energy-independent manner. In accordance with these findings endogenous PE was exposed to the outer plasma membrane leaflet following the Ca^{2+}-signal, while the plasma membrane itself remained intact.

These results provide novel insight into the dynamic regulation of the transbilayer lipid distribution across the parasite plasma membrane and reveal that exposure of PS and PE is not crucial for invasion of the host cell by *Leishmania donovani* promastigotes.

Keywords: *Leishmania*, lipid asymmetry, type 4 P-type-ATPase, scrambling, phosphatidylserine

1 Index

2 List of abbreviations

Abbreviation	Meaning
9-AA	9-aminoacridine
ABC-transporter	ATP binding cassette transporter
ADP	adenosine-5´-diphosphate
ATP	adenosine-5´-triphosphate
BSA	bovine serum albumin
CCCP	carbonyl cyanide m-chlorophenylhydrazone
CFP	cyan fluorescent protein
CID	collision induced dissociation
CL	cardiolipin
CR1 / CR3	complement receptors 1 or 3
CRP	C-reactive protein
DDM	n-dodecyl-β-D-maltopyranoside
DHB	2,5-dihydroxybenzoic acid
DIC	differential interference contrast
EC50	effective concentration
ER	endoplasmic reticulum
ESI-MS	electron spray ionisation mass spectrometry
FA	fatty acid
FcγR	Fcγ receptor
FITC	fluorescein isothiocyanate
FRET	Förster Resonance Energy Transfer
GFP	green fluorescent protein
gp63	glycoprotein 63
GPI	glycosylphosphatidylinositol
GPILs	glycoinositol phospholipids
HPLC	high performance liquid chromatography

iC3b	inactivated complement 3b
IgG	immunoglobulin gamma
IL	interleukin
IP	immunoprecipitation
IPC	inositol phosphorylceramide
LdMT	*Leishmania donovani* Miltefosine transporter
LPG	lipophosphoglycan
MALDI-TOF	matrix assisted laser desorption ion time of flight mass spectrometry
Miltefosine	hexadecylphosphocholine
MTT	3-(4,5-dimethyl-2-thiazolyl)-2,5-diphenyl-2H-tetrazolium bromide
NBD	7-nitro-2-1,3-benzoxadiazol-4-yl
P_4-ATPase	type 4 P-type ATPase
PA	phosphatidic acid
PAGE	polyacrylamide gel electrophoresis
PC	phosphatidylcholine
PCD	programmed cell death
PCR	polymerase chain reaction
PE	phosphatidylethanolamine
PG	phosphatidylglycerol
PI	phosphatidylinositol
p-PE	plasmalogen PE
ProI	propidium iodide
PS	phosphatidylserine
PSD	post source decay
SDS	sodium dodecyl sulfate
SERCA	sarcoplasmatic reticulum calcium transporter
SIM	selected ion monitoring

SM	sphingomyelin
SMP	serum mannan binding protein
TGF-β	transforming growth factor beta
Th 2	T helper cell type 2
TLC	thin layer chromatography
TMD	transmembrane domains
wt	wild-type
YFP	yellow fluorescent protein

3 Introduction

3.1 Leishmaniasis

Leishmaniasis is a disease caused by protozoan parasites of the *Leishmania* species, which belong to the order of Trypanosomatidae. Like all trypanosomatids they depend on their insect vector to run through the whole life cycle (**Figure 1**). Consequently, the parasites geographical distribution reflects the habitat of its insect vector. In case of *Leishmania* these insect vectors are sand flies of the genus *Phlebotomus* and *Lutzomyia* in the Old and New World, respectively, which can be found in the temperate or tropical regions. The infected female sandfly transmits the parasite to vertebrate hosts (hyraxes, canids, rodents and humans) during its blood meal. The disease occurs at least in four major forms in man caused by the distinct *Leishmania* species (**Figure 2**). Firstly, the cutaneous leishmaniasis, caused by species of the *L. mexicana* complex and the *L. major* complex, is characterised by frequently self-healing skin lesions around the bite. Nevertheless, multiple and disfiguring scars remain. Secondly, the diffuse cutaneous leishmaniasis occurs in individuals with defective cell-mediated immune response. In these patients the lesions disseminate, never heal spontaneously and often reoccur after treatment. Thirdly, the mucocutaneous leishmaniasis causes extensive destruction of the oral-nasal and pharyngeal cavities with disfiguring lesions, mutilation of the face and great suffering for life. This form is predominantly caused by *Leishmania* species of the Viannia subgenus in the New World but was also reported for *L. donovani* and *L. major* in the Old World. Fourthly, the most severe and nearly always fatal form of leishmaniasis is the visceral leishmaniasis or ‘kala azar’ caused by *L. donovani* and *L. infantum*. It is characterised by undulating fever, loss of weight, splenomegaly, hepatomegaly and/or lymphadenopathies and anemia [1,2]. Currently around 12 million people are infected and two million new cases are reported annually. About 350 million people live under risk of becoming infected [3].

3.2 Life Cycle

The *Leishmania* life cycle is divided by the two different hosts (**Figure 1**). Parasites taken up by the sandfly during blood meal differentiate to motile flagellated promastigotes, which attach to the midgut epithelium of the sandfly to prevent excretion and to initiate proliferation. These fast replicating procyclic promastigotes show only low virulence. Upon transformation to metacyclic promastigotes (low proliferation but high virulence) the parasites detach from midgut epithelium and migrate anterior to the cuticle-lined foregut. There some attach by

forming hemidesmosomes while others remain mobile being susceptible for bite-induced transmission to a mammalian host [4]. The sandfly inoculates about 100 - 3000 metacyclic promastigotes into the skin of the mammalian host [5].

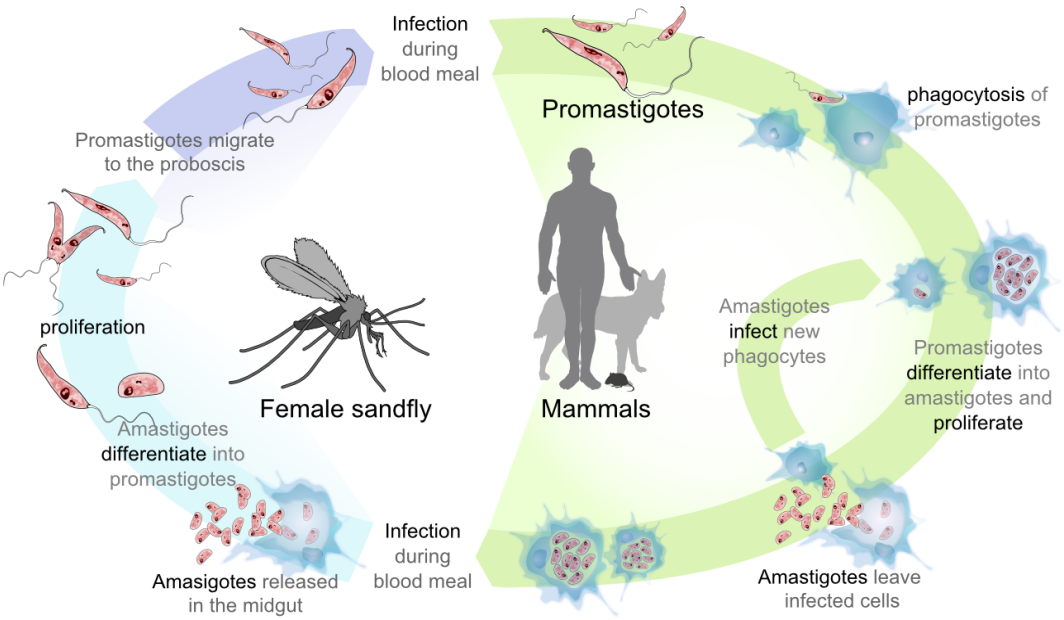

Figure 1: Life Cycle of *Leishmania* species.

Adapted from Mariana Ruiz Villarreal.

In the vertebrate host these metacyclic promastigotes switch from extracellular to intracellular parasites by invasion of their preferred phagocytic host cells e.g. neutrophile granulocytes, macrophages and dendritic cells [6]. These immune cells are attracted to the site of infection by the sandfly saliva and a *Leishmania* chemotactic factor. The phagocytes take up the parasites by receptor-mediated phagocytosis. Inside the endosomal system the promastigote differentiates to the amastigote form of *Leishmania*. Upon formation of the parasitophorous vacuole by endosom-lysosom fusion the amastigotes start to proliferate. Migration of infected immune cells to the lymph nodes, the liver and the spleen facilitate the dissemination of the parasite to other organs [7].

While the whole *Leishmania* genus has the life cycle described above in common, differences among the distinct *Leishmania* species are known. The differences between the *Leishmania* species include the infectivity for distinct hosts, distinct organs and thus the clinical signs caused in the infected mammalian host.

Figure 2: Patients with clinical signs of leishmaniasis.

From left to right: cutaneous, mucocutaneous and visceral leishmaniasis [2] [3].

In general two epidemiological entities can be distinguished, firstly, zoonoses that include animal reservoir hosts and secondly, anthroponoses where man is the sole source of infection for the vector. Among the different *Leishmania* species 20 are known to be pathogenic for humans (**Table 1**) [1].

Differences in the clinical signs of leishmaniasis arise from distinct virulence factors modulating the host immune response and thus the organs affected. One of these virulence factors is the A2 protein expressed in *L. donovani* amastigotes which is required for survival in visceral organs. In *L. major* (cutaneous leishmaniasis) the corresponding gene is absent, but introduction of this gene into this species leads to a visceralisation in susceptible mice [8]. Although only a few virulence factors are known by now, more insight was gained in the modulations of the innate and adapted cellular immunity induced by different *Leishmania* species. The best studied examples in this respect are the Old World subspecies *L. major*, for cutaneous leishmaniasis and *L. donovani* for visceral leishmaniasis as well as species of the New World *L. mexicana* complex (cutaneous leishmaniasis). While the protective host response is generally T helper cell type 1-mediated, factors resulting in the non-healing disease vary among distinct species. In Old and New World species causing cutaneous leishmaniasis a T helper cell type 2 response accompanied by interleukin (IL)-4 and IL-13 production plays a crucial role during the chronic infection, whereas IL-10 and transforming growth factor (TGF)-β govern the manifestation of non-curing visceral leishmaniasis. Moreover, B-cells assist *L. donovani* and *L. mexicana* to establish a persistent infection, whereas their role is less pronounced in *L. major*. Besides the differences in cytokine and immune cell stimulation, a simi-

lar variety of chemokine and chemokine receptor modulation was found for the different *Leishmania* species. (Without claiming completeness) this listing shows differences between the *Leishmania* species, which result from diverged development within the last 40-80 million years between the Old and New World species as well as from specialisation for different organs [7,9].

	Main clinical pathology	Transmission cycle	Main geographical distribution
New World Leishmania species			
L. (Viannia) braziliensis	LCL, mucosal	Zoonotic	South America, parts of Central America, Mexico
L. (Viannia) panamensis	LCL, mucosal	Zoonotic	Northern South America and southern Central America
L. (Viannia) peruviana	LCL	Zoonotic	Peru
L. (Viannia) guyanensis	LCL	Zoonotic	South America
L. (Viannia) lainsoni	LCL	Zoonotic	South America
L. (Viannia) colombiensis	LCL	Zoonotic	Northern South America
L. (Leishmania) amazonensis	LCL, DCL	Zoonotic	South America
L. (Leishmania) mexicana	LCL, DCL	Zoonotic	Central America, Mexico, USA
L. (Leishmania) pifanoi	LCL	Zoonotic	South America
L. (Leishmania) venezuelensis	LCL	Zoonotic	Northern South America
L. (Leishmania) garnhami	LCL	Zoonotic	South America
Old World Leishmania species			
L. (Leishmania) aethiopica	LCL, DCL	Zoonotic	Ethiopia, Kenya
L. (Leishmania) killicki	LCL	Zoonotic	North Africa
L. (Leishmania) major	LCL	Zoonotic	central Asia, north Africa, middle east, East Africa
L. (Leishmania) tropica	LCL	Anthroponotic	central Asia, middle east, parts of north Africa, southeast Asia
L. (Leishmania) donovani	Visceral, LCL	Anthroponotic	Africa, central Asia, southeast Asia
Old and New World Leishmania species			
L. (Leishmania) infantum	Visceral, LCL	Zoonotic	Europe, north Africa, Central America, South America

Table 1: *Leishmania* species which are pathogenic to humans.

The subgenus is given in parentheses. LCL, localised cutaneous leishmaniasis; DCL, diffuse cutaneous leishmaniasis. Southeast Asia includes the Indian subcontinent and China. [10]

3.3 Cell Biology

Like all eukaryotes *Leishmania* parasites show a complex intracellular compartmentalisation (**Figure 3**). In addition to common cell organelles such as nucleus, endoplasmic reticulum (ER) and Golgi apparatus, they exhibit characteristic organelle structures including the kinetoplast [11], a large mitochondrion with mitochondrial DNA in close proximity to the flagellar

pocket, the multivesicular tubule, an elongated lysosome as well as the flagellum at the anterior side of the promastigote. The invagination of the plasma membrane next to the flagellum, the so-called flagellar pocket, serves as the main spot for endocytosis.

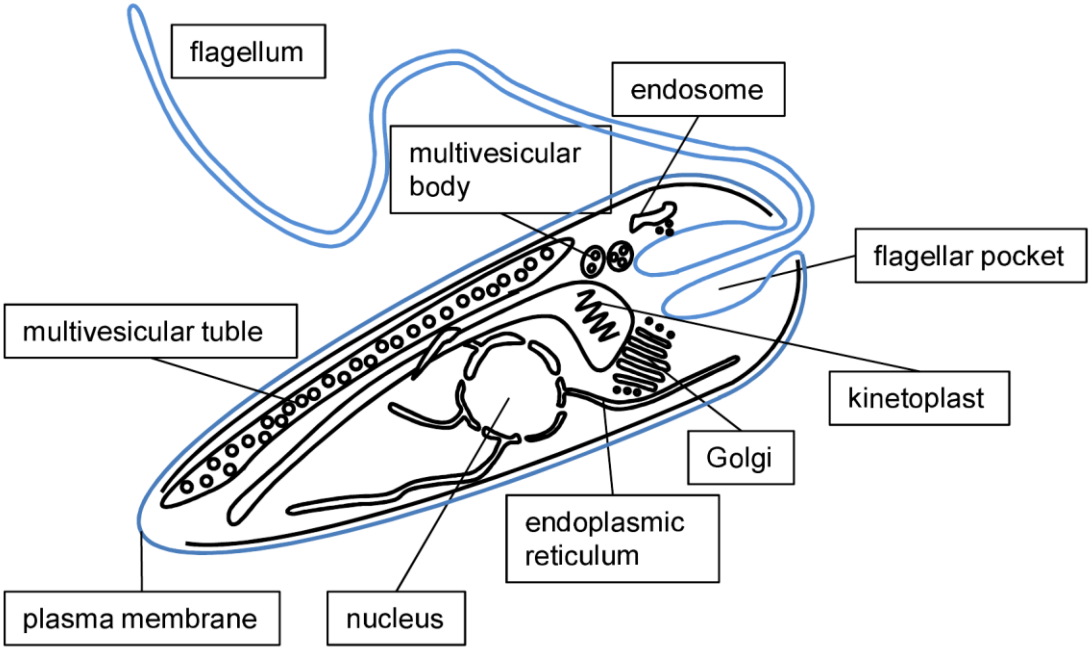

Figure 3: Schematic draw of a *Leishmania* promastigote and its characteristic organellar structure.

Adapted from various authors.

Leishmania parasites are perfectly adapted to each environmental niche they encounter during their life cycle. This is reflected by stage-specific protein expression, lipid modification and alterations in metabolic pathways [12].

In the sandfly *Leishmania* species satisfy their energy needs by glycolysis of sugar probably provided by nectar or sap feeding of the insect vector, whereas the intracellular stage of the parasite metabolises fatty acids and amino acids acquired from the host [13]. While most intracellular parasites avoid the proteolytic environment of the lysosomal compartment it serves as a place for proliferation of *Leishmania* amastigotes. There the continuous fusion with endosomes, phagosomes and autophagosomes containing macromolecular biomolecules guarantees the sufficient supply with nutrients. At the same time the parasite takes advantage of the hydrolytic environment of the lysosomal compartment that rapidly degrades these macromolecular nutrients into low molecular weight compounds. The latter typically serve as substrates for membrane transporters. The parasite exploits the strong proton gradient across the plasma membrane for co-transport of nutrients such as amino acids. To maintain the near neu-

tral cytosolic pH the amastigote expresses both, the constitutively expressed proton extrusion pump LDH1A and the proton pump LDH1B [14]. Functioning in concert both plasma membrane H^+ ATPases enable the parasite to survive at pH 4 [15].

Stage-specific binding of different lectins to distinct forms of the parasite during its cell cycle demonstrates molecular changes in the glycocalyx [16]. Changes in the major component of the promastigote glycocalyx, e.g. in the glycosylphosphatidylinositol (GPI)-anchored phosphoglycan (LPG), are important in the defence against lytic activities of the mammalian host. While LPG protects the procyclic promastigote against hydrolases in the midgut of the insect vector [17], it is not capable of blocking complement-mediated lysis. Increased infectivity of the metacyclic promastigote is mediated by elongated LPG, which has an increased number of phosphorylated disaccharide repeat units [18,19].

Besides the adaptation to its environment the parasite also modulates its hostile environment according to its needs. Following receptor-mediated endocytosis the decreased pH in the early endosome stimulates the promastigotes to differentiate into ovoid non-flagellated amastigotes. Here again LPG plays an important role in delaying the endosome-lysosome fusion allowing the promastigote to differentiate to an amastigote before the endosomal compartment is further acidified by phagosome-derived H^+ ATPases [20,21]. Furthermore, LPG is under cloud to scavenge oxygen radicals generated during the respiratory burst [22], to inhibit protein kinase C activity [23], to suppress macrophage NOS_2, and NO production [24].

3.4 Receptor-mediated phagocytosis

To initiate a successful infection *Leishmania* parasites have to gain entry into phagocytes. The invasion depends on receptor-mediated phagocytosis. Therefore surface antigens like LPG, which is recognised by serum mannan-binding protein and C-reactive protein (CRP), play a crucial role. In turn, the binding of CRP and serum-mannan binding protein results in complement-mediated lysis of procyclic, but not metacyclic promastigotes of *Leishmania donovani* and *Leishmania major*. In the latter case the GPI-anchored metalloprotease gp63 protects the parasite from degradative activities in the vertebrate host. It cleaves complement C3b into the inactive iC3b form and thus blocks complement-mediated lysis. Nevertheless, iC3b can opsonise the parasite via complement receptors 3 and 1 (CR3 and CR1) thereby targeting the parasite for uptake by macrophages. By preferentially accessing the macrophage via CR3 and CR1, the promastigote does not trigger a respiratory burst [25]. Nevertheless, differentiation to amastigotes goes along with a downregulation of the biosynthesis of LPG and gp63.

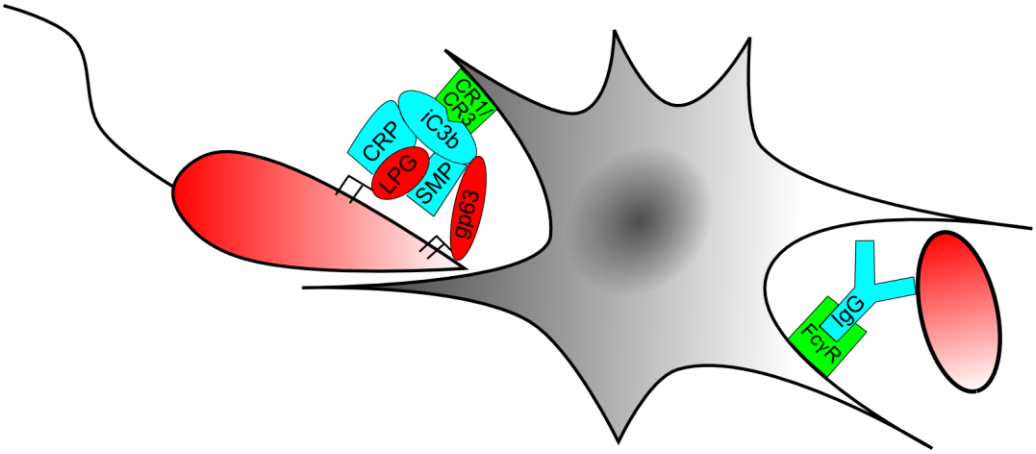

Figure 4: *Leishmania* antigens and phagocyte receptors important for the invasion.

Leishmania surface components Lipophosphoglycan (LPG) and glycoprotein 63 (gp63) are shown in red. Soluble components of the innate and adapted immune system like the C-reactive protein (CRP), serum mannan-binding protein (SMP), inactivated complement (iC3b) and immunoglobulin gamma (IgG) are shown in cyan. Phagocyte complement-receptors 1 and 3 (CR1/CR3) as well as the Fcγ receptor (FcγR) are marked green.

With progression of the infection antibody-mediated phagocytosis of amastigote forms via Fcγ receptors gain importance for parasite internalisation.

Moreover, it was suggested, that the surface exposure of the apoptotic lipid marker phosphatidylserine (PS) leads to recognition via the PS-receptor. Besides receptor-mediated phagocytosis this lipid is under cloud to stimulate the non-inflammatory response by macrophages to the parasite as known from apoptotic cells.

3.5 *Leishmania* Lipids

Lipids are a diverse class of biomolecules that play a major role not only as membrane components, but also as cellular signalling molecules. Chemically, lipids can be classified on basis of their headgroup (choline, ethanolamine, inositol and serine), their backbone (glycerol or sphingosine) or on basis of their lipid anchors (acyl, alkyl, alkenyl). In *Leishmania* species the choline, ethanolamine and inositol head groups dominate. The lipids in *Leishmania* are predominantly phospholipids (70% of total lipids) [26,27] and among them the glycerophospholipids constitute more than 50%. For example the glycerophospholipid phosphatidylcholine (PC) holds 30-40% of the total phospholipids (**Figure 5**).

Glycerophospholipids are based on a glycerol backbone, usually with two fatty acids bound via an ester or ether bond to the sn1 and sn2 position. Bound to the sn3 position of these diacylglycerols are hydrophilic moieties like choline, ethanolamine, serine or sugars. Synthesis

of diacyl ester and ether lipids follows different routes in *Leishmania*. Interestingly, inhibition of the ether lipid synthesis pathway by deletion of the required acyltransferase leads to a loss in virulence, whereas inhibition of the ester lipid metabolism does not show important alterations in virulence [28,29]. In contrast to other mammalian cells *Leishmania* contain high levels of ether lipids. For example most of the *Leishmania* phosphatidylethanolamines (PE) carry an ether acyl chain in the sn2 position (80-90% plasmalogens) [30,31].

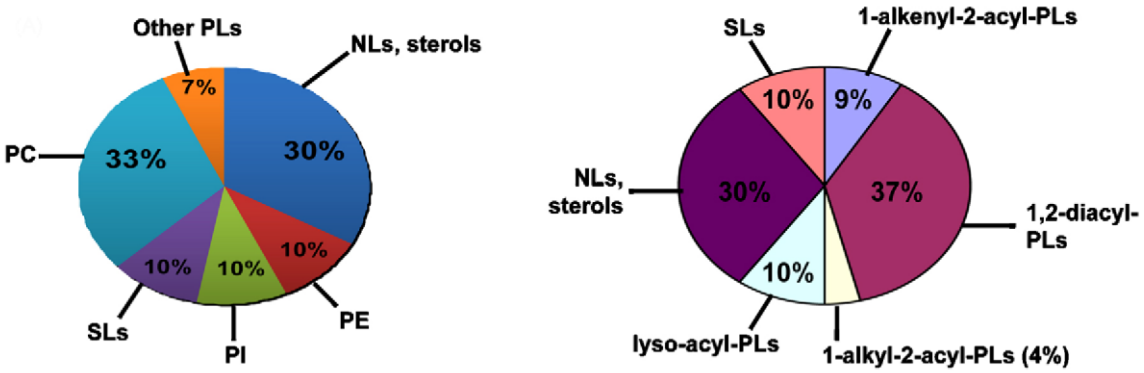

Figure 5: Lipid composition of *L. major*.

Lipids were classified either according to their backbone and head group (left) or according to their lipid anchors (right) [32]. Phospholipids (PLs); neutral lipids (NLs); sphingolipids (SLs); phosphatidylcholine (PE); phosphatidylethanolamine (PE); phosphatidylinositol (PI)

Among the ether lipids plasmalogens, lipids with an α-β-unsaturated ether at the sn1 position (**Figure 6**), might play an important role in protecting *Leishmania* from oxidative stress by scavenging oxidants and thus preventing polyunsaturated fatty acids from oxidation [33,34]. A prominent plasmalogen member is LPG mentioned above. It is an unusual complex glycolipid that contains a lyso-alkyl-PI lipid anchor linked to a hexasaccharide, followed by 15–30 repeats of the disaccharide mannose–galactose-phosphate, and ends with a small oligosaccharide [35]. Likewise, glycoinositol phospholipids (GPILs) and GPI-anchored proteins are tethered to the membrane by an ether lipid-based 1-alkyl-2-acyl-phosphatidylinositol anchor. Besides their function as anchor for certain surface components GIPLs constitute a dense glycocalyx directly adjacent to the promastigote surface. LPG and gp63 project through this glycocalyx [36]. GIPLs inhibit the protein kinase C activity [37] and thus probably the oxidative burst. Furthermore, they are under cloud to strongly inhibit NOS_2 expression [38].

Cardiolipins are diphosphatidylglycerols synthesised at the luminal side of the inner mitochondrial membrane and the major lipid component of this organelle. They are supposed to fulfil manifold functions. Although not essential for viability they support fitness and are suggested to interact with most mitochondrial proteins, to form lateral domains, to help bending the membrane due to their small head group area in comparison to the big fatty acid tail region, and to function as a proton trap for oxidative phosphorylation (for review see [39]).

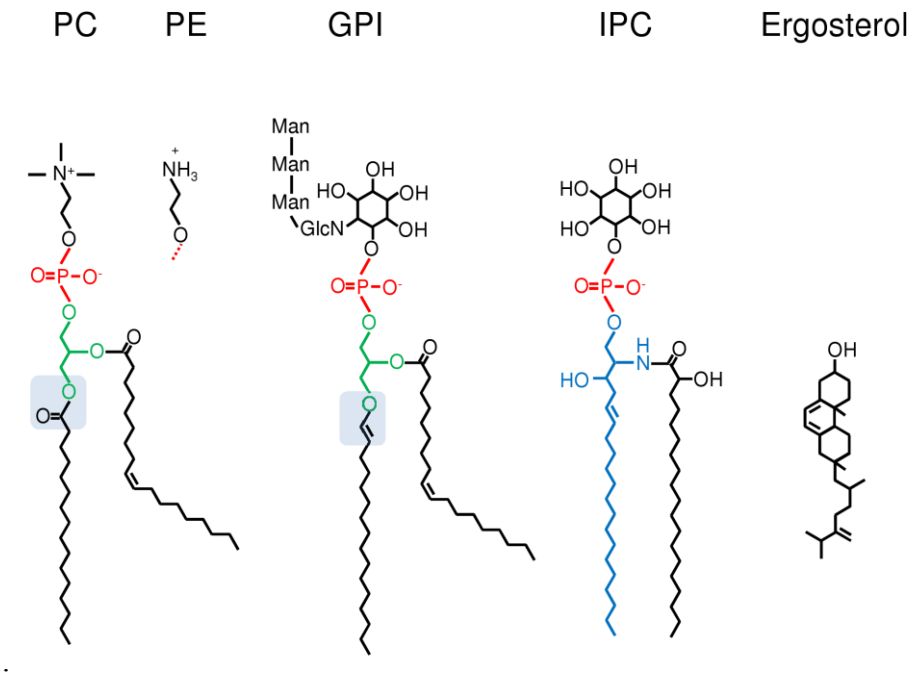

Figure 6: Chemical structures of important *Leishmania* phospholipids and ergosterol.

The glycerol backbone of glycerophospholipids is marked green, whereas the sphingosine backbone of sphingolipids is marked blue. The acyl bond in the sn1 position of phosphatidylcholine (PC) and the vinyl ether bond characteristic for plasmalogens in the sn1 position of glycosylphosphatidylinositol (GPI) are marked by boxes.

Another important group of *Leishmania* lipids are sphingolipids with sphingosine serving as the backbone moiety. While in host mammals sphingomyelin (SM) is the major member of this lipid class, SM is absent in *Leishmania*. Instead the protozoan parasite predominantly synthesises inositol phosphorylceramide (IPC, **Figure 6**). The deletion of enzymes important for sphingolipid synthesis leads to viable procyclics which fail to differentiate into metacyclics [30].

Sterols such as cholesterol and ergosterol are important amphipaths regulating the order, viscosity, and thus the permeability of lipid membranes. Synthesis of sterols takes place mainly in the ER. While mammalian cells synthesise cholesterol, synthesis of phyto- and ergosterols

dominates in plants and fungi, respectively. Isolated lipids of *Leishmania* parasites contain both, cholesterols and ergosterol. However, only the latter one is synthesised by the parasite itself. Cholesterol seems to be acquired from cell culture medium or the host cell itself.

As mentioned in the previous chapter the glycerophospholipid PS plays a vital role in signalling apoptosis to phagocytic cells like macrophages when exposed to the cells surface. The recognition of this moiety results in phagocytosis and production of non-inflammatory cytokines. Although genes homologous to a PS-synthase and a PS-decarboxylase are encoded by the *Leishmania* genome, contradictory results regarding the existence of PS in lipid extracts derived from parasites were published [31,40,41,42].

3.6 Lipid asymmetry (establishment and maintenance)

Phospholipid biosynthesis takes place only on one side of the membrane, e.g. PC and PE are formed in the cytosolic leaflet of the ER. This asymmetric lipid synthesis would lead to an imbalanced growth of the membrane. Hence, Bretscher et al. suggested the existence of a flippase[1] protein that facilitates the transversal motion of lipids in these biogenic membranes [43]. Indeed, later on it was demonstrated that phospholipids can flip in a fast bidirectional manner across the membrane of intact ER vesicles [44]. Moreover, it was shown that this motion requires proteins, but is ATP-independent. Although many attempts were made to identify this protein class, no candidates were found yet [45]. Anyway, during vesicle transport via the Golgi apparatus to the plasma membrane this random distribution of phospholipids disappears in favour of an asymmetric distribution. Since long it has been assumed that members of the type 4 P-Type (P_4) ATPase family and ABC-transporters play a fundamental role in establishing and maintaining this phospholipid asymmetry [46,47].

[1] Nowadays the term flippase is almost exclusively used for lipid transporting P_4-ATPases.

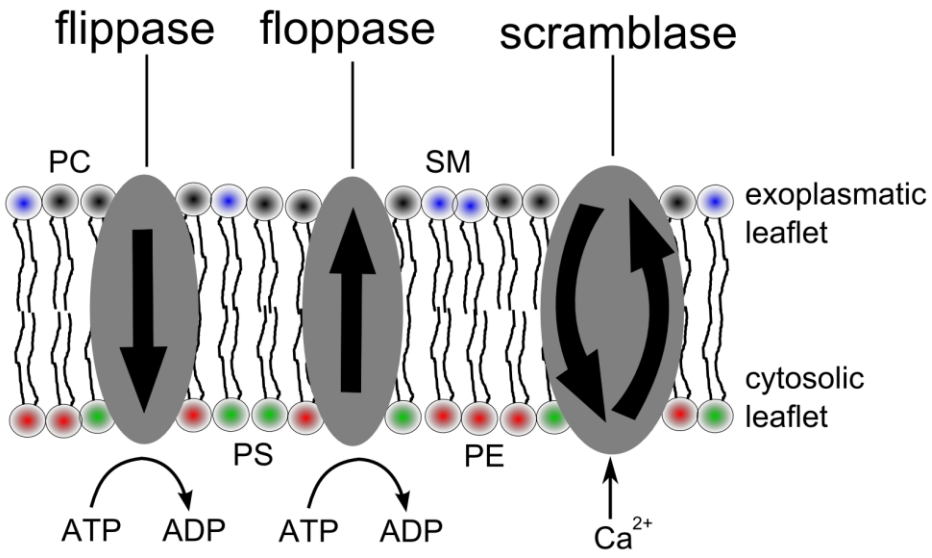

Figure 7: Scheme of the asymmetric lipid distribution at the plasma membrane of eukaryotic cells.

PS (green) and PE (red) are enriched in the cytoplasmic leaflet while PC (black) and SM (blue) reside in the exoplasmic leaflet. The ATP-dependent transporters, flippase and floppase, required for lipid flip-flop to establish and maintain phospholipid asymmetry at the plasma membrane of eukaryotic cells are depicted. Moreover, the ATP-independent scramblase was suggested to abrogate this gradient by facilitating the bidirectional flip-flop of phospholipids during apoptosis or activation by increased intracellular Ca^{2+} levels. The scramblase activity leading to an exposure of PS at the plasma membrane is crucial during apoptosis, since exposed PS serves as an apoptotic marker. Arrows indicate the direction of the respective transport activity. The scheme was adapted from Pomorski [46]

The members of either protein class transport their substrates across membranes in an energy-dependent manner. For this adenosine-5´-triphosphate (ATP) becomes hydrolysed to adenosine diphosphate (ADP) and orthophosphate on the cytosolic side of the membrane. While the ATP binding cassette (ABC)-class of lipid transporters moves their substrates from the cytoplasmic to the extracellular leaflet of the membrane, P_4-ATPases direct lipids the opposite way. Besides their distinct transport directions both protein families differ in their overall structure and mode of action.

3.6.1 The type 4 subclass of P-type-ATPases (flippases)

P-type-ATPases are a conserved family of ion transporters. While three of the five known subclasses transport indeed ions, P_1 (K^+, Cu^{2+} and Cd^{2+}), P_2 (Ca^{2+}, Na^+/K^+ and H^+/K^+) and P_3 (H^+ and Mg^{2+}), the P_4-ATPases were proven to transport lipids [48,49]. To date there is no substrate known for the P_5-ATPases [50]. Structurally, they consist of a membrane domain

with eight to ten membrane-spanning helices, a so-called actuator domain, a nucleotide binding domain, and most notably the name-giving phosphorylation domain containing the reversibly phosphorylated aspartate residue (**Figure 8**). The best studied P_4-ATPase is the yeast Drs2p. This transporter is located in the trans-Golgi network and transports PE and PS towards the cytosolic leaflet [47]. Screening the *L. infantum* genome for homologues of the yeast Drs2p results in five members of the P_4-ATPase subfamily. In **Figure 9** the typical p-type ATPase motifs of yeast Drs2p and the deduced amino acid sequence in *Leishmania* are shown. To date no crystal structure of a P_4-ATPase is available.

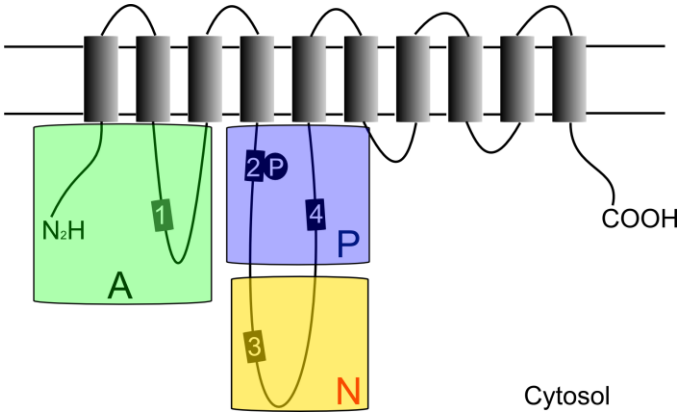

Figure 8: Topology model of P-type ATPases.

The membrane domain with the characteristic ten transmembrane helices (grey) and the conserved cytoplasmic domains are depicted. The actuator domain (A) with the amino-terminal end and the first cytoplasmic loop containing the motif 1 are highlighted in green. The phosphorylation domain (P) with the characteristic motive 2 containing the aspartic acid residue necessary for phosphorylation and motif 4 are marked with blue. And the nucleotide binding domain (N) containing motif 3 is framed in orange. The model was adapted from Lenoir [51].

Thus, most structure function relations for the P_4-ATPase family were obtained by analogy models derived from the sarcoplasmic reticulum calcium ATPase (SERCA) and the sodium-potassium ATPase [52,53]. The modified Post-Albers cycle for the P_4-ATPases is depicted in **Figure 10**. In the left sketch the catalytic cycle of the P_{2A}-ATPase SERCA is depicted. Here Ca^{2+} binds to a site with high affinity to this ligand, which is accessible from cytosol in the E1 conformation of the transporter. Next, the aspartate residue in the above mentioned DKTGTLT motif of the phosphorylation domain is amenable to phosphorylation by γ-phosphate of ATP in the presence of Mg^{2+}. In this high energy conformation, called E1P, the ligand is occluded in the transmembrane domain. The downhill transition towards the low-energy phosphorylated intermediate E2P starts with the release of ADP from the nucleotide

binding domain. This liberates the ligand into the exoplasmic space. Now, the transporter has high affinity for counter-ions, e.g. protons in the case of the Ca^{2+}-ATPase. In the following, hydrolysis of the phosphorylated aspartate mediated by the DGET motif in the actuator domain results in the E2 conformation. Transition from E2 to E1 is characterised by release of phosphate and Mg^{2+} and attended by dissociation of the counter-ions into the cytoplasm.

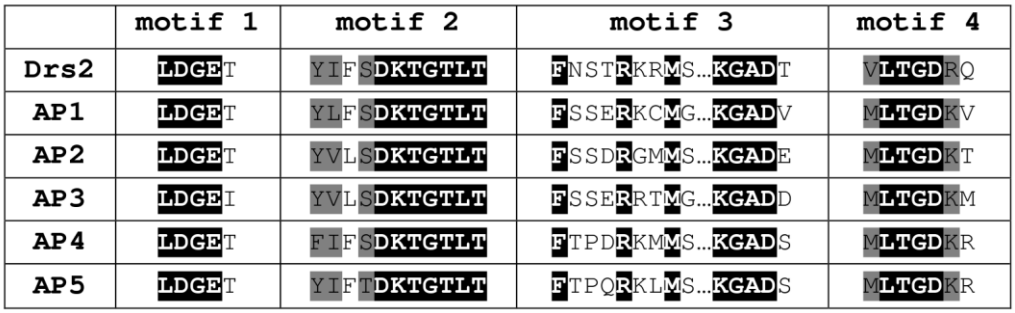

Figure 9: Conserved motifs of P-type-ATPases in yeast Drs2p and the five *Leishmania* homologues.

Leishmania protein sequences were derived from *L. infantum* genome and aligned using ClustalW2 tool at the website of the European Bioinformatics Institute. The complete comparison is shown in **Figure 34** in the appendix. The names AP1 to AP5 are given according to the similarity to the Drs2 while AP4 represents LdMT.

Based on structural homology, biochemical and biophysical analysis Lenoir suggested a similar function of P_4-ATPases [52]. With respect to Ca^{2+} transported by SERCA the motion of lipids mediated by P4-ATPases is antipodal (**Figure 10**).

In yeast mutants lacking the plasma membrane-resident or the trans-Golgi network-resident flippases are characterised by a defect in endo- and exocytosis, respectively. Besides creating and maintaining the phospholipid asymmetry of the Golgi and the plasma membrane, the phospholipid translocases support vesicle formation. The unidirectional translocation of phospholipids towards the cytosolic leaflet of a membrane was suggested to create a mass imbalance and hence surface tension, which results in bending of the bilayer towards the cytosol. Thus, flippases in concert with coat proteins were thought to be required for vesicle formation of relatively rigid membranes, such as trans-Golgi network and plasma membrane [54,55].

In *L. donovani*, a member of the P_4-ATPase family was found in a screening for drug resistance against miltefosine, a hexadecylphosphocholine with leishmanicidal effect [56]. With respect of this function, it was named *Leishmania donovani* miltefosine transporter (LdMT). In the same screening another mutant lacking LdRos3, a CDC50 homologue, with similar phenotype was found [57].

The function of most P_4-ATPases reported so far was found to be sensitive to the expression of members of the CDC50 protein family. The first member described, Cdc50p, was found in a screening for cold-sensitive yeast mutants deficient in cell division [58]. Later, another member, Lem3p/Ros3p, was found to be crucial for insensitivity to the PE binding antibiotic Ro09-0198 and for sensitivity to the toxic PC analogues miltefosine and edelfosine [59,60]. Members of this protein family share a common topology with two membrane-spanning helices and a large exoplasmic loop, which is N-glycosylated and stabilised by disulfide bonds. Three members each were found in yeast [61], man [62] and *Leishmania* [57], whereas five members were found in Arabidopsis [63]. In yeast four of the five P_4-ATPases form a complex with a CDC50 member [52,61].

Figure 10: The modified Post-Albers cycle of P-type ATPases for the sarcoplasmic reticulum calcium ATPase (SERCA, left) and for P_4-ATPases (right) [52]**.**

The mechanism is described in detail in the text.

Since CDC50 proteins were found to be required for the ER export of P_4-ATPases, Seito et al. suggested that these proteins function like chaperones for the transporter [61,64,65]. In addition, the yeast Cdc50p and the human CDC50A are crucial to render the P_4-ATPase in a phosphorylation competent state. Moreover, the strength of the physical interaction between yeast Cdc50p and Drs2p fluctuates throughout the catalytic cycle, being strongest in the ligand-bound phosphorylated E2-P conformation. These findings suggest that CDC50 proteins are vital components of the translocation machinery [52]. The molecular mechanism of CDC50-dependent activity of the flippase machinery is not known yet. A model described by Lenoir et

al. proposes that the two transmembrane domains of the CDC50 proteins provide additional cavity space crucial for binding of the bulky phospholipid substrate. In addition, the ectodomain of the CDC50 binding partner might promote the occlusion of the phospholipid substrate at the E2P state. The tight binding between both interaction-partners found in the E2P state is potentially lost by conformational changes occurring in the P_4-ATPase upon dephosphorylation. This allows the substrate to be released from the catalytic complex into the cytoplasmic leaflet of the lipid bilayer (**Figure 11**).

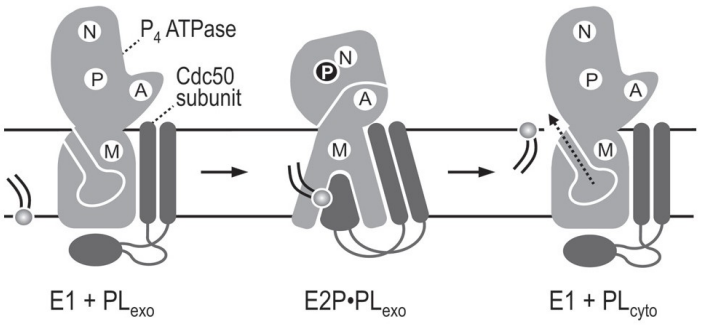

Figure 11: Model for the functional interaction of a CDC50 protein (dark grey) with a P_4-ATPase (light grey) during the catalytic cycle of the transporter [52]**.**

E1 and E2P correspond to conformations of the P-type-ATPase described in the Post-Albers cycle. The nucleotide binding domain (N), the phosphorylation site (P), the actuator (A), and the membrane domain (M) are marked. A phospholipid in the exoplasmic leaflet (PL_{exo}) binds to the high-affinity binding site available in the E2P conformation of the P_4-ATPase/CDC50 protein complex ($E2P{\cdot}PL_{exo}$). The ectodomain of the CDC50 binding partner facilitates occlusion of the bulky phospholipid substrate and hence, conversion of the P_4-ATPase to the E2 form. Upon acquiring the E1 state, the P_4-ATPase loses its tight interaction with the CDC50 protein allowing the phospholipid substrate to be released into the cytoplasmic leaflet of the membrane (PL_{cyto}).

3.6.2 ABC Transporters (floppases)

The ATP binding cassette (ABC)-transporter class is a highly conserved family of membrane proteins that translocate a broad spectrum of substrates across membranes. Substrates such as amino acids, sugars, inorganic ions, peptides, proteins, lipids, and various organic and inorganic compounds are transported with high affinity even against strong concentration gradients (up to 10 000 fold). Transporters of this family are composed of transmembrane domains (TMDs), usually with six membrane-spanning α-helixes, and nucleotide binding domains (NBDs) for the binding and hydrolysis of ATP. In eukaryotes often two TMDs and two NBDs form a functional transporter. The different domains can be organised as separate proteins or as a full-size protein [66].

During the transport cycle one substrate molecule binds to a cavity at the cytosolic side, subsequently two molecules of ATP bind to the NBDs. Following, the two distant NBDs close up to form a tight dimer. This conformational change is transmitted to the TMDs causing them to tilt. Thereby the cytosolic cavity with the bound substrate closes and opens towards the exoplasmic side, followed by substrate release. Hydrolysis of ATP to ADP and Pi might cause detachment of the NBDs and return to the starting conformation [67].

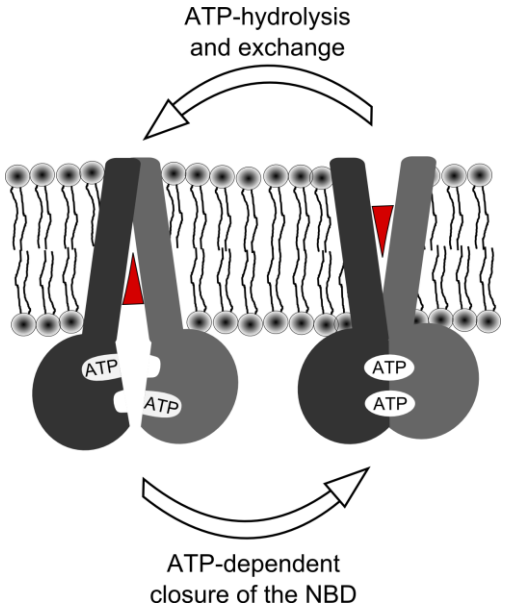

Figure 12: Simplified model for the translocation of substrates across the bilayer by ABC-transporters.

Following substrate binding to a cytosolic cavity two molecules of ATP bind to the Walker A and B motifs. Next, the two NBDs form a dimer and thereby tilt the α-helices in the membrane domain. This conformational change presents the substrate to the exoplasmic side and triggers substrate release. Upon ATP hydrolysis both NBDs detach from each other rendering the transporter competent for ATP and substrate binding. Adapted from Procko [67].

In *Leishmania*, several transporters of the ABC class were found to transport NBD-lipid analogues. Overexpression of both, LtrABCA2 and LtrABC1.1 in *Leishmania tropica* show less accumulation of fluorescently labelled lipid analogues of PC, PE, and to a lesser extent of PS compared to wild-type parasites [68,69]. LtrABCA2 localises to the flagellar pocket and to intracellular membranes, whereas LtrABC1.1 is located at the plasma membrane and the flagellar pocket. Both ABCG homologues, LiABCG6 and LiABCG4 from *Leishmania infantum* localise to the plasma membrane, but differ in substrate specificity. While LiABCG6 transports fluorescent NBD-PC, -PE, and to a lesser extend NBD-PS, LiABCG4 transports only PC analogues [70,71].

3.6.3 Scramblases

The lipid asymmetry established and maintained by flippases and floppases as described above is a feature of living eukaryotic cells. This phospholipid distribution was found to be abrogated in activated platelets, in macrophages during phagocytosis, in B-lymphocytes and many other cell types. Importantly, PS exposed due to loss of the lipid asymmetry at the plasma membrane of apoptotic cells serves as a crucial eat me signal for phagocytes [72].

The ability to undergo a regulated decay during cell death is a feature of metazoan as well as a small number of unicellular eukaryotes. For multicellular organism, apoptosis is important for proper development during embryogenesis, tissue homeostasis and protection from bacterial, viral and parasitic infections as well as cancer development [73,74,75,76,77,78,79]. An early event during apoptosis is the loss of the plasma membrane lipid asymmetry. This was shown to occur following caspase activation and disruption of the mitochondrial outer membrane [80]. Like other eukaryotes, *Leishmania* is capable to undergo apoptosis which is characterised by loss of the mitochondrial membrane potential, release of cytochrome c, activation of caspases, nicked DNA in the nucleus as well as high molecular weight DNA fragmentation and morphologically by loss of motility, rounding and shrinkage of the cell and blebbing of the plasma membrane [81,82,83]. Finally, the impermeability of the plasma membrane is compromised, which can be visualised by DNA binding dyes, like propidium iodide that in turn is excluded from cells with intact plasma membrane.

Independent from apoptosis elevation of cytosolic calcium levels in erythrocytes, platelets, T-cells, and many other cell types leads to facilitated flip-flop and thus to a loss in lipid asymmetry [84,85,86,87]. Although elevated intracellular calcium levels were described during cell death, this seems not to be a prerequisite for scrambling during apoptosis as demonstrated in lymphocytes derived from patients with Scott syndrome. In lymphoid cells from patients with this congenital bleeding disorder scrambling cannot be activated by Ca^{2+}, but is induced normally during apoptosis [88]. To this end, it is unclear whether apoptosis and elevated intracellular Ca^{2+} level trigger the same mechanism, but the latter was shown to be inhibited by protein modifying agents. Thus a protein, termed scramblase, was made responsible for calcium-induced bidirectional lipid movement across the plasma membrane of erythrocytes [89]. Henceforward, several protein candidates were suggested to transfer lipids energy-independently and bidirectionally across the plasma membrane of eukaryotic cells. Members of the PLSCR-family, the ABC transporter ABCA1 as well as the P_4-ATPase homologue Tat-1

from *C. elegans* were made responsible for calcium-induced scrambling and PS externalisation during apoptosis, respectively [90,91,92]. Contradictory results on ABCA1 and PLSCR1 questioned their role in lipid scrambling [93,94]. Another mechanism was suggested by Mirnikjoo et al. who found that elevation of intracellular calcium levels leads to fusion of lysosomes with the plasma membrane resulting in exposure of PS to the extracellular leaflet of the plasma membrane [95]. Moreover, Contreras et al. proposed another mechanism resulting in lipid scrambling during apoptosis. Sphingomyelinase activity catalysing the formation ceramide was suggested to facilitate the bidirectional flip-flop of phospholipids, too [96]. Whatever the identity of the scramblase or the mechanism mediating scrambling might be, it was found that the substrate specificity of the scramblase in erythrocytes depends on the head group size as well as on the lipid back bone, but is independent of the stereochemistry [97,98]. In general, scramblases seem to have broader substrate specificity than single P_4-ATPases or lipid transporting ABC-transporters. Thus, if scrambling is mediated by flippases or floppases, it would require the interplay of more than one member to cover all substrates.

In *Leishmania* no scramblase activity was reported so far, although staining with annexin V, a protein recognising charged lipids like PS, is used to assay the viability of parasites in laboratory. On the contrary increased intracellular Ca^{2+} levels were observed during apoptosis stimulated by miltefosine and H_2O_2, during the engulfment by macrophages as well as during temperature shift as required for differentiation [81,99,100,101,102].

4 Aim of the work

Despite the obvious importance of lipid surface components to gain entry into the host cell and to adapt to the different environmental niches the parasite faces during its life cycle, little is known about the composition and dynamics of membrane lipids in *Leishmania*. Likewise, the proteins involved in the regulation of the plasma membrane lipid distribution remain to be identified. Such knowledge may among others be important for the development of new drugs and strategies against the leishmaniasis.

In this work mechanisms regulating the lipid asymmetry have been investigated in detail. Firstly, a protein complex suggested to have a role in regulating the plasma membrane asymmetry was studied. Secondly, the presence of a calcium activated scramblase mechanism was investigated and thirdly, the phospholipid spectrum of the parasite was analysed by focussing on PS, since this lipid was suggested to be important for invasion of the mammalian host cells.

5 Material and Methods

5.1 Chemicals

If not stated otherwise, all substances were obtained by Sigma-Aldrich.

5.2 Equipment

Agarose gel electrophoresis System	Bio-Rad
Gel electrophoresis “Mini-Protean System”	Bio-Rad
PCR System “MyCycler”	Bio-Rad
pH meter 761 Calimatic	Knick
Phosphorimager “Image Analyser FLA3000”	Fujifilm
BASReader Software	Fujifilm
Photometer UV1	Thermo Scientific
Plate reader “FLUOstar Optima”	BMG Labtechnologies
Incubator Shaker Classic Series C25KC	New Brunswick Scientific
Thermoshaker	Gerhardt
Table top centrifuge Biofuge Fresco	Heraeus
Table top centrifuge Biofuge Stratos	Heraeus
Ultra centrifuge Avanti J-20 XP	Beckman Coulter
Ultra centrifuge XL-70	Beckman
Western-blot Semi-Dry	Bio-Rad
Cell Counter	CASY
Flow Cytometer “FACSCalibur”	Becton Dickinson
FACS Software “FACSDiva”	Becton Dickinson
FACS analysis software “Cyflogic”	Cyflogic
Microscope “FluoView FV1000”	Olympus
Axiovert	Zeiss
Multiporator	Eppendorf
Silica gel 60 DC TLC-plates	Merck

5.3 Biological material

5.3.1 *Leishmania* cell lines

All *Leishmania* cell lines were kindly provided by Santiago Castanys and Francisco Gamarro-Conde from the Institute of Parasitology and Biomedicine "Lopez Neyra", Spain.

Name	**description**
Leishmania donovani	(MHOM/ET/67/HU3)
Leishmania donovani	(MHOM/ET/67/HU3) ΔLdMT
Leishmania donovani	(MHOM/ET/67/HU3) ΔLdRos3
Leishmania infantum	(MHOM/ES/1993/BCN-99)
Leishmania tropica	LRC-L39 (LEM 2563, Montpellier, France)

5.3.2 Human cell lines

The THP-1 cell line was kindly provided by Juan Patron from the Max Planck Institute for Infection Biology, Germany.

Name	**description**
THP-1	$CD14^+$, $CD15^+$, derived from a patient with acute monocytic leukaemia

5.3.3 Yeast cell lines

Except for BS915, all *Saccharomyces cerevisiae* cell lines were created by Prof. Thomas Günther-Pomorski. BS915 was kindly provided by Birgit Singer-Krüger.

Name	**description**
SEY6210	MATa leu2-3,112 ura3-52 his3-Δ200 trp1-Δ901 suc2-Δ9 lys2-801; GAL
TPY248	6210-Δdnf1-ΔHIS-Δdnf2-ΔHIS-ΔRos3-ΔHIS
TPY249	6210-Δdnf1-ΔHIS-Δdnf2-ΔHIS-ΔRos3-ΔHIS
BS915	MAT**a** his4 ura3 leu2 lys2 neo1::kan^r bar1-1 + pRS315-neo1-37

5.3.4 Bacteria strains

Name	description
DH5α	F⁻endA1 hsdR17(r_K^-, m_K+) glnV44 thi1 recA1 gyrA96 relA1 Δ(lacIZYA-argF) U169 M15 Φ80Δ

5.3.5 Plasmids

Name	marker	produced by
pXG-neo-GFP-LdMT	G-418	F. Javier Pérez-Victoria
pXG-neo-CFP-LdMT	G-418	Maria Sánchez-Cañete
pXG-neo-CFP-AP2	G-418	Maria Sánchez-Cañete
pXG-neo-GFP-LdRos3	G-418	Maria Sánchez-Cañete
pXG-hyg-YFP-LdRos1	HYG	Maria Sánchez-Cañete
pXG-hyg-YFP-LdRos2	HYG	Maria Sánchez-Cañete
pXG-hyg-YFP-LdRos3	HYG	Maria Sánchez-Cañete
pXG-neo-FLAG-LdMT	G-418	Adrien Weingärtner
pESC-HIS-CFP-LdMT	HIS	Adrien Weingärtner
pESC-URA-YFP-LdRos3	URA	Adrien Weingärtner

5.3.6 Primers

Name	description
Forward MCS for pXG	P-CCGGG TCTAGA GCGGCCGC GGTACC TTAATTAA C
Reverse MCS for pXG	P-CCGGG TTAATTAA GGTACC GCGGCCGC TCTAGA C
Forward LdMT KpnI	CCC GGT ACC ATG CCC AAC CAA CCG CCG TGT TGG
Reverse CFP PacI	AA ATT AAT TAA TTA CTT GTA CAG CTC GTC CAT GCC GAG AGT GA
Forward LdRos3 KpnI	CCC GGT ACC ATG GCG CCT CTA CCC CCT AAG CC
Forward AP4 cfr9I	CCC GGG ATG CCC AAC CAA CCG CCG TGT TGG
Reverse AP4 FLAG cfr9I	CCC GGG TCA TTT ATC ATC ATC ATC TTT ATA ATC CAG CTT TCC ACC GTT TTG AAC AGC GTA C

5.3.7 Antibodies

Name	**description**	**produced by**
rabbit-α-LdMT	1:500, overnight, 4°C	Maria Sánchez-Cañete
rabbit-α-LdRos3	1:500, overnight, 4°C	Maria Sánchez-Cañete
mouse-α-gp63	1:10, overnight, 4°C	Robert Mc Master
goat-α-rabbit-horseradish peroxidise-conjugate	1:5000, 1h, 25°C	Thermo Scientific Pierce # 32260
goat-α-mouse-horseradish peroxidase-conjugate	1:5000, 1h, 25°C	Thermo Scientific Pierce # 32230

5.3.8 Growth media

Escherichia coli medium

LB-medium

1.0% (w/v)	Bacto™ Trypton
0.5% (w/v)	Bacto™ yeast extract
0.5% (w/v)	NaCl
1 ml/l	1M NaOH
50µg/l	Ampicillin

LB-agar

LB-medium supplemented with 1.5% Agar

Saccharomyces cerevisiae media

SD-Medium

0.17% (w/v)	Yeast nitrogen base
0.5% (w/v)	$(NH_4)_2SO_4$
Selective marker	
0.0055% (w/v)	Adenine
0.0055% (w/v)	L-Tyrosine
0.0055% (w/v)	Uracil
pH 7.4	
2.0%	L-Glucose
1.0%	Amino acid stock

YPD-Medium

2.0% (w/v)	Bacto™ Pepton
1.0% (w/v)	Bacto™ yeast ex-
2% (w/v)	L-Glucose

YPD-Agar

YPD-medium supplemented with 2% (w/v) Agar

SD-Agar

SD-medium sup-
with 2% (w/v) Agar

Leishmania medium

M199+

M-199 medium supplemented with

40mM	HEPES
100µM	Adenosine
0.5µg	Hemin
10µM	6-Biopterin
10%	heat-inactivated
selective marker	
50µg to 500µg/ml	Hygromycin
50µg to 500µg/ml	G-418 (PAA)

THP-1 medium

RPMI-1640+

RPMI-1640 supplemented with

2 mM	L-Glucose
50 µM	β-mercaptoethanol
1 mM	Na-Pyruvate
10%	FCS

5.3.9 Buffer

HPMI

132 mM	NaCl
20 mM	HEPES
3.5 mM	KCl
0.5 mM	$MgCl_2$
2 mM	$CaCl_2$
5mM	L-Glucose
1mM	Na-Pyruvate

Electroporation buffer

25 mM	KCl
0.3 mM	KH_2PO_4
0.85 mM	K_2HPO_4
90 mOsmol/kg	Myo-inositol
7.2	pH
3.5	mS/cm

5.4 Methods

5.4.1 Cell culture

Promastigotes of wild-type *Leishmania donovani* (MHOM/ET/67/HU3) and its derivative cell lines LdMT knockout (ΔLdMT) and LdRos3 knockout (ΔLdRos3) as well as wild-type *L. infantum* (MHOM/ES/1993/BCN-99) and wild-type *L. tropica* LRC-L39 (LEM 2563, Montpellier, France) were propagated under mild shaking with 40 rounds per minute (rpm) in M199+ at 26°C. The identity of the knockout strains was tested routinely by PCR and by miltefosine sensitivity assays. Cell lines overexpressing LdMT-green fluorescent protein (GFP), LdRos3-GFP or LdMT-cyan fluorescent protein (CFP) were cultured in M199+ supplemented with G-418, and cell lines overexpressing LdRos3-yellow fluorescent protein (YFP) were cultured in M199+ supplemented with hygromycin.

The human monocytic cell line THP-1 was cultured in RPMI-1640+ with 5% CO_2 at 37°C. The differentiation to macrophages was stimulated by adding 100ng/ml Phorbol 12-Myristate 13-Acetate (Biomol) to THP-1 cells (0.2 x 10^6 cells/ml) for 12h. Then adherent cells were washed three times with PBS and cultured for three days as described above.

The *Saccharomyces cerevisiae* wild-type (SEY6210) and knockout strains Δdnf1, Δdnf2, and Δros3 (TPY248 and TPY249) as well as the derivative neo1 knockout (BS915) were maintained at 30°C, on YPD-agar or in YPD-medium under constant shaking with 180 rounds per minute. For heterologous co-expression of LdMT-CFP and LdRos3-YFP, TPY248 or TPY249 cells were cultured on selective SD-agar or in selective SD-medium lacking histidine (HIS) and/or Uracil (URA).

5.4.2 CASY Cell-Counter

To determine the cell density in *Leishmania* cultures a 10µl sample of cell parasites suspension was mixed with 5ml of Casy-Flow™. Following, 200µl were soaked three times through the 60µm capillary of the Casy-Counter™, and the mean cell density was determined by using the 0-30µm settings with a cut off below 2µm and above 10µm.

5.4.3 Drug sensitivity and MTT assay

To determine parasite sensitivity to miltefosine (Zentaris), amphotericin B, papuamide B (Flintbox, Lynsey Huxham), and duramycin, 2.5 x 10^4 parasites were incubated in 96well

plates (100 µl) for three days at different drug concentrations before determining cell proliferation by the 3-(4,5-dimethyl-2-thiazolyl)-2,5-diphenyl-2H-tetrazolium bromide (MTT) colorimetric assay. For this, 50µl of a MTT solution (3.3 mg/ml) were added to each well. Then plates were incubated for 4h at 26°C under mild shaking to enable the mitochondrial reductase to convert MTT to the purple formazan. Subsequently, cells were lysed and formazan crystals dissolved by adding 100µl of a stop solution (50% isopropanol, 10% SDS) and further incubation for 30 minutes. Finally, the optical density was determined by measuring the absorbance at 570nm, using a FLUOstar Optima plate reader (BMG Labtechnologies). For all drugs and all cell lines used, the MTT assay correlated linear to cell numbers determined by cell counter (CASY).

The 50% effective concentration (EC50) was defined as the drug concentration required for half-maximal inhibition of the cellular growth rate. The EC50 for each line was calculated by nonlinear regression analysis using SigmaPlot 2000 for Windows (SPSS Inc.).

5.4.4 Phagocytosis of *Leishmania donovani* lines by macrophages

Macrophages were derived from the monocytic THP-1 cell line as described under cell culture. Three days post-differentiation macrophages (10^6/flask) were labelled for 40 minutes in 3 ml RPMI-1640 medium containing 0.5 µM CellTracker™ Dil (Invitrogen). Non-accumulated dye was removed by washing the cells 5 times with RPMI-1640^+ medium. Promastigotes (10^7) from early log phase were labelled for 40 minutes in 2.5 ml M-199 medium containing 0.5 µM CellTracker™ Green (Invitrogen). Then, parasites were washed five times with M-199^+ and finally suspended in RPMI-1640^+. For macrophage infection at a ratio of 1:10 (macrophages:parasites), about 10^7 CellTracker™-labelled parasites were added to 10^6 CellTracker™ Dil-labelled adherent macrophages. Sixteen hours after infection, unbound parasites were washed away with PBS and infected macrophages analysed by fluorescence microscopy or by flow cytometry. For flow cytometry, macrophages were trypsinised for 20 minutes at 37°C and finally suspended in supplemented RPMI-1640^+.

5.4.5 Annexin V and Bio-Ro Assay

To visualise endogenous PE at the cell surface, 5 x 10^6 promastigotes in logarithmic phase of growth were incubated in 20 µl HPMI containing 38 µM Bio-Ro (provided by Kazuma Tanaka). After 1h at 4°C, cells were washed with HPMI containing 0.5% (w/v) bovine serum albumin and then fixed with HPMI containing 5% (v/v) formaldehyde for 1 h at 30 °C. Pro-

mastigotes were washed in HPMI, suspended in 250 µl HPMI containing 5µg/ml Streptavidin-fluorescein isothiocyanate (FITC) and incubated for 30 minutes at 25°C prior to microscopy analysis. To measure exposure of endogenous PS on the cell surface, about 5 x 10^5 parasites were incubated on ice for 10 minutes in the dark with 125 ng annexin V-FITC and 1 µg PI in 0.5 ml of binding buffer (10 mM HEPES pH 7.4, 140 mM NaCl, 2.5 mM $CaCl_2$). Cells were washed, suspended in 0.5 ml of binding buffer and subjected to microscopy.

5.4.6 Fluorescence Microscopy

Epifluorescence microscopy and image acquisition were carried out using an inverse Axiovert 100 standard fluorescence microscope (Carl Zeiss, Oberkochen, Germany), equipped with a cooled CCD camera (Coolsnap, visitron systems, Puchheim, Germany) driven by Metamorph software (Universal Imaging, Downingtown, USA). NBD (7-nitro-2-1,3-benzoxadiazol-4-yl) fluorescence was observed using a Plan-APO 100x/1.3 NA oil objective with the following filter set: band pass 450–490 nm, beam splitter 510, and band pass 512–542 nm.

Confocal laser scanning microscopy was performed using an inverted Fluoview 1000 microscope (Olympus, Tokio, Japan) and a 60x (N.A. 1.35) oil-immersion objective. Fluorescence of NBD, FITC and CellTracker Green was excited with a 488 nm argon laser and recorded between 500 and 530 nm. Fluorescence of PI and CellTracker CM-Dil was excited with a 559 nm argon laser and recorded between 570 and 600 nm. Images with a frame size of 256 x 256 pixels were acquired

To measure Förster Resonance Energy Transfer (FRET) between cyan fluorescent protein (CFP) and yellow fluorescent protein (YFP) filter settings were optimised using cells expressing either CFP or YFP to prevent bleed through. Thus, excitation of CFP was achieved with a 440nm laser diode and emission detected between 460 nm and 490 nm, while YFP was excited using a 515 nm Argon laser and emission detected between 535 and 575nm. Next, cells co-expressing CFP and YFP were imaged first in sequential mode and then FRET was measured by excitation with the 440 nm laser and read out for YFP fluorescence. To verify the FRET signal detected, the acceptor was photo bleached applying the 515nm laser. Finally, the fluorescence of CFP and YFP as well as the FRET signal were measured once again.

5.4.7 Flow Cytometry Analysis

Flow cytometry analysis was performed on a Becton Dickinson FACS (San Jose, CA) equipped with an argon laser (488 nm) using the following fluorescence channels (log scale):

FL1 (530/30 nm, NBD, CellTrackerTM Green, Fluo-4, FITC), FL2 (585/42 nm, PI, CellTrackerTM Dil). Live cells were selected based on forward/side-scatter gating and propidium iodide exclusion. For this 5µl propidium iodide (1mg/ml) were added to 1ml cell suspension with 10^6 cells in HPMI at least ten minutes prior analysis. Next, aliquots of 100µl were transferred to a FACS tube and 4000 gated events were analysed. Further analysis was performed using Cyflogic software. Geometric mean values of the fluorescence in FL1 were calculated for at least three independent experiments.

5.4.8 NBD-lipid uptake in *Leishmania donovani* lines

Fluorescent lipid analogues 1-palmitoyl-2-{6-[(7-nitro-2-1,3-benzoxadiazol-4-yl)amino]hexanoyl}-sn-glycero-3-phosphatidylserine (NBD-PS), -phosphatidylethanolamine (NBD-PE), -phosphatidylcholine (NBD-PC), and N-[6-[(7-nitro-2-1,3-benzoxadiazol-4-yl)amino]hexanoyl]-sphingosine-1-phosphocholine (NBD-sphingomyelin; NBD-SM) were obtained from Avanti Polar Lipids (Birmingham, AL). Appropriate amounts of analogues (5 nmol of NBD-lipids for 10^7 cells) in chloroform/methanol (1:1) were transferred to a glass tube, dried under nitrogen and dissolved in 5 µl absolute ethanol.

To study the lipid uptake mediated by the LdMT-LdRos3 complex, *Leishmania* promastigotes in logarithmic growth phase were harvested by centrifugation (1000 x g, 10 minutes, 26°C) and washed twice with HPMI. To block the catabolism of NBD-lipids, the cell suspension (10^7 parasites/ml) was pre-incubated with 5 µM 3-(4-octadecyl)-benzoylacrylic acid (BIOMOL) and 1 mM phenylmethanesulphonylfluoride (PMSF) for 30 minutes at 26°C. Then, the parasite suspension was cooled down to 2°C and 5 µM NBD-lipids from ethanol stock were added. After 30 minutes, cells were washed twice in HPMI containing 4% (w/v) fatty acid free bovine serum albumin (FA-free BSA) to extract NBD lipids from the cell surface. Subsequently, parasites were analysed by flow cytometry.

The lipid uptake and extrusion mediated by a scramblase-like mechanism was studied by pre-treatment with the calcium ionophore ionomycin. For calcium depletion, 10^7 parasites were incubated in M199 supplemented with 50 µM BAPTA-AM (Invitrogen) for 30 minutes at 26°C, washed twice and suspended in HPMI without calcium but supplemented with 2 mM EGTA. Parasites were then incubated with or without calcium in the absence or presence of 20 µM ionomycin for 30 minutes at 26°C. In parallel, 20 mM NaN_3, 5 mM 2-deoxyglycose and 50 µM carbonyl cyanide m-chlorophenylhydrazone (CCCP) were added to deplete cells of ATP. Next, parasite suspensions (1 ml) were shifted to 4°C, labelled with NBD-lipids (final

5 µM) and incubated for 30 minutes to allow uptake of the lipid analogues. Subsequently, 1.5 ml of ice-cold FA-free BSA (0.3% w/v in HPMI) was added to 100 µl labelled parasite suspension, and incubation was continued to analyse the backward transport of NBD-lipids to the cell surface. At indicated time points, samples were subjected to flow cytometry. To facilitate the comparison of ionomycin-treated parasites with non-treated parasites, each data set was normalised to the maximum of the ionomycin-treated sample.

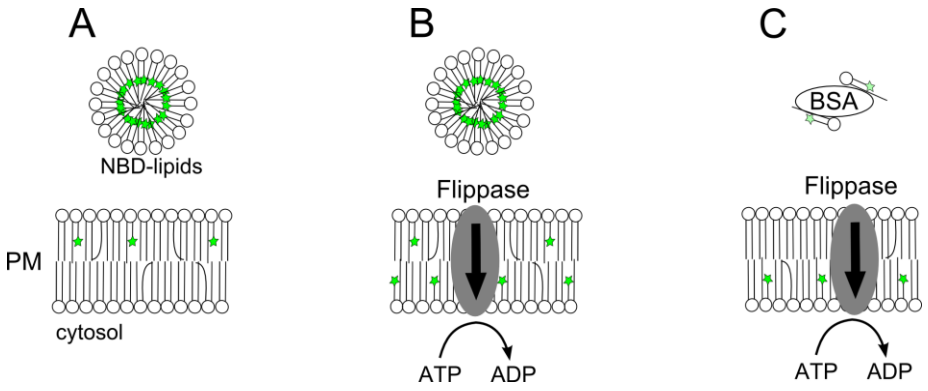

Figure 13: Schematic presentation of the BSA-back exchange assay.

Lipids with a fluorescent NBD-group attached to the C6-atom of the fatty acid chain in sn-2 position (NBD-lipids) form micelles in aqueous solutions and incorporate spontaneously into the outer leaflet of a bilayer (A). In the micelle the fluorescent groups are in close proximity, which leads to self-quenching of the fluorescent signal. Due to the increased distance between the NBD-groups upon incorporation into the membrane, an increase in the fluorescent signal can be detected. NBD-lipid analogues are translocated to the inner bilayer leaflet, when recognised as flippase substrates (B). Addition of albumin (BSA) extracts the fluorescent short chain lipid analogues from the outer membrane leaflet. Bound to BSA the quantum yield of the NBD-group is much lower than incorporated into the membrane.

5.4.9 Measurement of cytosolic Ca^{2+}

Promastigotes (10^7 cells/ml) in supplemented M-199 medium without FCS were loaded for 40 minutes with 5 µM Fluo-4/AM (from a 10 mM DMSO stock; Invitrogen) at 26°C to allow cytosolic esterases to cleave the acetomethyl (AM) ester group. After washing in supplemented M-199 medium, parasites were suspended in HPMI to a concentration of 10^7 cells/ml and stimulated with 20 µM ionomycin or left untreated at room temperature. At indicated time points, samples were analyzed by flow cytometry and fluorescence microscopy.

5.4.10 Genomics

Homology analyses were performed by using either the ClustalW2 tool provided by the European Bioinformatic Institute (EBI) website or the omniblast tool from Sanger Institute. Further editing of alignment files was performed using the BioEdit Sequence Alignment Editor published by Tom Hall [103].

Vectorial expression of GFP tagged *Leishmania* proteins was performed by using the pXG-GFP vector system kindly provided by Steven M. Beverly [104]. The GFP DNA-sequence was replaced by Maria Sanchez Cañete for the sequence of CFP or YFP to express cyan or yellow fluorescent tag proteins for the FRET screening.

Leishmania DNA was extracted by harvesting about 10^7 parasites, suspending in 1 ml DNA-zol (Invitrogen) and addition of 0.5 ml ethanol. Following centrifugation the supernatant was withdrawn, the precipitated DNA washed five times in ethanol (75%) and finally suspended in 100 µl NaOH (8 mM). To amplify *Leishmania* genes, wild-type genomic DNA was 500 times diluted and 1 µl was mixed with 1 µl of each primer (20 pmol/µl), one µl nucleotides (10mM), 46 µl buffer and 0.5 µl Phusion High-Fidelity DNA polymerase (Finzymes) according to the manufacturer's instructions manual. The polymerase chain reaction (PCR) was performed at 72°C in a MyCycler (Bio-Rad) according to the manufacturer's recommendation. PCR products were separated by electrophoresis in agarose gels (1%), exercised and purified with a gel purification Kit (Quiagen Gel Extraction Kid). Following, PCR products were either directly ligated into a Topo-vector (pGEM-T) or digested with restriction enzymes or according to the manufactuer's protocol. Ligation of digested PCR fragments with digested and dephosphorylated vectors was performed at room temperature for 2h. The ligation mix was used directly for transformation of chemo-competent *E. coli* (DH5α). Subsequently, the bacteria were plated on SD-agar plates and incubated over night at 37°C. Then, single colonies were tested by colony PCR. Right clones were cultured in liquid medium and Plasmids prepared with a purification Kit (Quiagen MiniPrep Kit). Vectors were tested again with restriction enzymes and/or sequencing.

For transformation of *L. donovani,* early log phase promastigotes were harvested, washed and suspended in electroporation buffer (10^8 parasites/ml). Next, 400 µl parasites suspension was placed into sterile electroporation cuvette, stored on ice for five minutes, supplemented by 40 µl purified vector, further cooled, and then electroporated in an Eppendorf Multiporator by using the prokaryotes program applying a pulse of 1200 V for 5 µs [105].

5.4.11 Protein analysis and immunoprecipitation

For preparation of membrane proteins, parasites were harvested, resuspended in ice-cold hypo-osmotic buffer (5 mM Tris-HCl pH 7.4) containing 1 mM PMSF, and lysed by vortexing with glass beads. The cell lysate was clarified by centrifugation at 500 x g (10 minutes, 4°C). Subcellular membranes were collected by centrifugation at 100,000 x g (1 h, 4°C) and suspended in sample buffer (750 mM 6-aminocarproic acid, 50 mM Bistris pH 7.0, 20% glycerol) to a protein concentration of 5 mg/ml. Protein concentration was measured using the bicinchoninic acid protein assay kit (BCA, Pierce Chemical Co.). Membranes were solubilised by adding 20 µl of n-dodecyl-β-D-maltopyranoside (DDM, 10%) to 100 µl of suspended membranes corresponding to a DDM/protein ratio of 4 (g/g). After incubation for 60 minutes on ice, insoluble material was removed by centrifugation (100,000 x g, 1 h, 4°C).

For Clear Native-PAGE, solubilised membrane proteins (1 mg) were loaded directly onto a 6%-15% gradient gel (6%-15% acrylamid / bisacrylamid in 50 mM Bis-Tris-HCl pH 7.0, 500 mM 6-aminocarproic acid). Electrophoresis was carried out at 4°C and 500 V for 16 h (electrophoresis buffer; 50 mM Tricine, 15 mM Bis-Tris-HCl pH 7.0, 0.05% Na-taurodeoxycholat, pH 7.0), and bovine serum albumin (monomer, 66 kDa; dimer, 132 kDa; trimer, 198 kDa; tetramer, 264 kDa) was used as molecular weight marker. Gels were scanned for GFP fluorescence using a Fuji FLA3000 phosphorimager equipped with a 473 nm argon laser and a 510 nm long-pass filter. Fluorescent bands were excised from the native gel and subjected to SDS–PAGE followed by western blot analysis.

GFP-co-immunoprecipitation assays were performed using anti-GFP microBeads (Miltenyi Biotec, Bergisch Gladbach, Germany). Per immuno-isolation, a 1ml reaction was prepared in lysis buffer containing 150 µl of anti-GFP microBeads slurry and 250 µl of detergent-solubilised protein. The suspensions were rotated gently for 30 minutes at 4°C. Beads were separated from the supernatants by means of µColumns with a µMACS separator (Miltenyi Biotec) and washed three times with lysis buffer containing 0.05% DDM. Membrane protein extracts and immuno-isolated membrane proteins were subjected to Western blot analysis. Immunoblots were probed with polyclonal antibodies raised against LdMT, LdRos3 [57], and gp63 (kindly provided by Robert McMaster). Horseradish peroxidase-conjugated secondary antibodies were obtained from Bio-Rad (Hercules, CA). Blots were developed using enhanced chemiluminescence (ECL plus Kit, GE-Healthcare). Protein mass spectrometry of the immunoprecipitates was performed as described elsewhere [106].

5.4.12 Metabolic labelling of lipids

Parasites (5 x 10^7) were inoculated in 100 ml of supplemented M-199 containing 100 µCi [^{32}P]H_3PO_4 (1mCi, Hartmann-Analytic GmbH) and grown for 48 h at 26°C. Cells were harvested by centrifugation, washed twice with PBS. Total cellular lipids were extracted by the method of Bligh and Dyer [107] and separated by two-dimensional thin layer chromatography (TLC) (I: chloroform/methanol/25% aqueous ammonium hydroxide, 90:54:7; II: chloroform/acetone/methanol/acetic acid/water, 50:20:10:10:5) using silica gel 60 coated glass plates (Merck). The ^{32}P-containing radiolabelled spots were imaged on a ^{32}P-sensitive screen and quantified on a Fuji Imaging System imager (FLA3000, Raytest, Straubenhardt, Germany). Lipids were also visualised with common lipid-locating agents such as iodine or ninhydrin.

5.4.13 Lipid analysis by ESI-MS

For lipid determination by electron spray ionisation mass spectrometry (ESI-MS) lipids were first fractionated by high performance liquid chromatography (HPLC, Agilent 1200 series) equipped with a BioBasic-4 column (C4, particle size 5 µm, 150mm x 1mm) coupled to a Finnigan LTQ Fourier transform ion cyclotron resonance mass spectrometer (Thermo Fischer Scientific). Lipid species were assigned according to their accurate masses in negative ionisation mode and their corresponding fragmentation spectra. The mass spectrometer was calibrated according to manufacturer's recommendations, and transfer optics were tuned with a lipid standard mixture containing PS (16:0/18:1), phosphatidylglycerol (PG; 16:0/18:1), phosphatidic acid (PA; 16:0/18:1), PE (16:0/18:1), PC (16:0/18:1) and cardiolipin (CL; 4x18:1) (Avanti Polar Lipids). Total lipid extracts were dried, or lipid spots from iodine stained 2D-TCL were scraped off, extracted as described above and dried. Before use, the HPLC column was rinsed with 70% Buffer B (70% acetonitril, 25% 2-propanol, 5 % H_2O, 10 mM triethylammonium acetate, 1 mM acetic acid) and 30% Buffer A (95% H_2O, 5% acetonitril; 10 mM triethylammonium acetate, 1 mM acetic acid). Dried lipids (about 0.5 mg) were dissolved in 200 µl of acetonitrile/methanol (1:1, v/v) and 4 µl were loaded to the column. The concentration of Buffer A was increased stepwise to 100%. The gradient elution used was as follows: 0-2 minutes 70% B, 2-48 minutes 70%-80% B, 48-50 minutes 80% -100 % B, 50-73 minutes 100% B, 73 - 75 minutes 100% - 70% B, 75 – 90 minutes 70% B at a flow rate of 50 µl/minutes and 40°C column temperature. Eluted fractions were directly injected to the ESI-MS and analysed in negative ion mode. The employed HPLC-MS method was adopted

from Hein et al. [108]. All solvents used were of HPLC grade (Mallinckrodt Baker, Deventer, Netherlands).

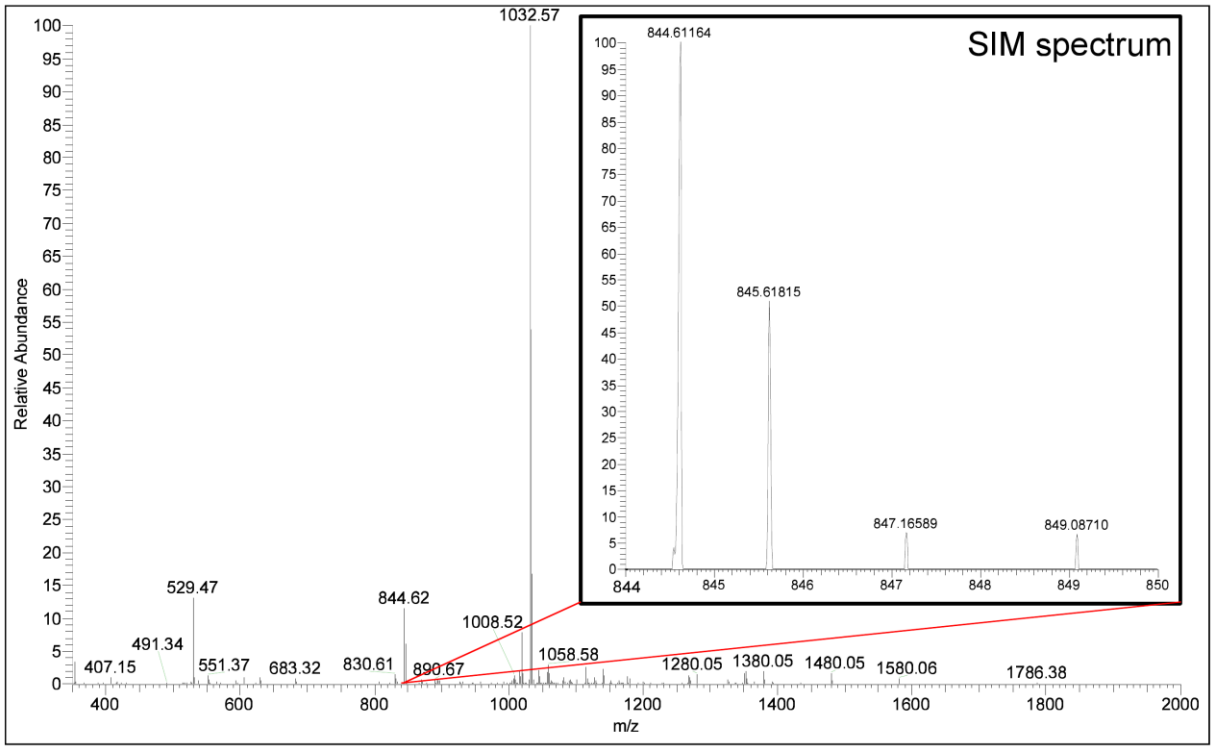

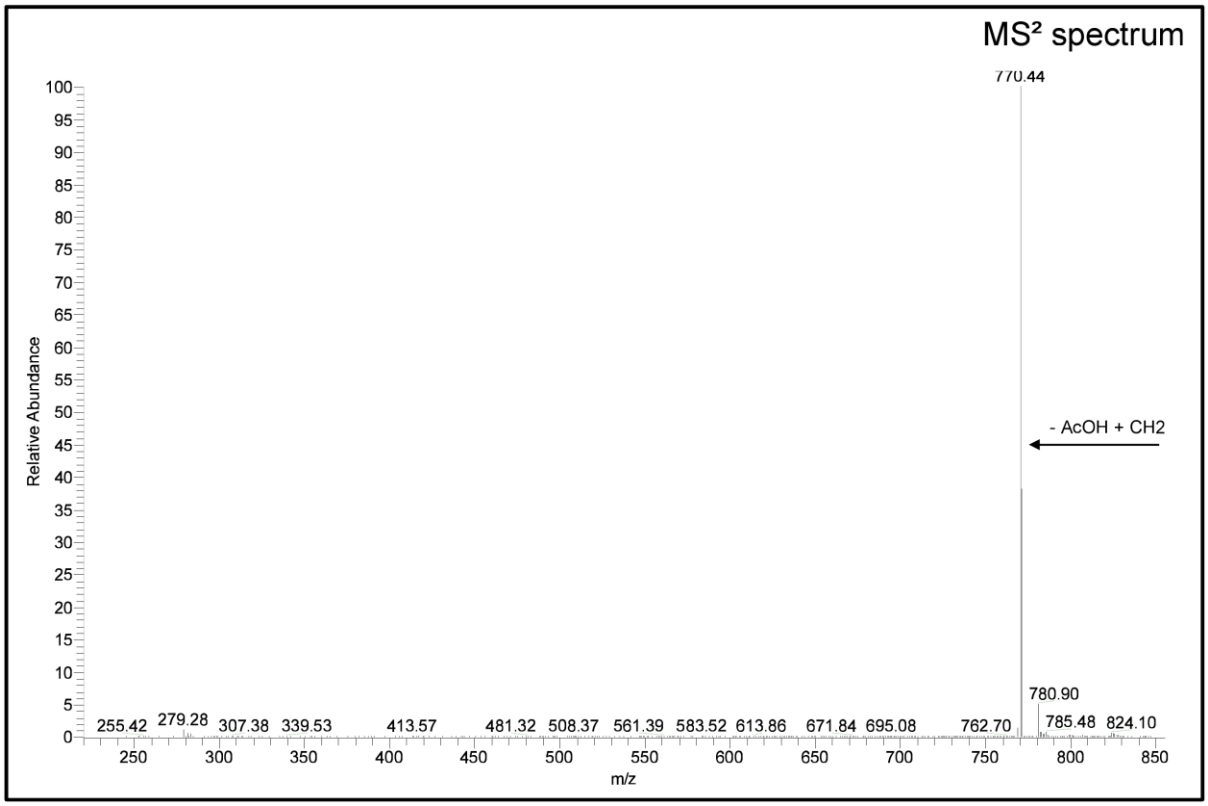

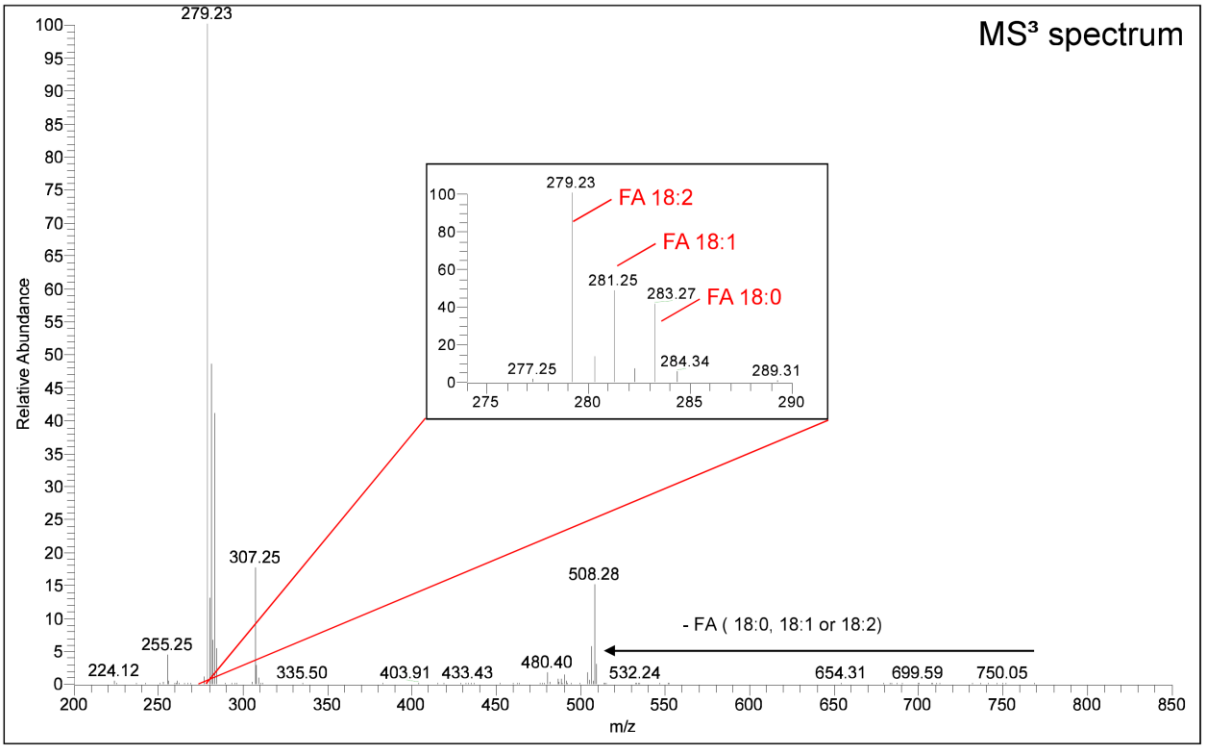

Figure 14: Example of the lipid determination by ESI-MS.

In the first diagram a panoramic spectrum of ionised lipids from *L. donovani* eluted from a 2D-TLC spot is depicted with a selected ion monitoring (SIM) inset for PC (36:2) with acetone bound (m/z: 844.6 u = 784.6 u + 60.0 u). The second diagram (MS^2 spectrum) shows the fragmentation following the first collision-induced dissociation (CID) detected in the MS^2. Here, acetone and carbene dissociated resulting in a diacyl-PC fragment of 770.4 u. The third diagram depicts the fragments detected following the second CID. The lyso-PC (m/z: 508.3 u) results from dissociation of the fatty acids (FA) in the sn2 position from the previous fragment. The inset shows a magnification of the three different FAs detected. Their masses correspond to FAs of 18 carbon atoms with none, one or two unsaturated bonds. Since the signal intensity for the double unsaturated FA is highest it belongs to the sn2 position. In conclusion, two PCs with the same mass were identified as PC (18:0,18:2) and PC (18:1,18:1), in which the first species clearly dominates, since its FA fragment is most intense and thus more abundant.

Data analysis was performed using the GP-merger, -analyser and –viewer software by Bertram Boedecker. For lipid identification, ions within the spectrum were selected (selected ion monitoring, SIM) and fragmented twice by collision-induced dissociation (CID). Absolute masses detected in the SIM and its corresponding CID spectra (MS^2 and MS^3) were analysed to identify certain lipids and their fatty acids (FA). Following the first CID lipids fragment according to their headgroup, whereas following the second CID the lipid backbone dissociates with high probability into a lyso-lipid and the fatty acid from the sn2 position. In **Figure 14** an example is given for the analysis of PC from *L. donovani*.

5.4.14 Lipid analysis by MALDI-TOF

For matrix-assisted laser desorption ion time of flight mass spectrometry (MALDI-TOF MS), dried lipid extracts were dissolved in isopropanol/acetonitrile (60/40, v/v) and mixed with a 0.5 M 2,5-dihydroxybenzoic acid (DHB) solution in methanol [109] or 10 mg/ml 9-aminoacridine solution (in isopropanol/acetonitrile (60/40, v/v)) prior to deposition onto the MALDI target.

All MALDI-TOF mass spectra were acquired on a Bruker Autoflex mass spectrometer (Bruker Daltonics, Bremen, Germany). The system utilises a pulsed nitrogen laser, emitting at 337 nm. The extraction voltage was 20 kV and gated matrix suppression was applied to prevent the saturation of the detector by matrix ions [110]. For each mass spectrum 128 single laser shots were averaged. The laser fluence was kept about 10% above threshold to obtain optimum signal-to-noise ratios. In order to enhance the spectral resolution all spectra were acquired in the reflector mode on delayed extraction conditions.

In the PSD (post source decay) experiments, the precursor ions of interest were isolated by means of a timed ion selector. The laser intensities for PSD spectra were maintained the same as in the reflector mode. The fragment ions were refocused onto the detector by stepping the voltage applied to the reflectron in appropriate increments. This can be done automatically by using the “FAST” (fragment analysis and structural TOF) subroutine of the Flex Control Program delivered by Bruker Daltonics. Further details are available in [111].

6 Results

6.1 The flipping machinery

Accumulating evidence indicate that P_4-ATPases catalyse phospholipid transfer from the exoplasmic to the cytosolic leaflet of cellular membranes. This flippase activity enables eukaryotic cells to create and maintain a non-random lipid distribution between the two leaflets. Hence, the aminophospholipids PS and PE are largely confined to the cytosolic leaflet in compartments along the endocytic and late secretory pathway, whereas sphingolipids like SM and glycosphingolipids are enriched in the exoplasmic leaflet of these organelles [112,113]. Studies aimed at identifying the molecular mechanism of miltefosine (hexadecylphosphocholine) resistance in *Leishmania* led to the identification of two membrane proteins, LdMT, a P_4-ATPase and LdRos3, a potential non-catalytic subunit of LdMT related to the Cdc50 family [56,57]. Both proteins are primarily localised to the plasma membrane and are required for intracellular uptake of alkylphosphocholine drugs and fluorescent 7-nirobenz-2-oxa-1,3-diazol-4-yl (NBD)-labelled phospholipids, suggesting a role for these proteins in controlling lipid asymmetry in the parasites plasma membrane. In this work, it is shown that LdMT forms a complex with LdRos3 which is necessary for headgroup specific transport of PE and PC across the plasma membrane. Moreover, it is demonstrated that loss of this flippase complex alters the asymmetric distribution of endogenous PE across the plasma membrane.

6.1.1 *Leishmania* LdMT and LdRos3 form a stable complex

To investigate the ability of the P_4-ATPase LdMT and the Cdc50p homologue LdRos3 to form a stable complex like their homologues e.g. in yeast, a C-terminally green fluorescent protein (GFP)-tagged version of LdRos3 was expressed in parasites lacking either LdRos3 or LdMT. The GFP-fused version of LdRos3 was functional, since it could suppress resistance of ΔLdRos3 parasites to the alkyl-phospholipid derivate miltefosine [57]. Total membrane preparations from LdRos3-GFP expressing parasites were subjected to solubilisation in the presence of mild detergent. Subsequently, the proteins were analysed by non-denaturing polyacrylamide gel electrophoresis (native-PAGE), in which complex formation between two proteins gives a new band with mobility different from that of either protein alone. Fluorimaging of the native gels identified one prominent fluorescent band of low molecular size for protein preparations obtained from ΔLdMT parasites expressing LdRos3-GFP (**Figure 15 A**). In protein samples obtained from ΔLdRos3 parasites expressing LdRos3-GFP, additional fluo-

rescent bands of reduce mobility were detected (**Figure 15 B**, bands II–III). To test for the presence of LdMT in the GFP-labelled complexes, the fluorescent bands were excised from the native gel and subjected to SDS–PAGE followed by Western blot analysis. Immunoblotting with antibodies to LdMT and LdRos3 showed that the fluorescent band of low molecular size (band I) only contained LdRos3-GFP while the more slowly migrating bands (band II-III) corresponded to a complex of LdMT and Ros3-GFP.

To corroborate that LdMT and LdRos3 form a stable complex, a C-terminally GFP-tagged version of LdMT was introduced into the ΔLdMT *Leishmania* line, and co-immunoprecipitation experiments were performed using anti-GFP-MicroBeads. Non-transfected wild-type parasites served as a control. As shown in **Figure 15 C**, the GFP antibodies efficiently precipitated GFP–LdMT and LdRos3 from detergent-solubilised membrane preparations, obtained from parasites expressing GFP–LdMT. In contrast, an unrelated integral plasma membrane protein (metalloprotease gp63) was not present in the immunoprecipitate. As a control, a parallel immunoprecipitation from an extract obtained from a wild-type strain lacking the GFP–LdMT fusion did neither precipitate LdMT nor LdRos3, indicating that the co-immunoprecipitation was specific.

Analysis of the GFP–LdMT immunoprecipitates by mass spectrometry revealed that the preparations did not contain other Cdc50 members than LdRos3 (data not shown). Taken together, these results provide direct evidence that LdMT and LdRos3 reside in a stable complex in the membrane. Since in the native PAGE no fluorescent bands corresponding to larger complexes of LdMT and LdRos3 appeared the stoichiometry of both proteins in the complex must be one.

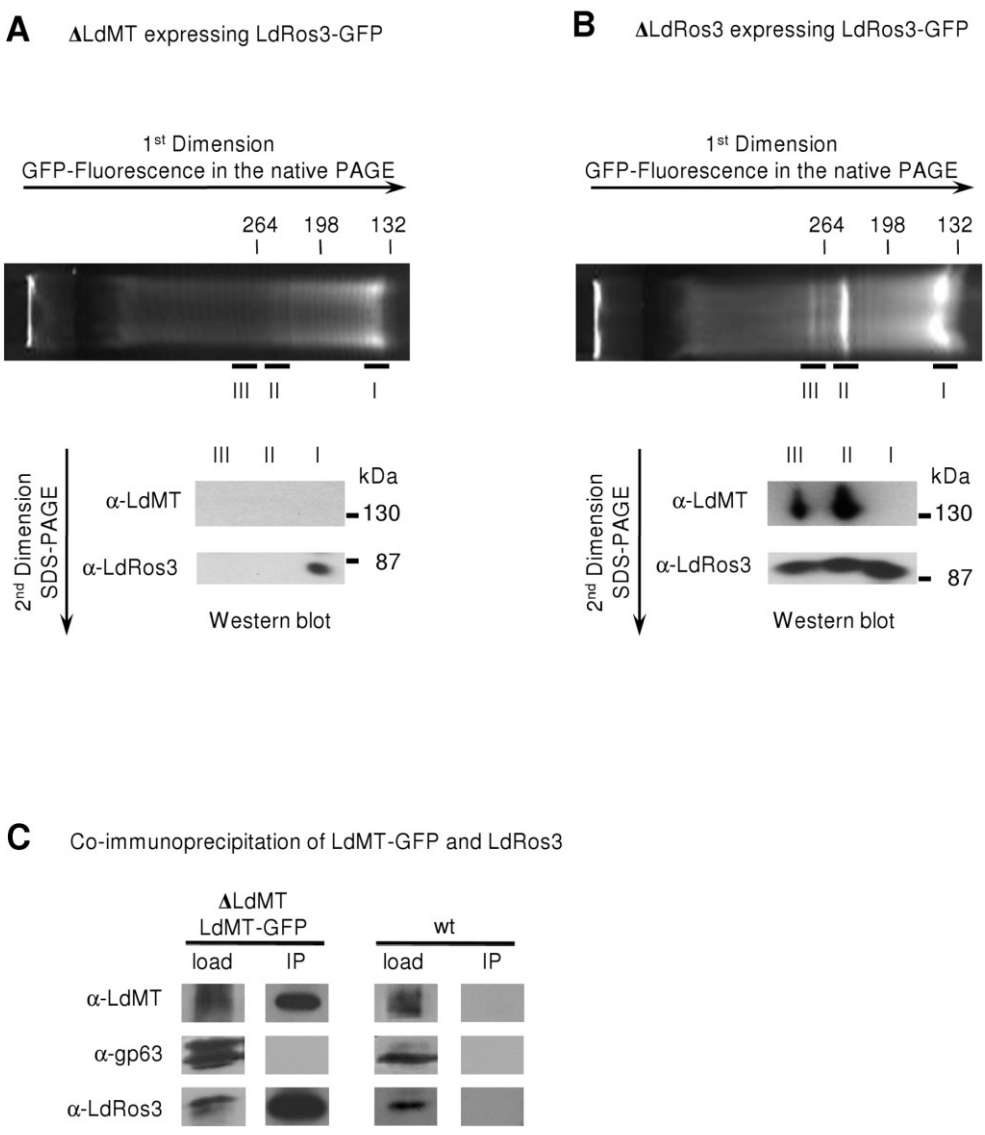

Figure 15: LdMT and LdRos3 form a stable complex in the *Leishmania* membrane.

(A, B) Native- and SDS-PAGE analysis of LdMT and LdRos3-GFP. LdRos3-GFP was expressed in ΔLdMT parasites (A) and in ΔLdRos3 parasites (B). Solubilised membrane proteins were separated by native PAGE and analyzed for GFP fluorescence. The membrane extract obtained from ΔLdRos3 parasites contained a prominent fast-migrating fluorescent band (band I). In addition to band I, the membrane protein extract derived from ΔLdMT parasites also contains slow-migrating fluorescent protein bands (band II and III). Regions of the gel corresponding to the fluorescent bands were excised and loaded onto SDS-PAGE gels, subsequently analysed by immunoblotting using polyclonal antibodies against LdRos3 (α-LdRos3) and LdMT (α-LdMT). Size markers indicate relative mobility of proteins in kDa. (C) Immunoblots from co-immunoprecipitation assays. LdMT-GFP was immunoprecipitated from a detergent-solubilised membrane fraction (load) obtained from ΔLdMT parasites expressing LdMT-GFP as well as non-transfected wild-type parasites (wt) using anti-GFP-MicroBeads. Immunoprecipitates (IP) were subjected to immunoblot analysis using antibodies recognising LdMT (α-LdMT), LdRos3 (α-LdRos3) and metalloprotease gp63 (α-gp63).

6.1.2 *In vivo* FRET analysis of the LdMT/LdRos3 complex formation

In order to investigate the interaction of all *Leishmania* P_4-ATPase family members with their potential CDC50 protein binding partners *in vivo*, a vector-based Förster Resonance Energy Transfer (FRET) screening system was establish in collaboration with the laboratory of Francisco Gamaro Conde. CFP and YFP fusion proteins of all proteins of interest were cloned into *Leishmania* expression vectors (Maria Sánches Cañete, Institute of Parsitology and Biomedicine 'Lopez Neyra', Spain). Our previous *in vitro* studies described in chapter 6.1.1 revealed that the C-terminally fused GFP-tag did not interfere with P_4-ATPase/Cdc50 protein complex formation. Hence, we decided to create C-terminally tagged CFP and YFP fusion proteins for the FRET analysis as well.

Initial attempts to detect FRET signals in a *Leishmania donovani* wild-type strain expressing P_4-ATPase-CFP and CDC50 protein-YFP variants, failed. While LdRos3-YFP co-expressed with LdMT-CFP stained intracellular membranes, the fluorescence derived from the CFP-tagged P_4-ATPase appeared diffuse (**Figure 17 A**). Similar results were obtained for the CFP-marked *Leishmania* P_4-ATPase AP2 when co-expressed with any of the three YFP-tagged *Leishmania* CDC50 homologues, LdRos1, LdRos2 and LdRos3 (**Figure 18**). Since a double knockout line of *Leishmania* lacking both, LdMT and LdRos3, was unavailable, preferred complex formation between fusion proteins and endogenous P_4-ATPases or CDC50 proteins might have occurred in the wild-type parasites preventing a FRET signal. To exclude binding to endogenous interaction partners, fusion proteins were expressed in a yeast cell line lacking all plasma membrane flippases (Dnf1p, Dnf2p) and the CDC50 homologue Ros3p. Here, LdRos3-YFP stained membranes in close proximity to the yeast plasma membrane, while LdMT-CFP stained ER and perinuclear membranes (**Figure 17 B**). The weak signal detected in the YFP channel while exciting CFP did not vanish after acceptor bleaching, which in addition was not accompanied by an increase in the signal intensity for the FRET donor (CFP, **Figure 17 C**). Concluding that double tagging of *Leishmania* P_4-ATPases and their possible partners from the CDC50 protein family with rather bulky fluorescent proteins at the C-terminus hinders their interaction. Due to the immense expenditure of time for cloning different constructs to visualise the interaction of LdMT with LdRos3 as well as other members of either family *in vivo* this approach was stopped at this stage.

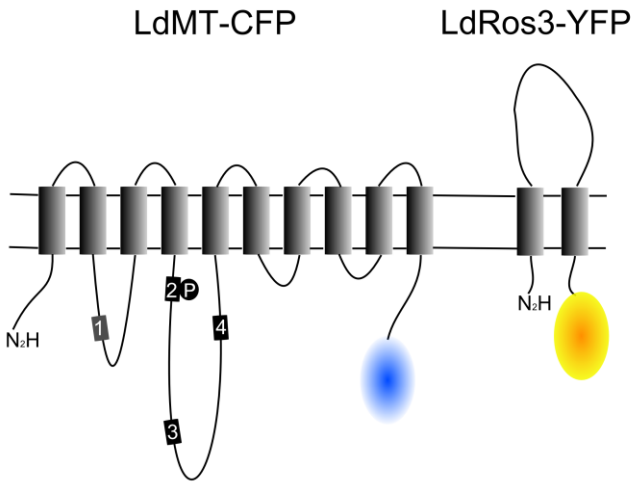

Figure 16: Scheme of the CFP and YFP tagged P_4-ATPase and Cdc50 protein, respectively.

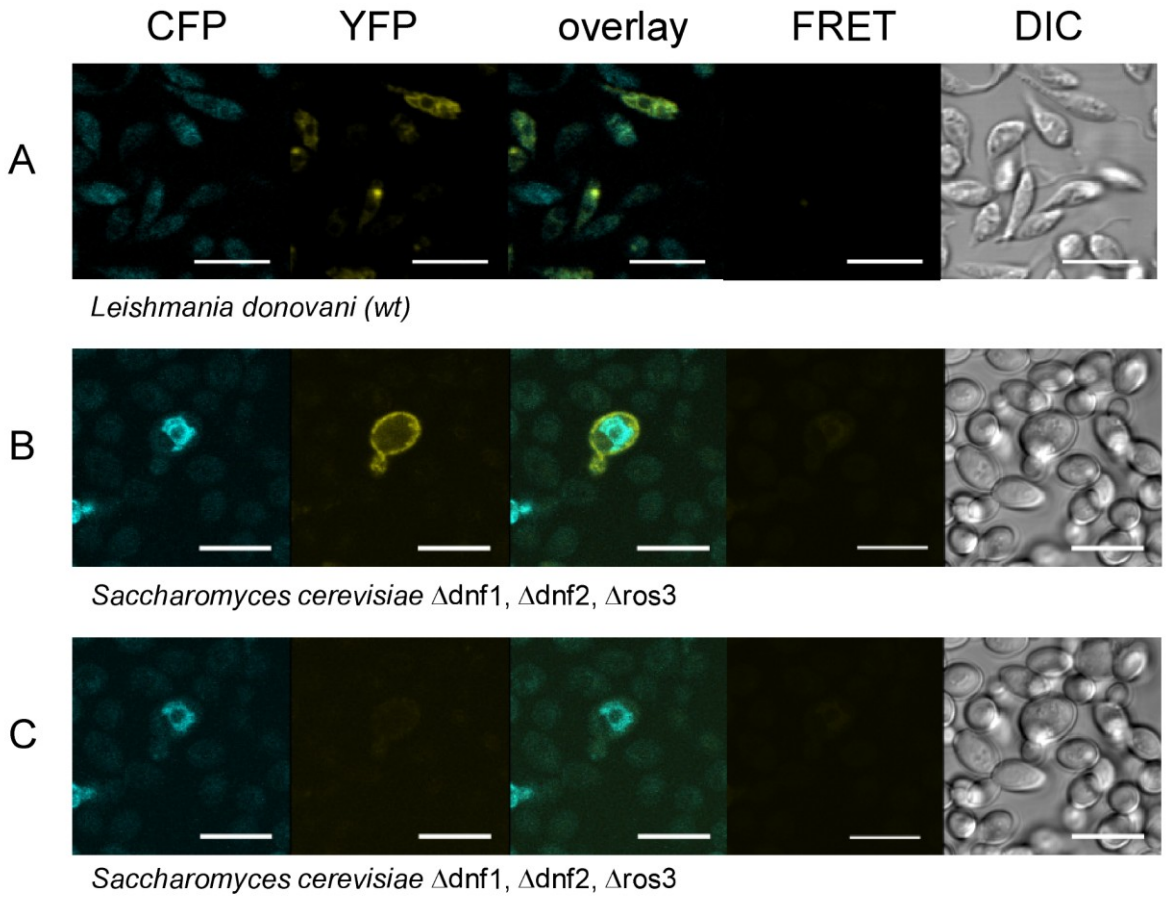

Figure 17: FRET analysis of the LdMT/LdRos3 complex.

Microscopic images of *L. donovani* (A) and *S. cerevisiae* (B and C) co-expressing LdMT-CFP and LdRos3-YFP are depicted. From left to right fluorescence images of CFP and YFP, the overlay of both, Förster resonance energy transfer (FRET) and the differential interference contrast (DIC) pictures are shown. (C) The same sector as displayed in B is depicted following photo bleaching of YFP. Bar, 10µm.

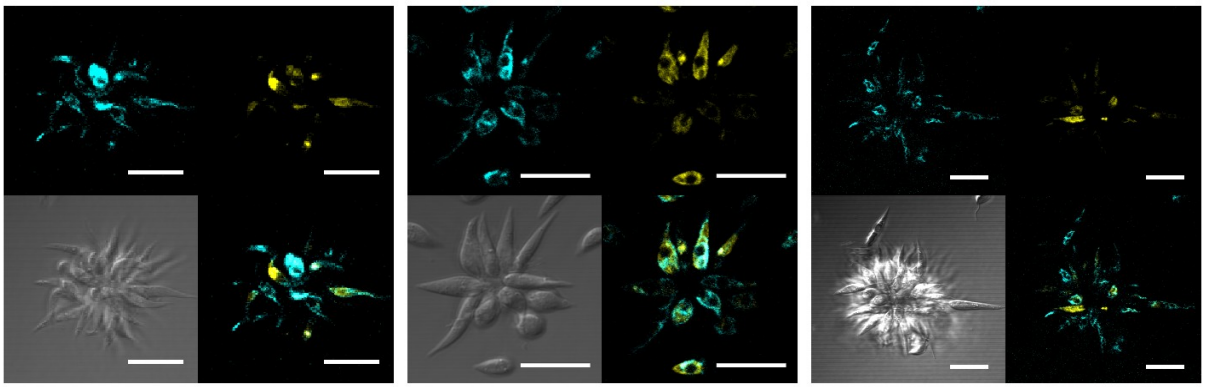

Figure 18: Co-expression of AP2-CFP with LdRos1-YFP (left), LdRos2-YFP (middle) or LdRos3-YFP (right) in *L. donovani* wild-type.

In each set, the CFP- (upper left) and the YFP-fluorescence (upper right) as well as, the overlay of both fluorescence pictures (lower right) and the dichroic interference contrast picture (lower left) is depicted. Bar, 10µm.

6.1.3 LdMT and LdRos3 are required for the ATP-dependent inward translocation of NBD-PC and -PE

To characterise the lipid transport activity of the LdMT/LdRos3 complex in the plasma membrane the uptake of NBD-lipids was examined in wild-type, ΔLdMT and ΔLdRos3 parasites by flow cytometry and by fluorescence microscopy. Experiments were performed at 2°C to suppress endocytosis, lipid flop mediated by ABC-transporters and degradation of the NBD-lipids (consistently <10%, **Figure 29**). Under these conditions wild-type parasites efficiently internalised NBD-PC and NBD-PE, while NBD-PS and NBD-sphingomyelin (NBD-SM) were hardly taken up at all. The efficient uptake of NBD-PC and NBD-PE was significantly inhibited in ATP-depleted parasites pre-treated with sodium azide and 2-deoxyglucose or the protonophore carbonyl cyanide m-chlorophenylhydrazone (CCCP) dissipating the proton electrochemical gradient (**Figure 19 A**). Consistent with these results, fluorescence microscopy of wild-type parasites labelled with NBD-lipids and washed with BSA-containing buffer revealed an intensive labelling of intracellular membranes with NBD-PC and -PE but not with NBD-PS and -SM (**Figure 19 D**). In contrast to wild-type parasites, ΔLdMT and ΔLdRos3 parasites were found defective in NBD-PC and NBD-PE uptake at low temperature (**Figure 19 B**). These defects were solely due to the loss of LdMT and LdRos3, as lipid uptake was restored by re-expression of LdMT-GFP and LdRos3-GFP in ΔLdMT and ΔLdRos3 mutants, respectively (**Figure 19 C**). In summary, the LdMT-LdRos3 complex is essential to sustain an energy-dependent influx of NBD-PC and -PE across the parasite plasma membrane.

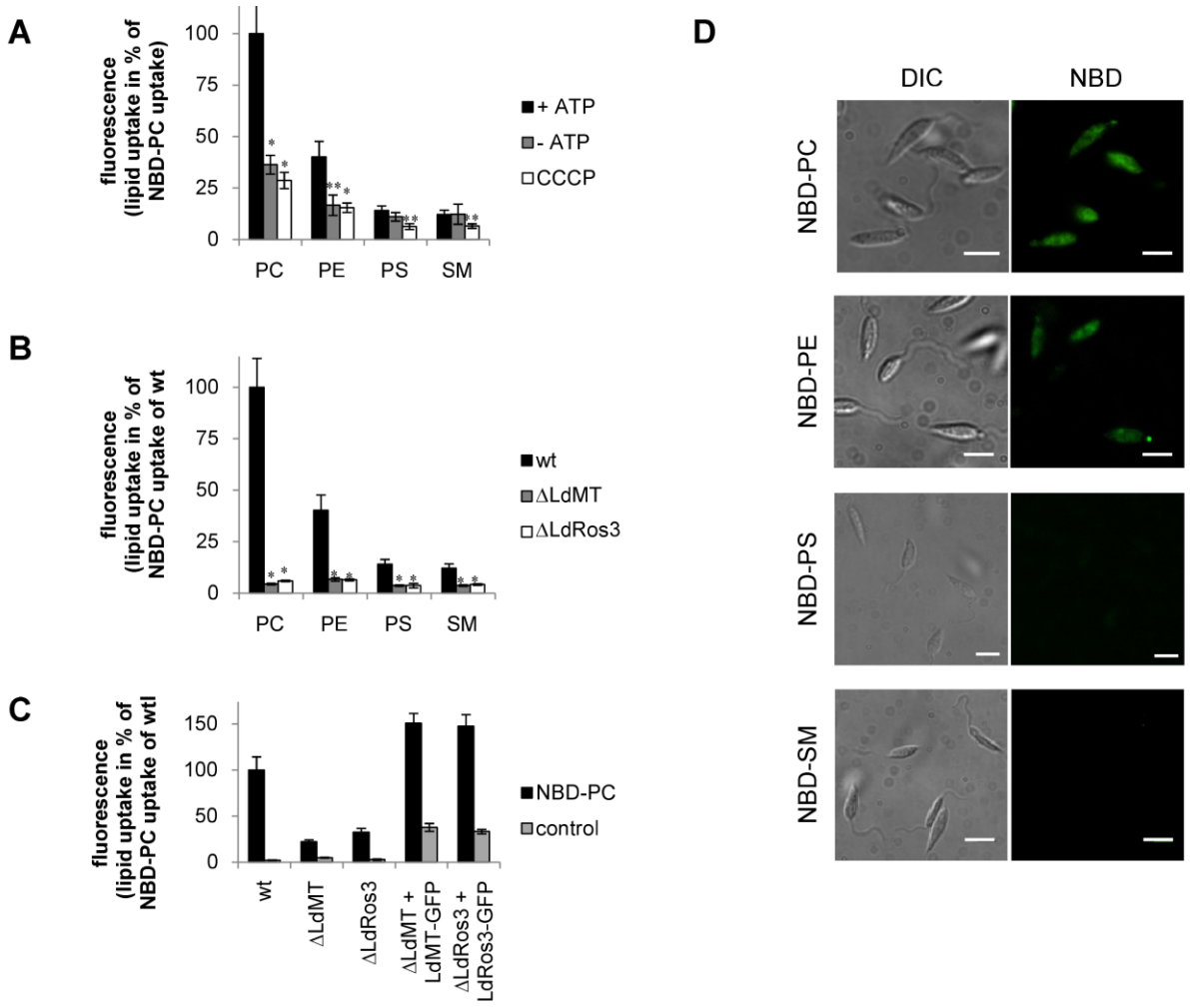

Figure 19: Inward translocation of NBD-PC and NBD-PE across the plasma membrane of *Leishmania* requires LdMT and LdRos3.

Promastigotes of wild-type (wt), ΔLdMT and ΔLdRos3 lines were labelled with NBD-lipids for 30 minutes at 2°C and than washed with BSA and analysed by flow cytometry (A-C) or visualised by fluorescence microscopy (D). ATP depletion was achieved by preincubation with 5 mM 2-deoxyglucose and 20 mM sodium azide. To abolish the proton electrochemical gradient, promastigotes were treated with 50 µM of the protonophore CCCP. As a control LdMT-GFP and LdRos3-GFP on episomal *Leishmania* expression vectors were reintroduced in ΔLdMT and ΔLdRos3 mutants, respectively; control, non-labelled cells showing the intrinsic fluorescence of the GFP fusion proteins. Data are normalised to NBD-PC internalisation of wild-type parasites; 100% corresponds to 468 ± 96 a.u. NBD-PC. Data represent the means ± SE of at least three independent experiments. For statistical analysis Welch´s test was performed. Significant differences in the lipid uptake of the mutants compared to the wild-type are denoted by asterisks (** p=0.05; * p=0.01).

6.1.4 LdMT and LdRos3 sustain plasma membrane PE asymmetry in *Leishmania donovani*

To test whether the LdMT/LdRos3 complex is required for maintenance of the tight asymmetric distribution of aminophospholipids at the plasma membrane, promastigote stages of *Leishmania* wild-type, ΔLdMT and ΔLdRos3 lines were incubated with different concentrations of duramycin and papuamide B. These cytolytic peptides require binding to cell surface-exposed PE (duramycin) and PS (papuamide B), respectively, to exert their cytotoxicity [114]. As shown in **Figure 20 A**, both cell lines, ΔLdMT and ΔLdRos3 were more sensitive to duramycin-induced cytolysis as compared to the wild-type line with an EC_{50} for duramycin which was approximately 1.8-fold lower than that for wild-type cells. Restoration of LdMT and LdRos3 expression returned the duramycin sensitivity profile back to the wild-type pattern (Figure 3A). To visualise more directly that deletion of LdMT or LdRos3 affects the lipid asymmetry in the plasma membrane, the exposure of PE was analysed by labelling with biotinylated Ro09-0198, a peptide that specifically binds to PE [115,116]. As shown in **Figure 20 B**, both, the ΔLdMT and the ΔLdRos3 *Leishmania* lines, bound more PE-sensing biotinylated Ro09-0198 peptide visualised by streptavidin-FITC than the wild-type cell line. For a quantitative assessment of Ro09-0198 peptide binding, the FITC fluorescence associated with mutant and wild-type cells was measured by flow cytometry. As shown in **Figure 20 B**, deletion of LdMT or LdRos3 caused a 10-fold increase in Ro09-0198 peptide/streptavidin-FITC binding compared to wild-type parasites. With respect to the sensitivity to papuamide B (**Figure 20 A**) and to the binding of annexin V-FITC (**Figure 20 B**) no significant difference between viable parasites of ΔLdMT and ΔLdRos3 *Leishmania* lines as compared to wild-type cells was observed. This result is in line with NBD-PS uptake studies described above what indicates that NBD-PS represents a minor substrate of the LdMT/LdRos3 complex. Moreover, wild-type and mutant parasites were screened for sensitivity to amphotericin B, a polyene macrolide antibiotic that binds to membrane ergosterol and induces cellular leakage [117]. Again, no difference between the mutant and the wild-type *L. donovani* cell lines could be observed, indicating that the deletion of LdMT or LdRos3 does not affect plasma membrane ergosterol levels.

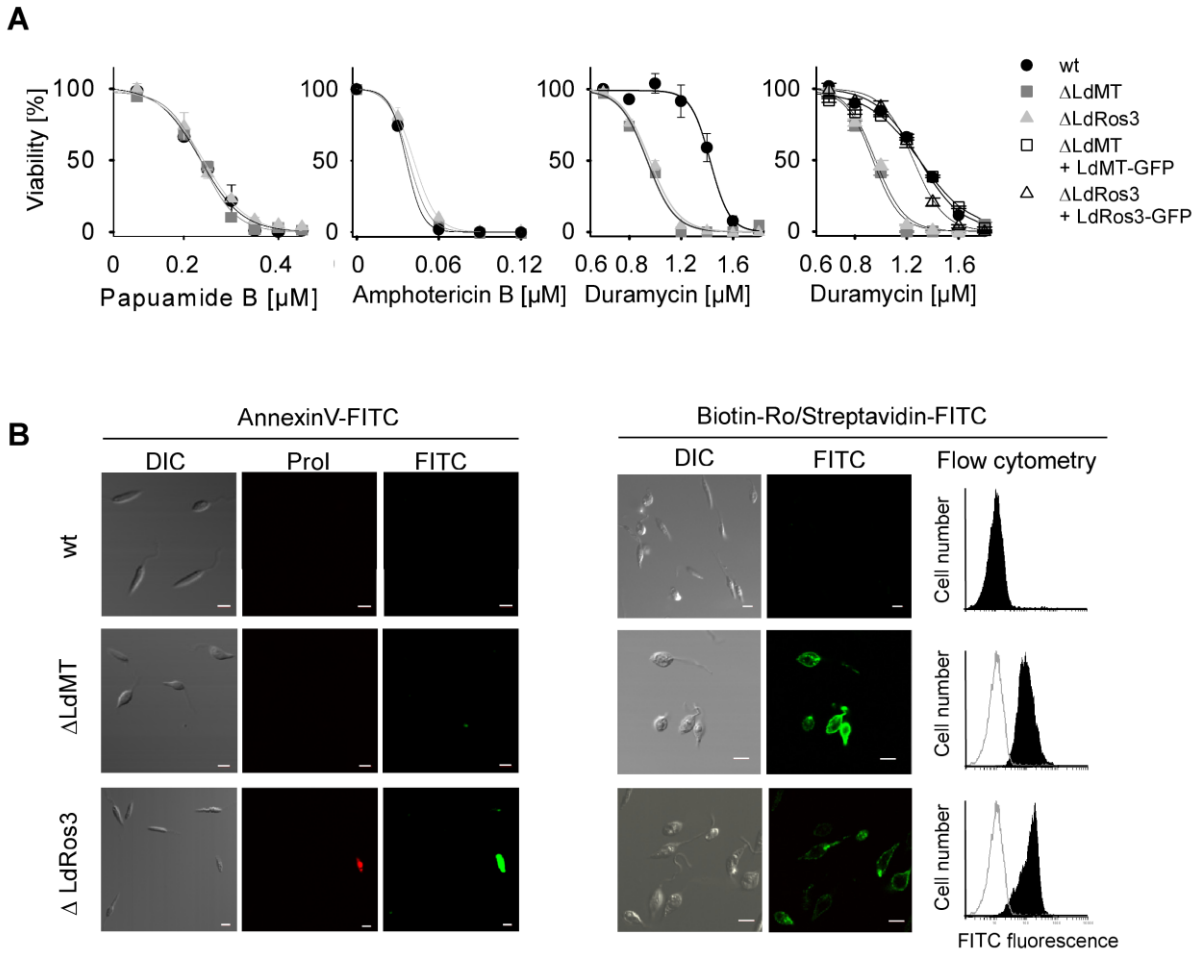

Figure 20: LdMT and LdRos3 are required to sustain plasma membrane PE asymmetry in *Leishmania*.

(A) Sensitivity of wild-type (wt), ΔLdMT and ΔLdRos3 *L. donovani* parasites to the PE-binding peptide duramycin, the PS-binding peptide papuamide B, and the sterol-binding amphotericin B. Parasites were diluted to 0.25 x 10^6 cells/ml in medium containing duramycin, papuamide B or amphotericin B at the indicated concentrations. After 72 h viability was analysed as described in the 'Material and Methods'. As a control LdMT-GFP and LdRos3-GFP on episomal *Leishmania* expression vectors were reintroduced in ΔLdMT and ΔLdRos3 mutants, respectively. Means ± S.E. of at least three independent experiments are shown as percentage of untreated control parasites. (B) Endogenous PS and PE at the exoplasmic leaflet of the plasma membrane of these strains was visualised by annexin V-FITC and Biotin-Ro/Streptavidin-FITC binding, respectively. Cells were analyzed by phase contrast (DIC) and fluorescence microscopy for propidium iodide (PrpI) and FITC. Bar, 10 µm. Fluorescence intensity histograms were obtained by flow cytometry as described under "Materials and Methods." WILD-TYPE cells incubated in with biotinylated Ro09-0198 peptide and Steptavidin-FITC served as controls (dashed line).

To rule out the possibility that the observed differences in PE exposure resulted from substantial increase in the PE level of endogenous lipid in the ΔLdMT and the ΔLdRos3 lines as

compared to wild-type parasites, the total phospholipid composition of *Leishmania* parasites labelled to steady state with ^{32}P-phosphate was analysed. Four major phospholipids could be

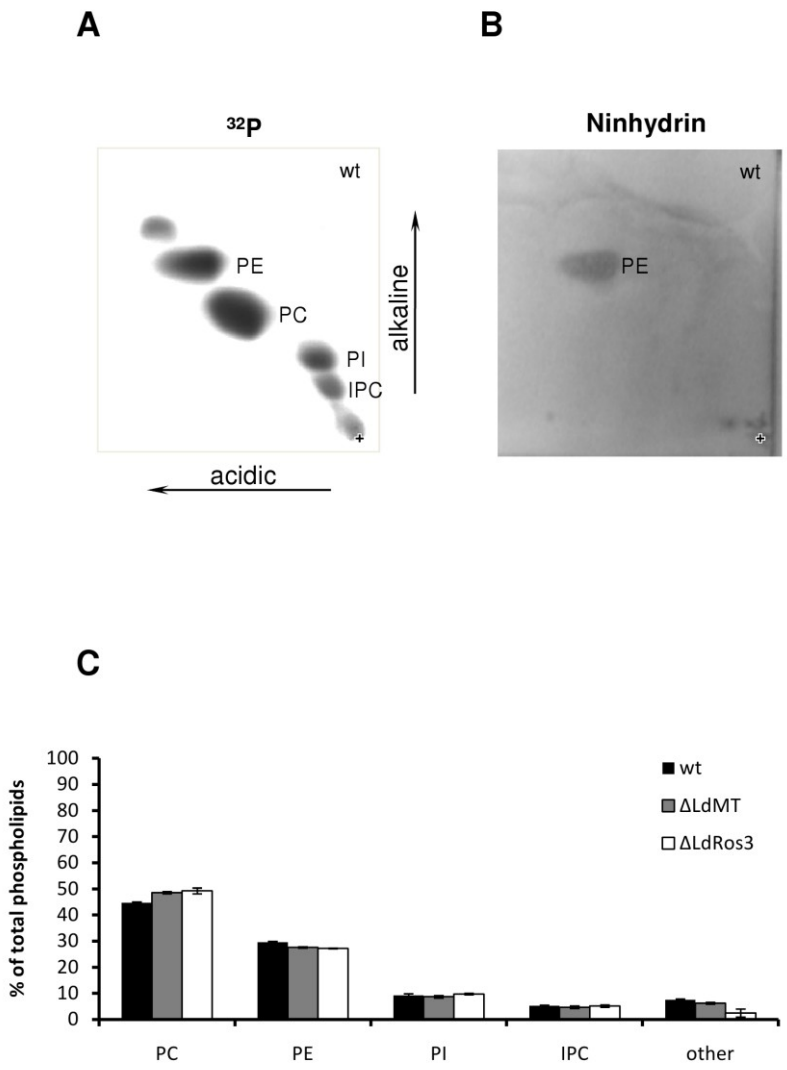

Figure 21: Total phospholipid composition of wild-type, ΔLdMT and ΔLdRos3 *L. donovani* parasites.

Promastigote stages of wild-type (wt), ΔLdMT and ΔLdRos3 lines were labelled for 48 h with 32P-phosphate. Lipids were extracted, separated by two-dimensional thin layer chromatography, and then visualised by phosphorimager scanning (A) or ninhydrin staining (B). Representative two-dimensional TLC plates are shown. The location of individual species was verified by ESI-MS. Unidentified lipids are not marked. In (C) the quantification of phospholipids in wild-type, ΔLdMT and ΔLdRos3 parasites is shown. Data are expressed as the percentage of total phospholipids and represent the means ± S.E. of three independent experiments. PC, phosphatidylcholine; PE, phosphatidylethanolamine; PI, phosphatidylinositol; IPC, inositol phosphorylceramide.

identified, showing comparable levels in all strains tested: PC (44%-49%), PE (27%-29%), phosphatidylinositol (PI, 9%) and Inositolphosphorylceramide (IPC, 4-5%), see **Figure 21 A**. Thus, the possibility that increased cell surface exposure of PE (**Figure 21 B**) was caused by

increased PE synthesis can be ruled out. Notably, no significant levels of PS could be detected by this method. Likewise, lipid analysis by HPLC-coupled ESI-MS did not reveal the presence of PS, suggesting that *L. donovani* does, if at all, synthesise very low amounts of this phospholipid (**Figure 21 C**). The presence of only very low amounts of PS explains the equal sensitivity of the parasite lines to papuamide B and the lack of annexin V-FITC binding on intact parasites (**Figure 20 A**).

6.1.5 Phagocytosis of ΔLdMT and ΔLdRos3 *Leishmania* lines by THP-1-derived macrophages is unaltered

Judged by annexin V-binding, PS exposure on the exoplasmic leaflet of the *Leishmania* plasma membrane has been shown to be important for entry of the parasite into host cells [118,119,120]. The availability of two *Leishmania* lines displaying an altered plasma membrane lipid asymmetry and the apparent lack of PS provided an opportunity to test whether other phospholipids are relevant for the recognition of *Leishmania* parasites by macrophages using the human monocytic cell line THP-1. THP-1 cells share many characteristics with human monocytes including morphology, surface-membrane receptor presentation as well as the capacity to undergo maturational changes when induced with phorbol esters [121,122]. Parasites and THP-1-derived macrophages were pre-labelled with CellTrackerTM Green and CellTrackerTM Dil, respectively, and co-incubated at a ratio of 1:10 (cells : parasites). Sixteen hours after the infection, 30 to 70% of the THP-1-derived macrophages were found to be infected. At this moment the number of intracellular parasites per infected macrophage ranged from 1 to 19 (**Figure 22 A**). The mean numbers of intracellular parasites per infected cell were similar: 2.6 for wild-type, 2.5 for ΔLdMT and 2.7 for ΔLdRos3 parasites. The total numbers of THP-1-derived macrophages infected by ΔLdMT and ΔLdRos3 parasites were not markedly different from that of wild-type parasites (**Figure 22 B**) indicating that at least in this infection model system changes in the plasma membrane PE arrangement of *Leishmania* parasites do not affect specific recognition and removal of the parasites by macrophages.

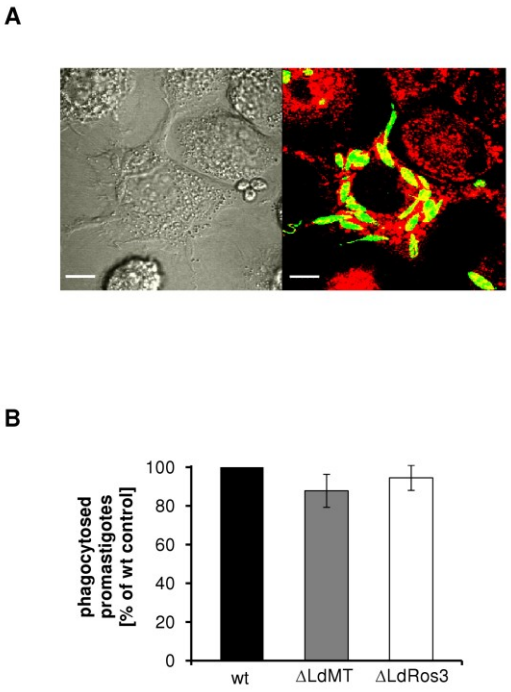

Figure 22: Phagocytosis of ΔLdMT and ΔLdRos3 parasites by THP-1-derived macrophages is unchanged.

CellTrackerTM Green-labelled parasites were added (10:1) to THP-1-derived macrophages pre-labelled with CellTrackerTM Dil (red) and co-incubated for 16 h at 37°C. (A) Micrograph of double-fluorescence labelling of THP-1-derived macrophages phagocytosing *Leishmania* parasites. Bar, 10 µm. (B) Percentage of phagocytosing THP-1-derived macrophages was determined by flow cytometry. Values are means ± SD of three independent experiments expressed as percentage of control (number of phagocytosed wild-type parasites by TPH-1-derived macrophages). The population of phagocytosing THP-1-derived macrophages ranged from 30 to 70% in control cultures.

6.2 Scramblase activity

Under physiological conditions eukaryotic cells lose their plasma membrane lipid asymmetry during apoptosis. This process, called scrambling, is characterised by energy-independent lipid flip-flop, while the barrier function of the plasma membrane is unaffected. Similarly, the loss of plasma membrane lipid asymmetry can be provoked by increased intracellular calcium levels. Although stimulated through different routes the same scrambling mechanism seems to be activated [87]. In the following, activation of lipid scrambling by increased cytosolic calcium concentration induced by the calcium selective ionophore ionomycin was studied.

6.2.1 Ionomycin elicits intracellular Ca^{2+} in *Leishmania donovani*

Ionomycin treatment of mammalian cells was shown to rapidly elicit intracellular calcium levels, followed by lipid scrambling in the mammalian plasma membrane [98,123,124,125]. To confirm that under our experimental conditions treatment with ionomycin also triggers elevation of intracellular Ca^{2+} levels in *Leishmania*, promastigotes were loaded with the cytosolic Ca^{2+} probe, Fluo-4/AM, and alterations in Ca^{2+} levels were assessed by confocal microscopy and flow cytometry. Addition of 20 µM ionomycin provoked a rapid and sustained increase in Fluo-4/AM signals, which was induced simultaneously in all parasites under investigation (**Figure 23 A**). Flow cytometric analysis revealed that the Fluo-4/AM signals in ionomycin-stimulated parasites were 20 to 50-fold higher as compared with untreated control cells (**Figure 23 B**). Furthermore, the majority of cells did not show significantly increased propidium iodide fluorescence indicating that the cell membrane integrity was not affected by the addition of ionomycin. Notably, ionomycin-induced elevation of intracellular Ca^{2+} levels was biphasic consisting of a rapid initial elevation within 5 minutes after ionomycin treatment followed by a sustained elevation. Upon removal of external Ca^{2+} by 3 mM EGTA, the fast initial increase in Fluo-4/AM fluorescence in response to ionomycin addition could not be observed. However, the slower sustained elevation in cytosolic Ca^{2+} remained suggesting that the normal response consists both of Ca^{2+} influx and of Ca^{2+} release from intracellular compartments.

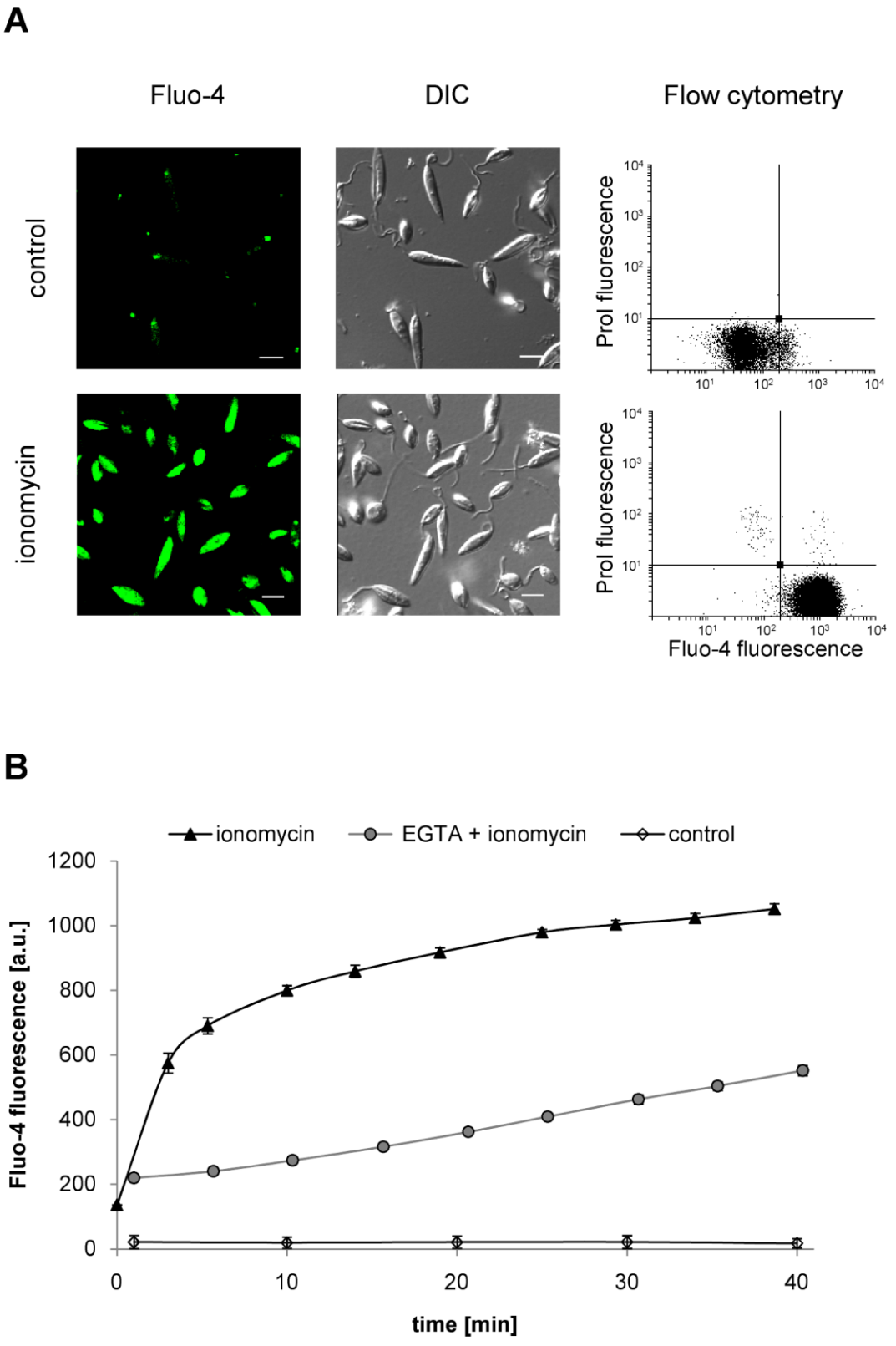

Figure 23: Cytosolic Ca^{2+} elevation in *Leishmania* promastigotes upon ionomycin treatment.

(A) Parasites were loaded with Fluo-4/AM, left untreated (control) or treated with 20 µM ionomycin at 25°C for 30 minutes and subsequently analyzed by confocal fluorescence microscopy or flow cytometry. Bar, 10 µm. (B)

Fluo-4/AM geo-mean fluorescence intensity was monitored at different time intervals by flow cytometry with and without addition of ionomycin. Removal of external Ca^{2+} using 3 mM EGTA reduced the increase in Fluo-4/AM signals in response to ionomycin. Results of three independent experiments are shown as mean ± SEM. Cells with impaired membrane integrity were excluded by propidium iodide (ProI) staining.

6.2.2 Stimulation of PE exposure by ionomycin

Next it was tested whether stimulation of parasites with ionomycin in the presence of calcium ions triggers lipid redistribution and loss of lipid asymmetry at the plasma membrane. PE in the outer leaflet of the plasma membrane can be probed in living cells with biotinylated Ro09-0198, a peptide that specifically binds to PE [126]. When parasites stimulated with ionomycin in the presence of calcium were incubated with biotinylated Ro09-0198 and stained with Streptavidin-FITC, their plasma membranes and flagellar pockets became highly fluorescent (**Figure 24**). The staining with Streptavidin-FITC was dependent on incubation with biotinylated Ro09-0198 (**Figure 24**, control). In contrast to the intense fluorescence of ionomycin-treated parasites, untreated promastigotes did not display any FITC labelling and thus binding of biotinylated Ro09-0198 peptide (**Figure 20**). These results indicate that PE usually resides in the inner leaflet of the plasma membrane and becomes exposed on the parasite surface upon ionomycin treatment.

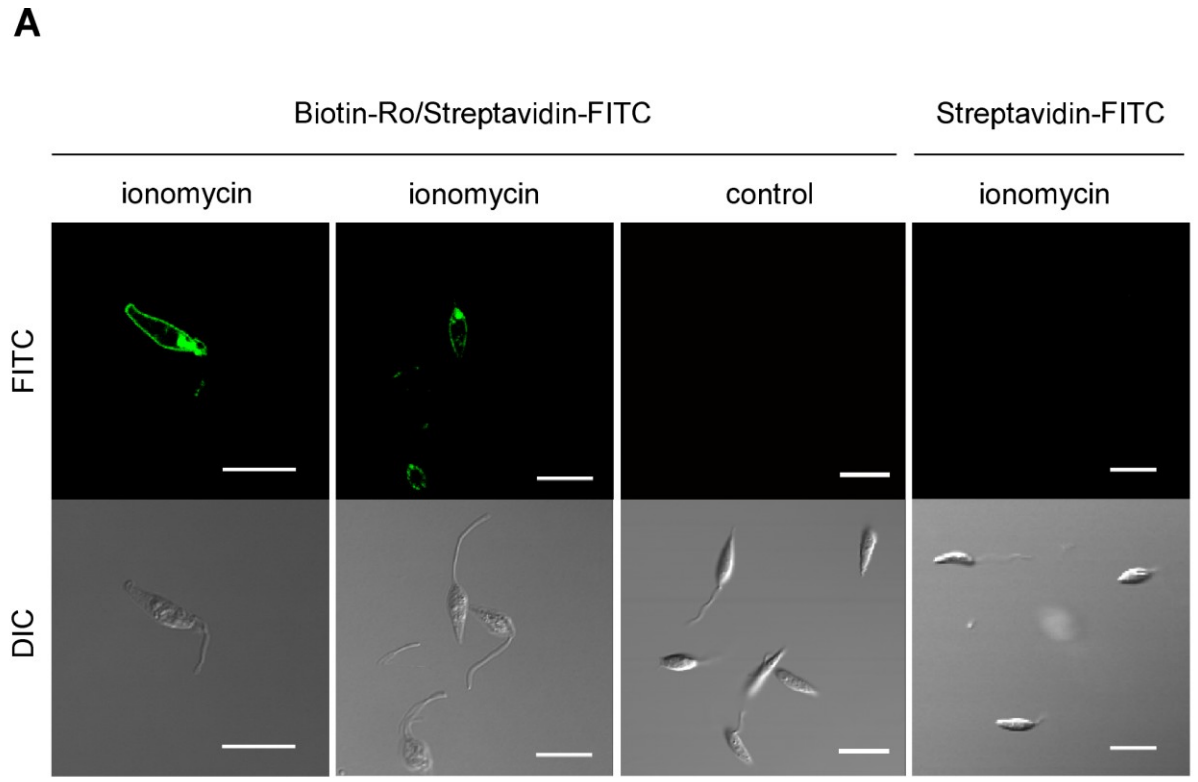

Figure 24: Surface-exposed PE in *L. donovani* promastigotes upon ionomycin treatment.

In the presence of 2mM Ca^{2+}, parasites were stimulated with (ionomycin) or without (control) ionomycin and incubated with (Bio-Ro) or without biotinylated Ro-peptide. Binding of Bio-Ro was visualised by Streptavidin-FITC.

Exposure of PS on the outer plasma membrane leaflet was tested by measuring the binding of annexin V to the cell surface. Annexin V is a lipid binding protein which preferentially interacts with membranes containing negatively charged lipids like PS in the presence of calcium [127]. Specific recognition of PS depends on the calcium concentration, which should not exceed 3 mM. Higher Ca^{2+} levels lead to unspecific binding e.g. to PC [128]. In this work binding of annexin V-FITC in the presence of 2.5 mM Ca^{2+} to propidium iodide-negative *Leishmania* promastigotes could be detected neither for untreated nor for ionophore-stimulated parasites. To probe the capability of ionomycin to induce PS-scrambling detectable with annexin V-FITC, the human monocyte cell line THP-1 was treated identically to the promastigotes (**Figure 25**).

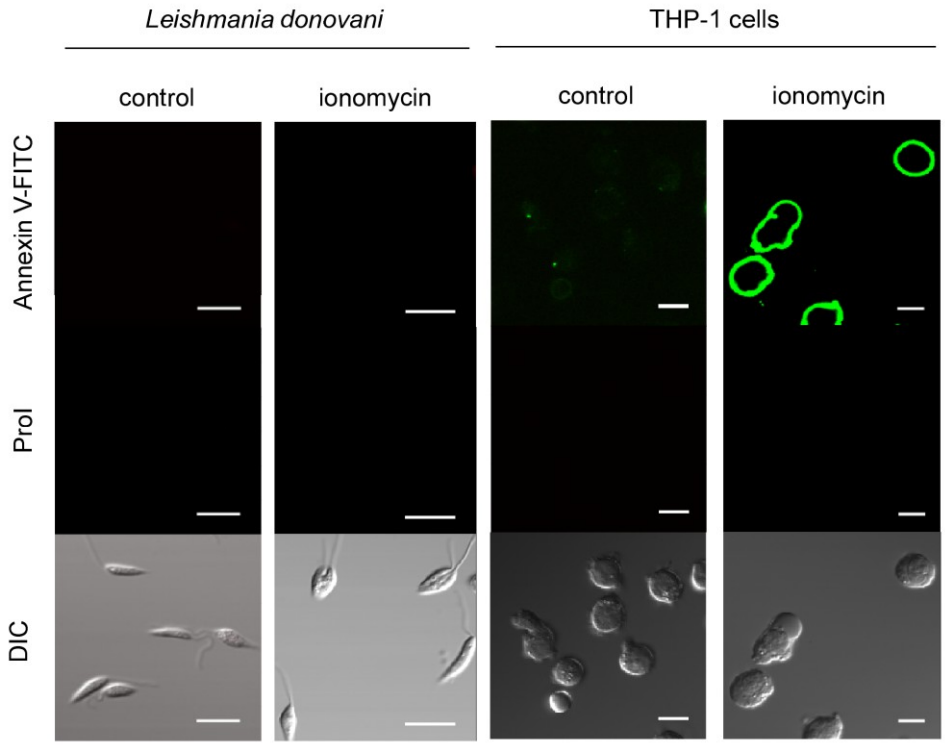

Figure 25: Viable *Leishmania* promastigotes do not bind annexin V-FITC following stimulation with ionomycin.

L. donovani promastigotes and THP-1 cells were treated with ionomycin (ionomycin) or left untreated (control) and incubated with propidium iodide (ProI) and annexin V-FITC on ice fort ten minutes. Representative confocal images are shown. Bar, 10µm.

6.2.3 Ionomycin induces scrambling of fluorescent phospholipids

To obtain further evidence for Ca^{2+}-activated scramblase activity in *Leishmania* parasites, the translateral lipid dynamic in the plasma membrane upon ionomycin treatment was characterised. For this purpose, parasites were incubated for 30 minutes at 2°C with NBD-labelled lipids and analysed by confocal microscopy. At this temperature endocytosis is blocked [68,129] and internalisation depends on the lipid flip to the inner leaflet of the plasma membrane. Once inside, NBD-lipids with a shortened acyl chain (6-carbon) at the *sn*-2 position spontaneously redistribute to intracellular membranes because of their partial water solubility and accumulate intracellularly. As described above internalisation of NBD-lipids by untreated wild-type parasites was strongly headgroup dependent: NBD-PE and NBD-PC were rapidly accumulated intracellularly, while NBD-PS and -SM were only incorporated into the plasma membrane (**Figure 26**). By contrast, internalisation of all NBD-lipids was observed after stimulation of parasites with ionomycin (**Figure 26**). Analysing the uptake dynamics via flow cytometry revealed a biphasic kinetic with a fast increase during the first two minutes for all NBD-lipids, reflecting the incorporation of the lipid analogue into the external leaflet of the plasma membrane.

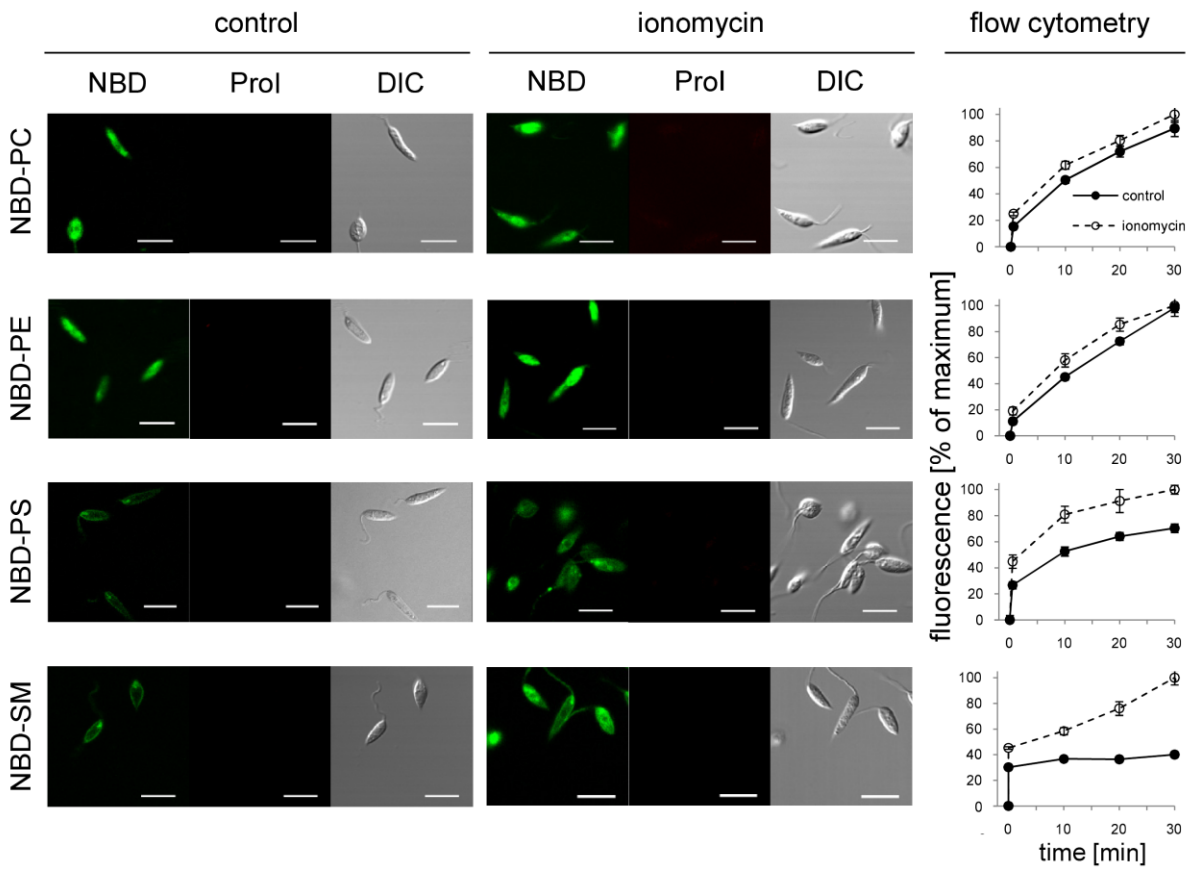

Figure 26: Ca^{2+}-induced inward transbilayer movement of fluorescent phospholipids in *Leishmania* promastigotes.

Untreated (Control) and ionomycin-stimulated (Ionomycin) wild-type promastigotes were incubated with NBD-lipids at 2°C as described in Material and Methods. After 30 minutes, propidium iodide (ProI) was added and cells were examined by differential interference contrast (DIC) and confocal microscopy (NBD, ProI). Representative micrographs are shown. Bar, 10 µm. Analysis by flow cytometry was used to follow cell-associated NBD fluorescence of living cells over time. Data are expressed as a percentage of NBD fluorescence intensity associated with ionomycin-stimulated parasites after 30 minutes of labelling at 2°C in HPMI medium and represent the means ± SEM of five independent experiments. One hundred percent corresponds to 389 ± 23 arbitrary units (NBD-PC), 223 ± 18 arbitrary units (NBD-PE), 286 ± 26 arbitrary units (NBD-PS), and 739 ± 41 arbitrary units (NBD-SM).

In untreated parasites this was followed by further increase for NBD-PC and –PE while for NBD-PS and –SM only a little increase was detected. Stimulation with ionomycin led to continuous increase for all lipid species. This inward directed flip induced by ionomycin treatment of the parasites was not ATP dependent. Depletion of cellular ATP decreased the fluorescent signals for NBD-PC and –PE obtained after 30 minutes of labelling in control parasites, whereas ionomycin treated parasites were still highly fluorescent (**Figure 27**). Moreover, the lipid flip induced by Ionomycin is independent from the functional LdMT-LdRos3 complex

and requires calcium. To visualise these aspects in lipid scrambling ΔLdMT parasites were stimulated with ionomycin, and uptake of NBD-PC during 30 minutes at 2°C was analysed (**Figure 28**). Again ionomycin treatment induced intracellular staining with the NBD-PC whereas untreated ΔLdMT parasites showed only plasma membrane labelling. In the kinetics measured by flow cytometry this is reflected by increased NBD-PC uptake following stimulation with ionomycin in comparison to unstimulated mutant parasites.

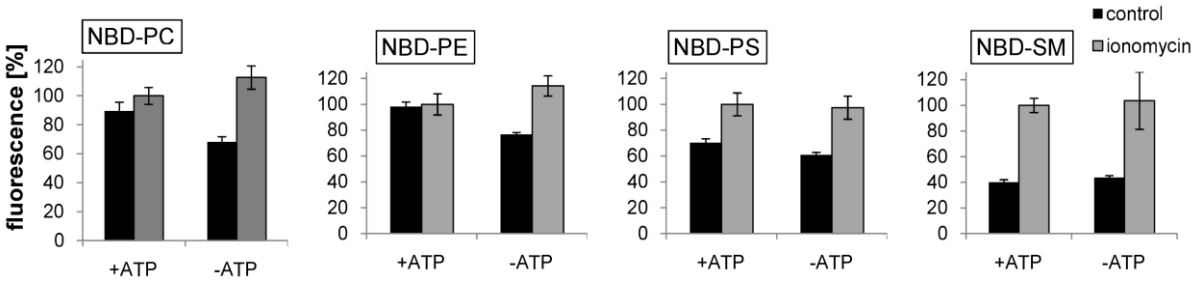

Figure 27: Ca^{2+}-induced flip of NBD-lipids is not ATP-dependent.

To probe the ATP dependence of the scrambling process, wild-type parasites were ATP-depleted (-ATP) as described under Material and Methods or left untreated (+ATP). Following, these untreated (control) or ionomycin-stimulated (ionomycin) parasites were labelled with NBD-lipids for 30 minutes at 2°C. Subsequently, samples were analysed by flow cytometry. Data are expressed as a percentage of NBD fluorescence intensity associated with non-ATP-depleted control parasites and represent the means ± SEM of five independent experiments.

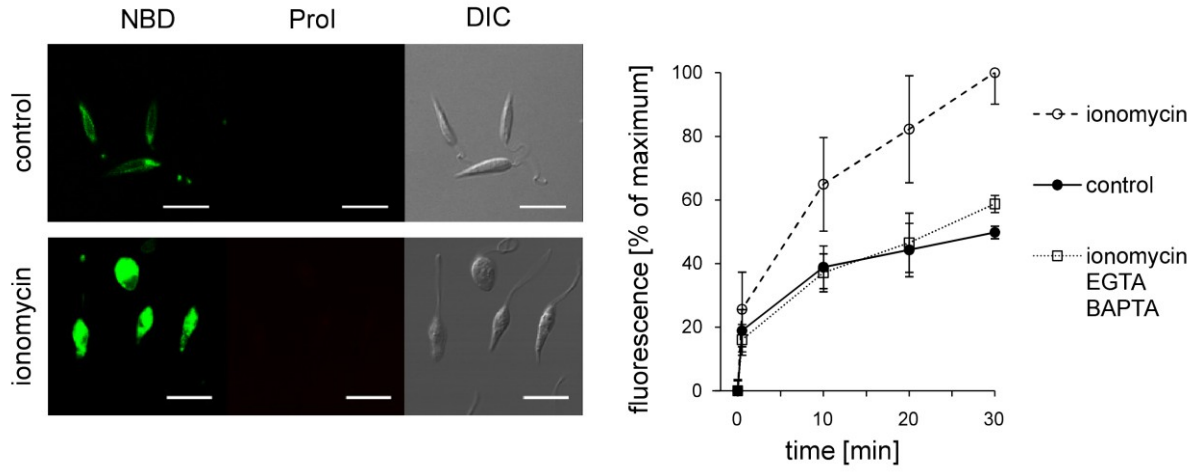

Figure 28: Ionomycin-stimulated flip of NBD-lipids is independent of the Flippase but requires intracellular Ca^{2+}.

Before labelling with NBD-PC for 30 minutes at 2°C ΔLdMT promastigotes were stimulated in presence of Ca^{2+} with ionomycin (Ionomycin) or loaded with BAPTA-AM and stimulated with ionomycin in presence of EGTA (ionomycin EGTA BAPTA) or left untreated (control). After 30 minutes, propidium iodide (PI) was added and cells were examined by differential interference contrast (DIC) and confocal microscopy (NBD, ProI). Represen-

tative micrographs are shown. Bar, 10 µm. Analysis by flow cytometry was used to follow cell-associated NBD-fluorescence of living cells over time. Data are expressed as a percentage of NBD-fluorescence intensity associated with ionomycin-stimulated parasites after 30 minutes of labelling at 2°C in HPMI medium and represent the means ± SEM of three independent experiments.

This increased uptake was similar to wild-type parasites stimulated with ionomycin. To make sure that ionomycin itself did not cause lipid flip-flop *Leishmania* parasites lacking LdMT were loaded with the calcium chelator BAPTA-AM and stimulated with ionomycin in the presence of 3mM EGTA. Under these conditions the increase in NBD-PC uptake was inhibited completely.

To make sure that these differences in lipid uptake following ionomycin stimulation of *L. donovani* do not reflect increased metabolism of NBD-lipids, lipid extracts were analysed. For this, control and ionomycin stimulated parasites were labelled with NDB-PC, -PE, -PS and –SM on ice for 30 minutes, and lipids were extracted according to the method of Bligh and Dyer [107]. Following, NBD-lipid stocks and lipid extracts were separated by TLC under neutral conditions and plates scanned with a phosphorimager (FUJI FLA-3000).

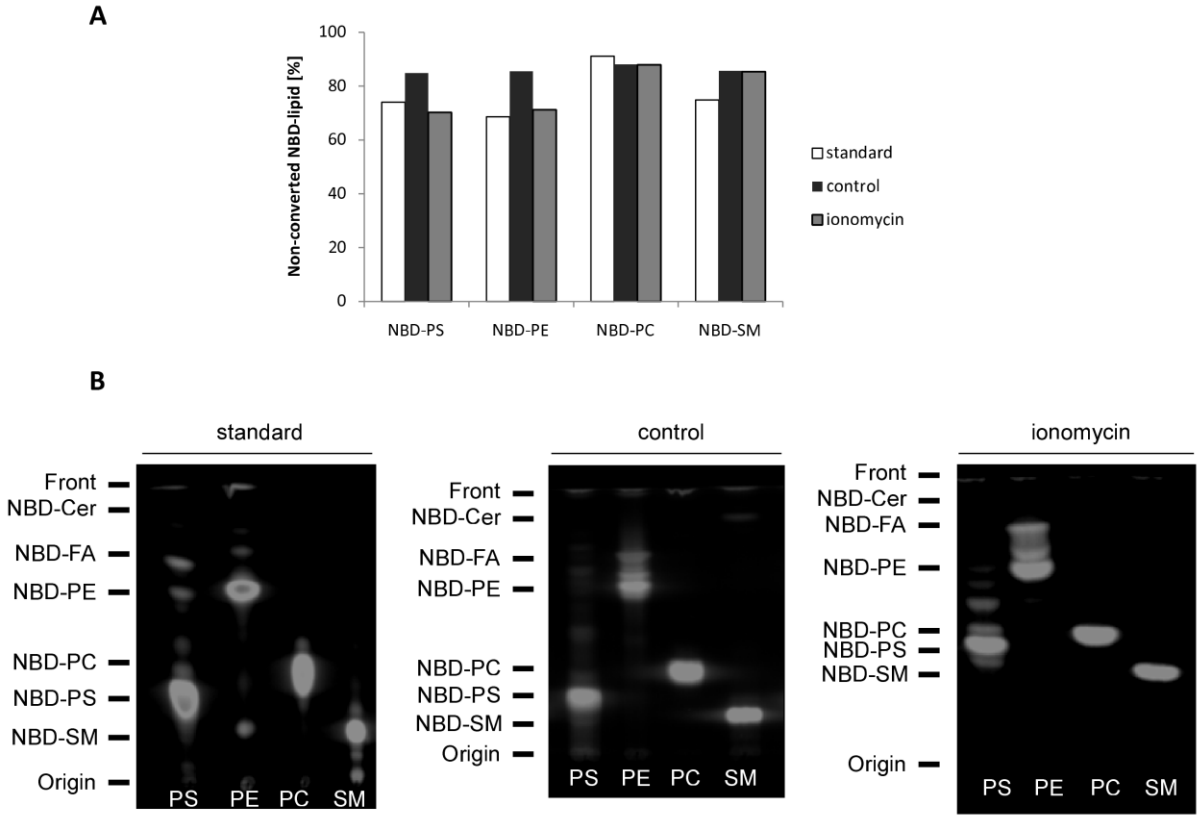

Figure 29: NBD-lipid metabolism in *L. donovani* quantified by TLC.

Lipid stocks (standard) and extracts from parasites following 30 minutes of lipid uptake on ice either stimulated by ionomycin (ionomycin) or not (control) were separated by thin layer chromatography (TLC) and NBD-fluorescence was visualised by means of a FUJI phosphorimager (B) as described under material and methods. Lipid species were quantified by using the AIDA analysis software. The percentage for each NBD-lipid-species was calculated with respect to fluorescent spots within the lane (A).

Quantification of NBD-fluorescence within each lane revealed no differences between NBD-PC and –SM in control and ionomycin treated parasites, whereas for NBD-PS and -PE the main spot lost intensity in ionomycin treated parasites (**Figure 29 B**). However, metabolism of NBD-lipids was consistently below 10% compared to control cells within the time course of the experiment (**Figure 29 A**).

To follow the back transport of NBD-lipids towards the cell surface, after 30 minutes of labelling incubation was continued in the presence of albumin. This acts as an extracellular sink for short-chain lipids by rapidly extracting NBD-lipids from the outer leaflet of the plasma membrane, thereby excluding analogues from inward transport. Under these conditions a fast decrease in cellular fluorescence was observed. In **Figure 30** the flop of NBD-PC and NBD-PE in control cells and following ionomycin stimulation is depicted exemplarily. While the fluorescence in control parasites initially decreased (until 10 minutes) similar to ionomycin stimulated parasites, indicating the removal of NBD-lipids from the outer leaflet, this decay was much slower for control cells in the following 20 minutes. Induced by ionomycin the extraction velocity of NBD-PC and -PE by albumin was altered what results in different fluorescence values 30 minutes following addition of albumin. The fluorescence associated with control cells was 46% of NBD-PC and 40% of NBD-PE, whereas in ionomycin-stimulated parasites, more than 70% of both NBD-lipid species became accessible to albumin.

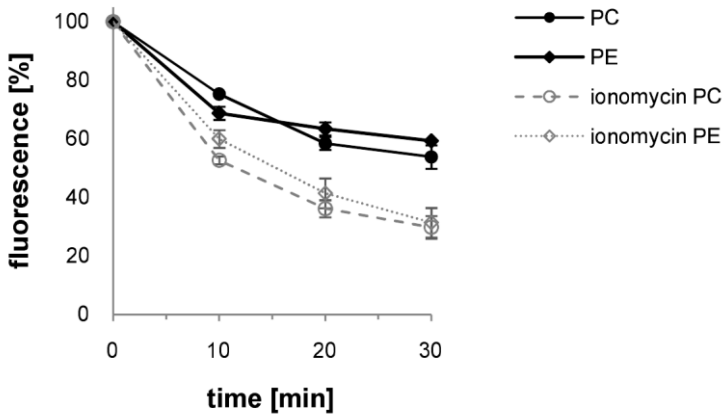

Figure 30: Ca^{2+} induced flop of NBD-lipids exceed that in nonstimulated control parasites.

L. donovani promastigotes stimulated with ionomycin (ionomycin) or not (control) were labelled for 30 minutes with NBD-PC or –PE at 2°C. Following, albumin was added and the incubation at 2°C continued. At indicated time points aliquots were withdrawn and analysed by flow cytometry. Data are expressed as a percentage of NBD fluorescence intensity associated with ionomycin-stimulated parasites after 30 minutes of labelling at 2°C in HPMI medium and represent the means ± SEM of five independent experiments.

The fast back transport of NBD-lipids towards the cell surface was not affected by ATP depletion (**Figure 35**, appendix).

Collectively, these results suggest that elevated Ca^{2+} levels in *Leishmania* parasites catalyse a rapid transbilayer lipid movement in the plasma membrane that is bidirectional, ATP-independent, and not specific to the polar head group of the lipid.

6.3 *Leishmania donovani* promastigotes lack PS

In the previous chapters it was already mentioned that PS could not be detected with the means applied in this work, neither in total lipid extracts separated by TLC and stained with the amino-reactive chemical ninhydrin nor by analysing the main spots with ESI-MS (**Figure 21 A and B**) nor by annexin V-binding to the outer plasma membrane leaflet of intact promastigotes (**Figure 20 B** and **Figure 25**). Since this lipid was reported to be exposed in certain developmental states of the parasite and suspected to silence the immune response [118,130], this aspect was studied more in detail. First of all, it was tested whether the extraction method used here to purify lipids from parasites is capable to extract this lipid species. For this, commercially available POPS was added to a *Leishmania* suspension and lipids were extracted according to the method of Bligh and Dyer [107].

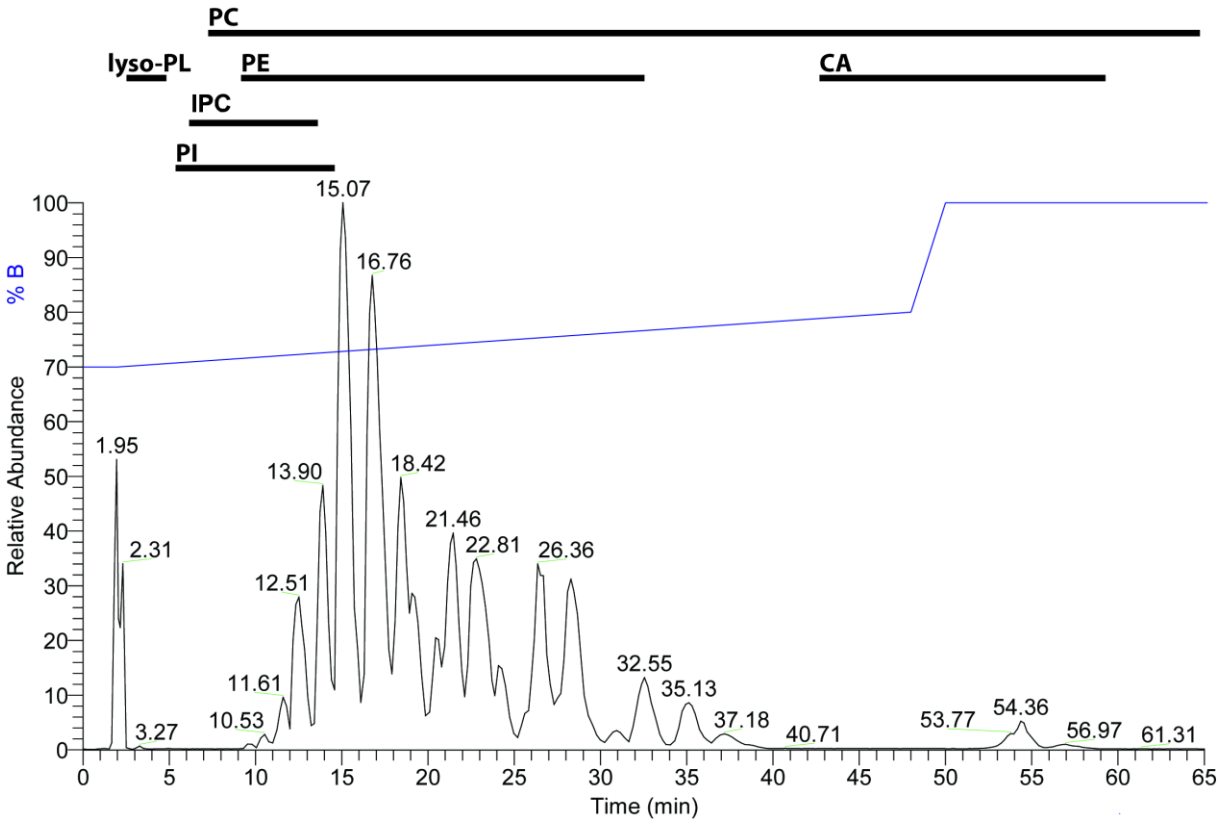

Figure 31: Spectrum of a total lipid extract from *L. donovani* obtained by HPLC coupled to ESI-MS.

Lipid extracts from *L. donovani* were separated by HPLC and eluted fractions directly injected in the ESI-MS. Analysis was performed in the negative ion mode. Numbers above the peaks indicate the elution time. Lipid species detected during the analysis are indicated above the spectrum with respect to their elution time. A detailed list of lipids detected can be found in **Table 2**. The percentage of buffer B in the elution solvent is indicated in blue.

lipid species	retention time (min)	abundance (%)
lyso-PC(18:2)	3.3	49.55
lyso-PC(18:1)	3.5	17.75
lyso-PC(18:3)	3.0	14.74
lyso-PC(18:0)	4.7	7.88
lyso-PC(20:2)	3.8	5.89
lyso-PC(16:0)	3.5	4.18
p-PC(34:3)	23.3	33.33
p-PC(36:2)	34.7	23.83
p-PC(36:3)	32.6	21.76
p-PC(34:2)	25.6	21.07
PC(40:8)	15.1	18.47
PC(36:4)	16.8	16.02
PC(40:7)	18.4	9.21
PC(36:5)	13.9	8.95
PC(36:3)	21.5	7.31
PC(38:4)	22.8	6.43
PC(36:2)	28.3	5.76
PC(40:9)	12.5	5.16
PC(38:5)	18.8	4.00
PC(34:2)	20.4	3.78
PC(36:6)	11.6	1.77
PC(36:1)	35.1	1.59
PC(40:6)	23.3	1.32
PC(38:3)	28.5	1.28
PC(32:2)	14.6	0.79
PC(38:6)	18.4	0.78
PC(34:1)	26.0	0.74
PC(39:6)	20.8	0.69
PC(40:5)	30.9	0.66
PC(39:7)	17.1	0.64
PC(38:2)	37.2	0.54
PC(40:10)	10.5	0.53
PC(42:8)	20.4	0.45
PC(44:12)	13.6	0.31
PC(37:4)	20.1	0.24
PC(42:9)	16.8	0.21
PC(36:7)	9.5	0.20
PC(37:3)	25.0	0.19
PC(40:4)	34.3	0.19
PC(42:7)	25.2	0.18
PC(32:3)	12.0	0.18
PC(40:3)	38.4	0.18
PC(32:1)	19.1	0.17
PC(37:5)	16.3	0.16
PC(44:11)	16.5	0.15
PC(35:3)	18.3	0.09
PC(39:5)	26.6	0.08
PC(37:2)	32.9	0.07
PC(32:0)	25.2	0.06
PC(39:4)	32.4	0.05
PC(42:6)	27.9	0.05
PC(40:7)-1	10.3	0.04
PC(38:1)	45.2	0.04
PC(30:2)	10.8	0.04
PC(40:2)	49.9	0.04
PC(44:3)	64.8	0.03
PC(38:5)-1	9.0	0.03
PC(39:3)	33.6	0.03
PC(36:4)-1	8.8	0.03
PC(42:2)	60.3	0.02
PC(34:5)	12.2	0.02
PC(40:8)-1	8.4	0.02
PC(37:1)	40.5	0.01
PC(36:5)-1	7.2	0.01
PC(30:3)	9.0	0.01
PC(39:9)	12.5	0.00
lyso-PE(18:2)	2.9	
p-PE(36:3)	26.4	33.09
p-PE(34:3)	19.1	25.04
p-PE(34:2)	24.1	15.70
p-PE(36:2)	32.6	13.47
p-PE(35:3)	22.0	6.93
p-PE(35:2)	27.5	3.18
p-PE(36:4)	20.1	2.05
p-PE(34:4)	15.9	0.54
PE(36:4)	13.4	25.39
PE(36:3)	17.4	21.79
PE(36:2)	23.0	16.21
PE(36:1)	28.7	11.85
PE(34:2)	16.3	6.84
PE(36:5)	11.0	6.59
PE(34:1)	21.0	5.62
PE(38:4)	18.4	3.39
PE(32:2)	11.8	2.32
PE(36:6)	9.0	0.01
PE(30:0)	14.6	
PE(30:1)	11.5	
p-PI(36:1)	5.3	
p-PI(34:1)	12.2	
PI(34:2)	9.0	
PI(36:3)	9.7	
PI(34:1)	10.8	
PI(36:2)	11.7	
PI(36:1)	14.6	
IPC(34:0)-2	6.1	
IPC(34:1)-1	7.1	
IPC(36:0)-2	8.3	
IPC(34:1)-2	8.8	
IPC(36:1)-1	9.6	
IPC(37:1)-1	11.5	
IPC(36:1)-2	12.2	
IPC(37:1)-2	13.8	
CA(80:15)	54.4	39.01
CA(80:16)	54.0	21.73
CA(80:14)	57.0	7.42
CA(80:13)	57.2	5.83
CA(76:12)	54.4	4.79
CA(84:19)	54.0	4.46
CA(78:13)	54.5	2.63
CA(76:10)	58.1	2.58
CA(76:11)	57.3	2.37
CA(80:17)	49.1	1.89
CA(78:12)	57.3	1.55
CA(78:11)	58.1	1.43
CA(76:9)	59.2	1.10
CA(84:17)	56.4	0.84
CA(84:18)	54.4	0.81
CA(80:12)	59.2	0.74
CA(84:20)	49.9	0.45
CA(80:18)	42.7	0.37

Table 2: Lipid species identified by ESI-MS in Figure 31.

Lipids are grouped within their subclass (lipid species) and presented in the order of their quantity (abundance) within each subclass as judged by the signal intensity. The lipids were eluted from the HPLC column at the time indicated (retention time) and identified by their absolute mass and their SIM spectrum obtained in the MS^2 and MS^3. Lipids not quantified were identified in different scans. The numbers in brackets indicate to the sum of carbon atoms and the number of unsaturated bonds in the fatty acid tails. If fatty acids are oxidised the number of hydroxyl groups is denoted following the bracket, e.g. IPC(34:1)-1 for Inositolphosphorylceramide with 34 carbon atoms one double bond and one hydroxyl group. PC (phosphatidylcholine) p-PC (plasmalogen PC), PE (phosphatidylethanolamine), PI (phosphatidylinositol), CA (cardiolipin).

These lipid extracts were separated by TLC and stained with ninhydrin. In comparison to pure *Leishmania* lipids where only PE gives a purple spot here a second spot appeared at the same

position were pure POPS was localised (data not shown). Second, total lipid extracts from early log phase *L. donovani* promastigotes were analysed by Frederic Müller applying ESI-MS and by Dr. Jürgen Schiller applying MALDI-TOF (Figure 31 and Figure 32).

Both methods were able to detect PS in standard calibration lipid mixtures and in a mixture of *E. coli* lipids enriched with 0.1% POPS (w/w) as well as a multitude of lipid species in the lipid extracts (**Table 2**) obtained from *Leishmania* promastigotes but not even traces of PS could be detected in the latter one. To make sure that the lack of PS is not a unique phenotype of our laboratory *L. donovani* strain, lipid extracts prepared from *L. infantum* and *L. tropica* promastigotes were probed by TLC and ESI-MS for this lipid. In line with the previous results neither of the two parasite strains contained detectable amounts of PS (data not shown). Indicating that in the promastigote state this lipid seems not to be present.

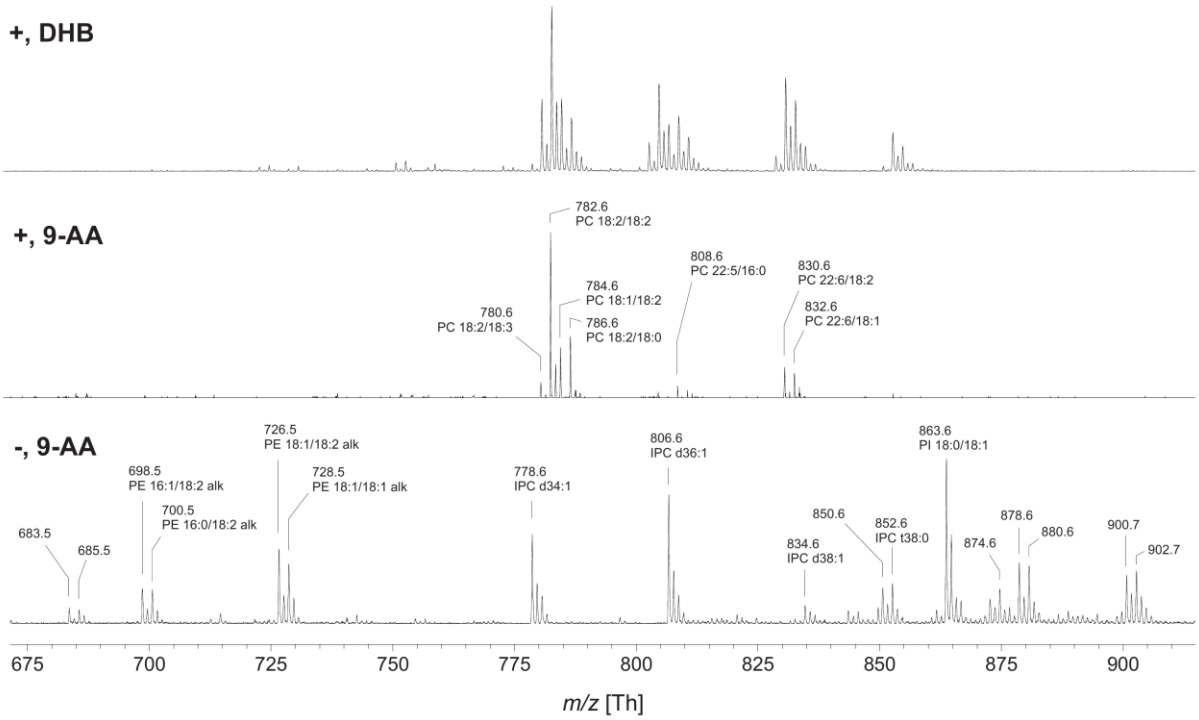

Figure 32: MALDI-TOF analysis of lipid extracts from *L. donovani.*

Lipid extracts were obtained as described under materials and methods and analysed using a 2,5-dihydroxybenzoic acid (DHB) or a 9-aminoacridine (9-AA) as matrix for ionisation by a 337 nm nitrogen laser. Ionisation of phosphatidylcholine (PC) was best in positive Ion mode using the DHB matrix (+, DHB) and less efficient by applying the 9-AA matrix. Detection of phosphatidylethanolamine (PE), inositol phosphorylceramide (IPC) and phosphatidylinositol (PI) was achieved by data acquisition in the negative ion mode using the 9-AA matrix. The molecular masses are indicated above the peaks in unified atomic mass units as well as the lipids derived from these masses and the selective fragmentation by post source decay experiments.

Nevertheless apoptotic *L. donovani,* judged by propidium iodide staining, bind annexin V. To bring to light if this is due to PS synthesised during apoptosis, promastigotes were incubated overnight with 40µM Miltefosine resulting in PI and annexin V-FITC positive apoptotic cells (**Figure 33**). Lipid extracts obtained from these dead parasites were analysed by ESI-MS and TLC stained with ninhydrin (**Figure 33**). Again both methods failed to detect any PS. Nevertheless annexin V-FITC binds to these dead parasites as well as to parasites damaged by electroporation (data not shown), indicating that the lipid recognised by annexin V is not necessarily synthesised during apoptosis.

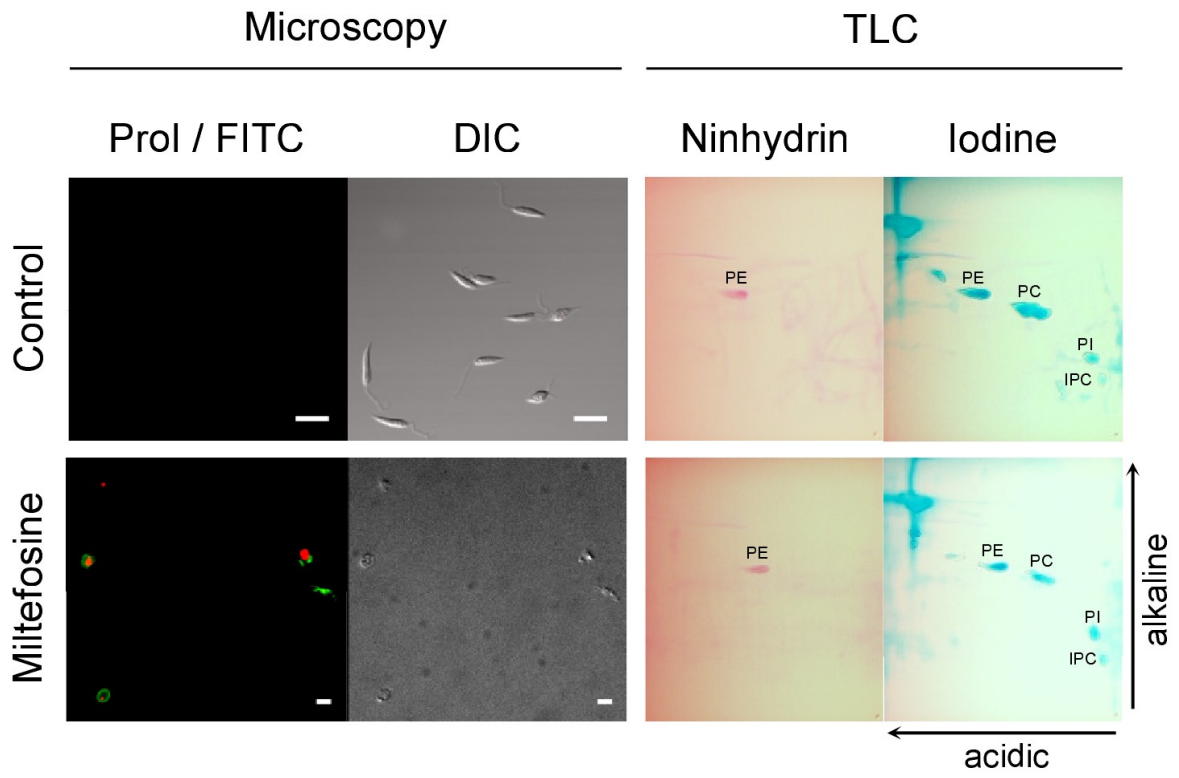

Figure 33: The lipid composition of apoptotic *L. donovani* is not altered.

Parasites were either cultured in absence (control) or presence of miltefosine (miltefosine). Following, an aliquot was withdrawn and parasites were stained with annexin V-FITC and propidium iodine (Microscopy, PI) and analysed by microscopy. Bar, 10µm. Moreover, lipids were extracted and separated by thin layer chromatography (TLC) using first an alkaline and second an acidic solvent. Next, Lipids containing terminal amino groups were stained with Ninhydrin and phospholipids with iodine. Lipid spots as determined by ESI-MS are indicated in the TLC: phosphatidylethanolamine (PE), phosphatidylcholine (PC), phosphatidylinositol (PI) and inositolphosphorylceramide (IPC).

In summary, these data indicate that the apoptosis marker annexin V recognises a different lipid moiety than PS in apoptotic *L. donovani*. If PS is synthesised in promastigotes at all, its

concentration in the total lipid extract ought to be below 1% of the phospholipids as quantified by radiolabelled phospholipids and below 0.1% since this amount is still easily detectable with ESI-MS.

7 Discussion

The surface of the *Leishmania* parasite is a major point of interaction with the host throughout the infectious cycle. A number of surface glycoconjugates such as lipophosphoglycans, GPI-anchored proteins (e.g. the metalloprotease gp63), and a heterogeneous group of small glycosylinositolphospholipids have been implicated in the ability of the parasite to infect and survive in host macrophages [131]. In addition, high levels of surface-exposed PS, judged on basis of annexin V-binding, have been associated with elevated parasite infectivity in metacyclic and amastigote cultures [118,120,130].

In this work, mechanisms implicated in the regulation of the lipid composition in the extracellular leaflet of the parasites plasma membrane were in focus of analysis. Firstly, a P_4-ATPase necessary for maintaining the lipid asymmetry by an inward-directed lipid transport was studied and the impact of its loss on the invasion of host cells analysed. Part of the data shown were published in Plos one [129]. Secondly, a scramblase mechanism activated by alterations in cytosolic calcium levels was described. And thirdly, the lipid composition with focus on PS was examined with different detection methods, since this lipid was suspected to be the basis for annexin V-binding to the parasite and thus to enhanced infectivity.

7.1 Functional LdMT/LdRos3 complex

Previous studies revealed a critical role for two proteins, namely the miltefosine transporter (LdMT) and LdRos3 in the uptake of alkylphosphocholine type drugs and in phospholipid translocation at the plasma membrane of *Leishmania* parasites [56,57,132]. The present study provides direct evidence that both proteins form a stable complex that is essential for maintaining the stady-state asymmetric lipid distribution of the parasite plasma membrane. Loss of plasma membrane PE asymmetry by disruption of the LdMT-LdRos3 complex did not alter the phagocytosis of the parasite by macrophages. Suggesting, that the loss of the asymmetric lipid distribution does not facilitate host cell invasion by *L. donovani*.

The formation of a stable complex between P_4-ATPases and Cdc50 family members seems to be indispensable for a proper targeting and functioning of P_4-ATPases. In yeast, the Cdc50 family members Cdc50p, Lem3p and Crf1p can be co-immunoprecipitated with Drs2p, Dnf1p/Dnf2p and Dnf3p, respectively. Formation of these complexes is required for proper expression and endoplasmic reticulum export of either partner [61,133]. The human P_4-ATPase ATP8B1 requires the Cdc50 family member CDC50A for ER exit and delivery to the

plasma membrane [134], and the Arabidopsis P_4-ATPase ALA3 requires its Cdc50 binding partner ALIS1 to complement the lipid transport defect at the plasma membrane in Δdrs2Δdnf1Δdnf2 yeast mutant [63]. These findings hold also true for LdRos3 and the P_4-ATPase LdMT. However, a closer analysis of the partially sequenced genome of *L. infantum* (http://www.genedb.org/genedb/linfantum/) revealed in total five genes encoding P_4-ATPases (LinJ09_V3.0940, LinJ13_V3.1590, LinJ30_V3.2270, LinJ30_V3.2270, LinJ34_V3.2460, LinJ34_V3.3000) and three genes encoding Cdc50 family members (LinJ09_V3.1080, LinJ32_V3.0540, LinJ35_V3.3450). It remains to be established if all of these P_4-ATPases require a Cdc50 binding partner for proper functioning and if they can interact with several Cdc50 proteins as shown for the Arabidopsis P_4-ATPase ALA3 [63] and the human P_4-ATPases ATP8A1, ATP8B1, ATP8B2, and ATP8B4 [64,65]. Results presented in this study revealed that *Leishmania* LdMT does not associate with other Cdc50 members than LdRos3 and that the stoichiometry of both proteins associated in the complex is one to one.

Incubation of parasites with fluorescent phospholipid analogues, (such as NBD-PC, -PE, -PS and -SM) served as an approach to analyze lipid transport activity of the LdMT-LdRos3 complex at the plasma membrane. We found that *L. donovani* parasites efficiently internalise NBD-PC and NBD-PE, while NBD-PS and NBD-SM are hardly taken up. Loss of either LdMT or LdRos3 completely blocked the ATP-dependent uptake of NBD-PC and NBD-PE, indicating that the LdMT-LdRos3 complex facilitates the energy-coupled transport of PE and PC from the outer to the inner leaflet of the parasites plasma membrane. In support of this notion, loss of either LdMT or LdRos3 led to an increased cell surface exposure of endogenous PE, as evidenced by enhanced hypersensitivity to PE-binding peptide and labelling by biotinylated PE-binding peptide. These results are in line with a direct role of the LdMT-LdRos3 complex in pumping endogenous PE to the cytosolic leaflet to generate an asymmetric membrane as recently reported for P_4-ATPases from other organisms [48,49]. The ability of wild-type parasites to take up NBD-PC suggests that PC is restricted to the inner leaflet of the parasites plasma membrane and that the outer leaflet is primarily composed of sphingolipids, since NBD-sphingomyelin is not taken up.

The substrate specificity of the inward translocation machinery appears to vary between *Leishmania* species. In contrast to *L. donovani*, *L. infantum* displays not only an ATP-dependent internalisation of NBD-PC and NBD-PE, but also an active transport of NBD-PS across its plasma membrane [135]. Thus, this parasite might express one or more P_4-ATPases of broader or different substrate specificity at the plasma membrane. The physiological rele-

vance of these species-specific differences in substrate specificity remains to be established. Previous studies suggested that the LdMT-LdRos3 complex of *L. donovani* also recognises NBD-PS as a substrate [56,57]. However, significant uptake of NBD-PS in this species was only observed when higher label concentrations were used as compared to NBD-PC and NBD-PE. It is noteworthy that in agreement with former reports [31,41] we could not detect endogenous PS in total lipid extracts prepared from *L. donovani* promastigotes, suggesting that this parasite does not synthesise considerable amounts of PS. Consequently, an inward-directed transport activity for PS at the plasma membrane might not be required in *L. donovani*. However, all experiments carried out in the present work were performed on the promastigote stage. It would be interesting to determine whether *L. donovani* amastigotes synthesise PS and regulate its distribution in the parasite plasma membrane. A stage-specific regulation of the plasma membrane asymmetry is conceivable, since amastigotes up-regulate the expression of two P_4-ATPases (LmjF30.2260, LmjF34.3220) and a plasma membrane ABC-transporter associated with lipid export (LmjF11.1260) [136]. *Leishmania* amastigotes replicate within the mature phagolysosome compartment and have complex nutritional requirements, which must be scavenged from the host cell [137]. It is therefore tempting to speculate that the LdMT-LdRos3 transporter complex or related P_4-ATPases are involved in the acquisition of host phospholipids.

The results on ΔLdMT and the ΔLdRos3 *Leishmania* mutant lines, which display an altered PE asymmetry, did not reveal major differences in terms of invasion efficiency into the human monocytic cell line THP-1. In line with these results, the ΔLdMT mutant remains infective and maintains virulence in cultures of primary isolated mouse peritoneal macrophages [138]. These results suggest that disruption of the LdMT-LdRos3 transporter complex and changes in the transbilayer distribution of PE, and probably PC, are not crucial for *L. donovani* promastigotes to invade host cell. Likewise, PS exposure is not mandatory for invasion of host cells. Future studies on other *Leishmania* species and mutants lacking the ability to synthesised PS may help to define the lipid types exposed on the cells surface and involved in parasite internalisation and phagocyte inactivation in more detail.

7.2 Scramblase activity

Disruption of the lipid asymmetry during apoptosis is an important signal for macrophages to engulf dying cells in order to maintain tissue homeostasis by preventing release of cytotoxicity substances. The mechanism resulting in loss of plasma membrane asymmetry due to facilitated flip-flop of lipids is called scrambling. Two different routes to trigger this mechanism are known. One is the apoptotic death and the other is an increase in cytosolic calcium. Here, evidence is provided that *Leishmania* parasites possess a Ca^{2+}-induced lipid scrambling activity.

As a first approach to explore the lipid distribution in the plasma membrane of the parasite and the impact of elevated intracellular Ca^{2+} levels on the lipid arrangement, we incubated parasites with lipid-binding proteins. We could demonstrate that under normal culturing condition, parasites do not expose PE at their cell surface in agreement with a preferential location of this phospholipid in the cytosolic plasma membrane leaflet. A rise in intracellular Ca^{2+} achieved by ionomycin treatment caused exposure of PE at the surface as revealed by strong binding of the PE-specific Ro09-0198 peptide [139,140]. Attempts to monitor the redistribution of PS in the plasma membrane by annexin V-FITC failed due to the absence or very low level of this lipid in *L. donovani* promastigotes. See chapter 7.3.

Further evidence for Ca^{2+}-induced lipid scrambling and loss of lipid asymmetry in the plasma membrane of the *Leishmania* parasites was provided by using fluorescent NBD-lipids. These lipid probes have been used successfully before to characterise lipid scrambling in a variety of cell types [90,141,142]. Similar to the situation in mammalian cells the rise of intracellular Ca^{2+} level in *Leishmania* promastigotes triggered a rapid bidirectional movement of lipid analogues across the plasma membrane. Lipid scrambling did not require cellular ATP and was nonspecific with respect to polar lipid head groups. This similarity in characteristics of the scrambling process in parasites and mammalian cells suggests that the same kind of scramblase activity is stimulated by an increase of intracellular Ca^{2+}.

The molecular identity of the scramblase activity has yet to be elucidated. In humans four putative phospholipid scramblase (hPLSCR) have been identified, named as hPLSCR1–hPLSCR4 [143]. In *in vitro* reconstitution assays and cell culture-based assays hPLSCR1 was found to be capable of triggering Ca^{2+}-dependent flip-flop [90]. However, the function of PLSCR1 as a phospholipid scramblase *in vivo* remains controversial [80]. The multiple, closely related phospholipid scramblases in mammals may act redundantly and prevent the

disclosure of gene function by single gene deletion analysis. Recently, the transmembrane protein 16F, a member of the TMEM16 family, has been identified as an essential component for the Ca^{2+}-dependent exposure of PS on the cell surface of mammalian cells [144]. Interestingly, we could not find any PLSCR homologue in the sequenced genome of *L. infantum*, *L. braziliensis* and *L .major* (www.tritryp.org), whereas TMEM 16F homologues exist in all three *Leishmania* species (LinJ13_V3.0630, LmjF13.0740, LbrM13_V2.0560). Future studies are required to uncover the function of this protein and its potential contribution to lipid scrambling.

It has been demonstrated that *Leishmania* parasites exhibit a rapid increase in cytosolic Ca^{2+} concentration from both, intracellular and extracellular pools during their differentiation [102] and during temperature shifts from 24°C to 34°C [101]. Furthermore, changes in intracellular Ca^{2+} have been shown during the interaction of the parasite with host cells [100]. Notably, suppressing the calcium signal by chelators or drugs blocking Ca^{2+} channels leads to a decreased infectivity due to reduced phagocytosis by macrophages. Elevated Ca^{2+} levels induced by ionophores lead to increased infectivity [100,145]. These findings reveal the importance of intracellular Ca^{2+} in the process of parasite–host cell interaction. The exact mechanism linking Ca^{2+} signalling with infectivity is not understood. Conceivably, transient activation of a lipid scramblase activity leading to a change in the cell surface lipid composition might be an opportunity to connect the change of intracellular calcium level with the interaction of *Leishmania* with host cells. Further analysis is warranted to fully uncover the physiological role of the lipid scramblase activity in *Leishmania* parasites.

7.3 Apoptotic mimicry

As mentioned in the previous chapter, surface-exposed PS is an apoptosis marker of eukaryotic cells [146]. Recognition of this moiety by phagocytes via a still unknown PS-receptor [147] or several PS opsonising proteins like annexins [148,149], lactadherin [150,151] or MFG-E8 and GAS6 [152] lead to the engulfment of apoptotic cells [153]. Thus, it is believed that presenting PS on the outer membrane leaflet might be a mechanism to guide pathogens into their host cells. Recently, this was shown for the vaccinia virus and for *Leishmania* amastigotes [118,154]. The entry of *Leishmania* into macrophages via this non-inflammatory route stimulates the secretion of TGF-β and the synthesis of IL-10 *in vitro* while NO production by the phagocytes was inhibited [118], similarly to the engulfment of apoptotic cells [155]. This modulation of the immune response results in an increased susceptibility to intracellular *Leishmania* [118,156]. Furthermore, amastigotes derived from infected mice of the T helper cell type 2 mouse line BALB/c result in amastigotes with higher amounts of PS exposed to the parasites surface than amastigotes obtained from T helper cell type 1 mouse line C57BL/6 [130]. Studies on promastigotes suggest that exposure of PS at this stage is a sign for apoptosis. During infection with mixed populations of living and apoptotic promastigotes, the vital parasites benefit from hiding in the apoptotic population, while either population alone is less or non-infectious [119,120].

So far, all articles mentioned in this chapter describing the detection of PS in *Leishmania* parasites judge the appearance of PS on basis of annexin V-binding. However, besides PS this lipid-binding protein recognises PE, PG, PI, Cardiolipin, PA, Sphingomyelin and phosphatidylinositol-4,5-bisphosphate in the presence of calcium ions [127,157]. Hence, annexin V provides a useful tool to detect apoptosis, but its binding selectivity is not sufficient to identify PS. Annexin V binds to charged lipids in a calcium-dependent manner with different affinities for the respective lipids. Ca^{2+} concentrations between 1 mM and 3 mM are recommended for the detection of PS, since higher concentrations promote unspecific binding of annexin V even to PC [128]. Interestingly, most of the studies mentioned above used annexin V in the presence of 5 mM Ca^{2+} to detect PS on the surface of *Leishmania* parasites. Similarly, the substrate specificity of a PS-antibody is somewhat broader as the name implies, since it binds to PS, PA and PI [157].

While studying the lipid asymmetry of the plasma membrane of *L. donovani* and the derivative line lacking the LdMT transporter, two contradictory results questioned the conclusion

that PS stimulates the phagocytosis and subsequently the non-inflammatory response of phagocytes.

Firstly, the lack of the LdMT transporter leads to a block of inward-directed lipid transport at the plasma membrane. Hence, the lipid asymmetry in the mutant lacking LdMT is altered, and PE is exposed to the outer plasma membrane leaflet. This was demonstrated by increased drug sensitivity against duramycin and by binding of biotinylated Ro-peptide as visualised by streptavidin-FITC. Increased annexin V-binding was reported for yeast mutants lacking the P_4-ATPase homologues localised in the plasma membrane [158]. Thus it was probed here as well. Surprisingly no annexin V-binding could be observed for life promastigotes in presence of 2.5 mM Ca^{2+}, neither for the wild-type nor for the LdMT knock-out line. A drug sensitivity assay exploiting alternative PS-sensing protein, the antibiotic papuamide B that binds to PS- but not to PE-containing membranes [114], led to the same result. Both, wild-type and mutant parasite lines, showed identical IC_{50} values of 0.25 µM papuamide B which is in a similar range like wild-type yeast [114]. Interestingly, there are only slight differences between wild-type yeast and yeast lacking the PS synthase in terms of sensibility to papuamide B [158]. On the one hand this underlines the efficiency of the yeast flippase, since the wild-type yeast exposes almost no PS. On the other hand it is a hint that the plasma membrane of the wild-type *Leishmania donovani* line tested here and its derivative lines ΔLdMT and ΔLdRos3 do not contain PS.

Secondly, to confirm the previous results, total lipid extracts derived from ^{32}P-radiolabelled *Leishmania donovani* wild-type, LdMT and LdRos3 were separated by TLC. The aminoreactive chemical Ninhydrin stained successfully *Leishmania* PE, while no PS could be detected. Spots separated by TLC as well as total lipid extracts were analysed by ESI-MS leading to the same outcome, namely that the concentration of PS in the total lipid extract is below the detection limit of the method applied (**Figure 21**). To make sure that this is not a unique feature of our wild-type *L. donovani* line or based on the detection limit of the ESI-MS, total lipid extracts from promastigotes of *L. infantum* and *L. tropica* as well as mixtures of total lipid extracts from *E. coli* supplemented with 0.1% DOPS were tested. While there was no PS detectable in lipid extracts obtained from *Leishmania* lines, the PS signal of the *E. coli* lipid-mixture was prominent.

Since it was described in the literature that PS synthesis in eukaryotic cells can be up-regulated during apoptosis [159,160], lipid extracts from miltefosine-treated apoptotic para-

sites were tested by ESI-MS and 2D-TLC. And indeed, upon miltefosine-treatment wild-type parasites could be stained with PI and annexin V-FITC (**Figure 33**). However, no PS could be detected by TLC, ESI-MS or MALDI-TOF. This is in accordance with comparable observation in *L. major* promastigotes where cellular levels of PS in ESI/MS/MS analysis were below the detection limit [31,41]. Nevertheless, *Leishmania* parasites contain a putative base-exchange enzyme (also called PS synthase 2) and a putative PS decarboxylase implying the existence of a functional PS metabolism. Conceivably, biosynthesis of PS might be highly regulated in *Leishmania* and depend on the developmental stage of the parasite.

Anyway, to this end it is unclear which lipid is recognised by annexin V in apoptotic *Leishmania* promastigotes, and it is questionable if the estimated amount of PS, which must be below 0.1% of total phospholipids is sufficient for recognition by macrophages. In erythrocytes from various mammals, the PS content was shown to vary between 10% and 20% of total phospholipids [161,162]. In a study investigating the PS bridging β_2-Glycoprotein I [163] the authors demonstrated that PC/PS vesicles with PS concentrations below 20% are hardly taken up by macrophages and half-maximal vesicle uptake was achieved at concentrations between 45% and 70% PS. Assuming a homogeneous lateral distribution of PS in PC/PS-vesicles, this poorly reflects the situation in the plasma membrane of living cells where even lower amounts of PS might be enriched in small domains as reported for activated $CD8^+$ T-cells or for PS and/or PE in yeast during fission [116,126,164,165,166].

The lack of significant amounts of PS in *L. donovani* promastigotes implies that this species cannot take advantage of surface-exposed PS during the initial infection process. However, binding of fluorescent conjugates of annexin V to amastigotes and an apoptotic subpopulation of promastigotes was accompanied by higher infectivity. Thus, the moiety recognised by annexin V in *L. donovani* parasites positive for propidium iodide staining might be the key to the mechanism termed apoptotic mimicry.

8 Outlook

In this work mechanisms altering the plasma membrane lipid asymmetry in *Leishmania donovani* promastigotes were studied.

The tools developed to investigate the LdMT/LdRos3 complex, its flippase activity, its impact on the lipid asymmetry and its relevance for the host cell invasion can be used to study the remaining members of the *Leishmania* P_4-ATPases family and their possible Cdc50 partners. Independently, the analysis of the expression and function of these proteins in the amastigotes stage is of great interest, since this is the infective stage in human. Differentiation of promastigotes to amastigotes is triggered by the drop of pH in the endosomal compartment. Since protons are discussed to function as counterions for P_4-ATPases, as known from other P-type ATPases, it might be of interest to investigate the pH dependency of the flip in this organism. Moreover, the altered plasma membrane asymmetry in mutants lacking LdMT or LdRos3 did not affect the uptake by macrophages. Nevertheless it was not investigated, if these mutants differ in stimulating cytokine production by the phagocyte.

Additionally, a calcium inducible scramblase activity was demonstrated. Future work is warranted to investigate its biological relevance and the molecular mechanism facilitating the lipid flip-flop.

Moreover, the binding of annexin V to apoptotic *Leishmania* promastigotes was demonstrated to be independent of PS. Nevertheless, annexin V binding to metacyclic promastigotes and to amastigotes is associated with increased infectivity [118,119,120,130]. Thus, the moiety recognised by annexin V might play a key role during the infection and should be identified.

Bibliography

[1] Desjeux, P (2004): Leishmaniasis: current situation and new perspectives., Comparative immunology, microbiology and infectious diseases (vol. 27), pp. 305-18.

[2] Chappuis, François; Sundar, Shyam; Hailu, Asrat; Ghalib, Hashim; Rijal, Suman; Peeling, Rosanna W.; Alvar, Jorge and Boelaert, Marleen (2007): Visceral leishmaniasis: what are the needs for diagnosis, treatment and control?, Nature reviews. Microbiology (vol. 5), pp. 873-82.

[3] WHO (2007): Report of the Fifth Consultative Meeting on Fifth Consultative Meeting, World Health Organization.

[4] Killick-Kendrick, R.; Wallbanks, KR; Molyneux, DH and Lavin, DR (1988): The ultrastructure of Leishmania major in the foregut and proboscis of Phlebotomus papatasi, Parasitology research (vol. 74), pp. 586-590.

[5] Warburg, A and Schlein, Y (1986): The effect of post-bloodmeal nutrition of Phlebotomus papatasi on the transmission of Leishmania major, American Journal Of Tropical Medicine And Hygiene (vol. 35), pp. 926-930.

[6] Visentini, Arrigo (1912): The Transmission of Leishmaniosis by means of Cultures, and the Mechanism of the Natural Immunity in Rats and Guinea-pigs., Quarterly Journal of Microscopical Science (vol. s2-58), pp. 373-384.

[7] Teixeira, Maria Jania; Teixeira, Clarissa Romero; Andrade, Bruno Bezerril; Barral-Netto, Manoel and Barral, Aldina (2006): Chemokines in host-parasite interactions in leishmaniasis., Trends in parasitology (vol. 22), pp. 32-40.

[8] Zhang, Wen-Wei; Mendez, Susana; Ghosh, Anirban; Myler, Peter; Ivens, Al; Clos, Joachim; Sacks, David L and Matlashewski, Greg (2003): Comparison of the A2 gene locus in Leishmania donovani and Leishmania major and its control over cutaneous infection., The Journal of biological chemistry (vol. 278), pp. 35508-15.

[9] McMahon-Pratt, Diane and Alexander, James (2004): Does the Leishmania major paradigm of pathogenesis and protection hold for New World cutaneous leishmaniases or the visceral disease?, Immunological reviews (vol. 201), pp. 206-24.

[10] Reithinger, Richard; Dujardin, Jean-Claude; Louzir, Hechmi; Pirmez, Claude; Alexander, Bruce and Brooker, Simon (2007): Cutaneous leishmaniasis, The Lancet Infectious Diseases (vol. 7), pp. 581-596.

[11] Visentini, Arrigo (1912): On the Morphology of the Leishmania of Italian Kala-Azar., Quarterly journal of microscopical science (vol. s2-58), pp. 353-371.

[12] Rochette, Annie; Raymond, Frédéric; Ubeda, JM; Smith, Martin and N (2008): Genome-wide gene expression profiling analysis of Leishmania major and Leishmania infantum developmental stages reveals substantial differences between, BMC Genomics (vol. 26), pp. 1-26.

[13] Rosenzweig, Doron; Smith, Derek; Opperdoes, Fred R; Stern, Shay and RW (2008): Retooling Leishmania metabolism: from sand fly gut to human macrophage, The FASEB Journal, pp. 1-9.

[14] Stiles, J.K.; Hicock, P.I.; Kong, Lan; Xue, Li and Meade, J.C. (1999): Leishmania donovani proton translocating P-type adenosine triphosphatases LDH1A and LDH1B: trans-splicing and polyadenylation of transcripts in amastigotes and promastigotes., Molecular and biochemical parasitology (vol. 103), pp. 105 - 109.

[15] Glaser, T A; Baatz, J E; Kreishman, G P and Mukkada, A J (1988): pH homeostasis in Leishmania donovani amastigotes and promastigotes., Proceedings of the National Academy of Sciences of the United States of America (vol. 85), pp. 7602-6.

[16] Wilson, Mary E and Pearson, Richard D (1984): Stage-Specific Variations in Lectin Binding to Leishmania donovani, Microbiology (vol. 46), pp. 128-134.

[17] Pimenta, PF; Turco, S.J.; McConville, M.J.; Lawyer, P.G.; Perkins, P.V. and Sacks, D.L. (1992): Stage-specific adhesion of Leishmania promastigotes to the sandfly midgut, Science (vol. 256), p. 1812.

[18] Sacks, D L; Pimenta, P F; McConville, M J; Schneider, P and Turco, S J (1995): Stage-specific binding of Leishmania donovani to the sand fly vector midgut is regulated by conformational changes in the abundant surface lipophosphoglycan., The Journal of Experimental Medicine (vol. 181), pp. 685-697.

[19] Saraiva, E M; Pimenta, P F; Brodin, T N; Rowton, E; Modi, G B and Sacks, D L (1995): Changes in lipophosphoglycan and gene expression associated with the development of Leishmania major in Phlebotomus papatasi., Parasitology (vol. 111 (Pt 3), pp. 275-287.

[20] Desjardins, M and Descoteaux, A (1997): Inhibition of phagolysosomal biogenesis by the Leishmania lipophosphoglycan., The Journal of Experimental Medicine (vol. 185), pp. 2061-2068.

[21] Vinet, Adrien F; Fukuda, Mitsunori; Turco, Salvatore J and Descoteaux, Albert (2009): The Leishmania donovani lipophosphoglycan excludes the vesicular proton-ATPase from phagosomes by impairing the recruitment of synaptotagmin V., PLoS pathogens (vol. 5), p. e1000628.

[22] Chan, J; Fujiwara, T; Brennan, P; McNeil, M; Turco, S J; Sibille, J C; Snapper, M; Aisen, P and Bloom, B R (1989): Microbial glycolipids: possible virulence factors that scavenge oxygen radicals, Proceedings of the National Academy of Sciences (vol. 86), pp. 2453-2457.

[23] Giorgione, J R; Turco, S J and Epand, R M (1996): Transbilayer inhibition of protein kinase C by the lipophosphoglycan from Leishmania donovani., Proceedings of the National Academy of Sciences of the United States of America (vol. 93), pp. 11634-11639.

[24] Proudfoot, L; Nikolaev, A V; Feng, G J; Wei, W Q; Ferguson, M A; Brimacombe, J S and Liew, F Y (1996): Regulation of the expression of nitric oxide synthase and leishmanicidal activity by glycoconjugates of Leishmania lipophosphoglycan in murine macrophages., Proceedings of the National Academy of Sciences of the United States of America (vol. 93), pp. 10984-10989.

[25] Brittingham, A and Mosser, D M (1996): Exploitation of the complement system by Leishmania promastigotes., Parasitology today Personal ed (vol. 12), pp. 444-447.

[26] Beach, D H; Holz, G G and Anekwe, G E (1979): Lipids of Leishmania promastigotes., The Journal of parasitology (vol. 65), pp. 201-16.

[27] Wassef, M K; Fioretti, T B and Dwyer, D M (1985): Lipid analyses of isolated surface membranes of Leishmania donovani promastigotes., Lipids (vol. 20), pp. 108-15.

[28] Zufferey, Rachel and Mamoun, Choukri Ben (2005): The initial step of glycerolipid metabolism in Leishmania major promastigotes involves a single glycerol-3-phosphate acyltransferase enzyme important for the synthesis of triacylglycerol but not essential for virulence., Molecular microbiology (vol. 56), pp. 800-10.

[29] Zufferey, Rachel and Mamoun, Choukri Ben (2006): Leishmania major Expresses a Single Dihydroxyacetone Phosphate Acyltransferase Localized in the Glycosome , Important for Rapid Growth and Survival at High Cell Density and Essential for Virulence *, Journal of Biological Chemistry (vol. 281), pp. 7952-7959.

[30] Zhang, Kai; Showalter, Melissa; Revollo, Javier; Hsu, Fong-Fu; Turk, John and Beverley, Stephen M (2003): Sphingolipids are essential for differentiation but not growth in Leishmania, The EMBO Journal (vol. 22), pp. 6016-6026.

[31] Zufferey, Rachel; Allen, Simon; Barron, Tamara; Sullivan, Deborah R; Denny, Paul W; Almeida, Igor C; Smith, Deborah F; Turco, Salvatore J; Ferguson, Michael A J and Beverley, Stephen M (2003): Ether Phospholipids and Glycosylinositolphospholipids Are Not Required for Amastigote Virulence or for Inhibition of Macrophage Activation by Leishmania major *, Biochemistry (vol. 278), pp. 44708 -44718.

[32] Zhang, Kai and Beverley, Stephen M (2010): Phospholipid and sphingolipid metabolism in Leishmania., Molecular and biochemical parasitology (vol. 170), pp. 55-64.

[33] Brosche, T. and Platt, D. (1998): The biological significance of plasmalogens in defense against oxidative damage, Experimental gerontology (vol. 33), pp. 363-369.

[34] Engelmann, B (2004): Plasmalogens: targets for oxidants and major lipophilic antioxidants, Biochemical Society Transactions (vol. 32), pp. 147-150.

[35] Mcconville, Malcolm J and Blackwell, Jenefer M (1991): Developmental changes in the glycosylated phosphatidylinositols of Leishmania donovani. Characterization of the promastigote and amastigote glycolipids., Journal of Biological Chemistry (vol. 266), pp. 15170-15179.

[36] Ferguson, M A (1997): The surface glycoconjugates of trypanosomatid parasites., Philosophical Transactions of the Royal Society of London - Series B: Biological Sciences (vol. 352), pp. 1295-1302.

[37] McNeely, TB; Rosen, G; Londner, MV and Turco, SJ (1989): Inhibitory effects on protein kinase C activity by lipophosphoglycan fragments and glycosylphosphatidylinositol antigens of the protozoan parasite Leishmania, biochemical journal (vol. 159), pp. 601-604.

[38] Proudfoot, L; O'Donnell, C A and Liew, F Y (1995): Glycoinositolphospholipids of Leishmania major inhibit nitric oxide synthesis and reduce leishmanicidal activity in murine macrophages., European Journal of Immunology (vol. 25), pp. 745-750.

[39] Schlame, Michael and Ren, Mindong (2009): The role of cardiolipin in the structural organization of mitochondrial membranes., Biochimica et biophysica acta (vol. 1788), pp. 2080-3.

[40] Straus, Anita H; Paulista, Escola and Ana, Departamento De (2006): Characterization of Leishmania (Viannia) braziliensis membrane microdomains , and their role in macrophage infectivity, Journal Of Lipid Research (vol. 47), pp. 2171-2178.

[41] Zhang, Kai; Pompey, JM; Hsu, FF; Key, Phillip and P (2007): Redirection of sphingolipid metabolism toward de novo synthesis of ethanolamine in Leishmania, The EMBO (vol. 26), pp. 1094-1104.

[42] Zheng, Liang; Kind, Ruben T; Decuypere, Saskia; Freyend, Simona John Von; Coombs, Graham H and Watson, David G (2010): Profiling of lipids in Leishmania donovani using hydrophilic interaction chromatography in combination with Fourier transform mass spectrometry, Rapid Communications in Mass Spectrometry, pp. 2074-2082.

[43] Bretscher, Marc S (1974): Some aspects of membrane structure. In: Perspectives in Membrane Biology, Academic Press, pp. 3-24.

[44] Marx, U; Lassmann, G; Holzhütter, H G; Wüstner, D; Müller, P; Höhlig, A; Kubelt, J and Herrmann, A (2000): Rapid flip-flop of phospholipids in endoplasmic reticulum membranes studied by a stopped-flow approach., Biophysical Journal (vol. 78), pp. 2628-2640.

[45] Vehring, Stefanie; Pakkiri, Leroy; Schröer, Adrien; Alder-Baerens, Nele; Herrmann, Andreas; Menon, Anant K and Pomorski, Thomas (2007): Flip-flop of fluorescently labeled phospholipids in proteoliposomes reconstituted with Saccharomyces cerevisiae microsomal proteins., Eukaryotic Cell (vol. 6), pp. 1625-1634.

[46] Pomorski, Thomas; Holthuis, Joost C M; Herrmann, Andreas and van Meer, Gerrit (2004): Tracking down lipid flippases and their biological functions., Journal of Cell Science (vol. 117), pp. 805-813.

[47] Alder-Baerens, Nele; Lisman, Quirine; Luong, Lambert; Pomorski, Thomas and Holthuis, Joost C M (2006): Loss of P4 ATPases Drs2p and Dnf3p disrupts aminophospholipid transport and asymmetry in yeast post-Golgi secretory vesicles., Molecular Biology of the Cell (vol. 17), pp. 1632-1642.

[48] Coleman, Jonathan a; Kwok, Michael C M and Molday, Robert S (2009): Localization, purification, and functional reconstitution of the P4-ATPase Atp8a2, a phosphatidylserine flippase in photoreceptor disc membranes., The Journal of biological chemistry (vol. 284), pp. 32670-9.

[49] Zhou, Xiaoming and Graham, Todd R (2009): Reconstitution of phospholipid translocase activity with purified Drs2p, a type-IV P-type ATPase from budding yeast, Proceedings of the National Academy of Sciences (vol. 106), pp. 16586-16591.

[50] Axelsen, K B and Palmgren, M G (1998): Evolution of substrate specificities in the P-type ATPase superfamily., The Journal of Molecular Evolution (vol. 46), pp. 84-101.

[51] Lenoir, Guillaume; Williamson, Patrick and Holthuis, Joost C M (2007): On the origin of lipid asymmetry: the flip side of ion transport., Current Opinion in Chemical Biology (vol. 11), pp. 654-661.

[52] Lenoir, Guillaume; Williamson, Patrick; Puts, Catheleyne F and Holthuis, Joost C M (2009): Cdc50p plays a vital role in the ATPase reaction cycle of the putative aminophospholipid transporter drs2p., Journal of Biological Chemistry (vol. 284), pp. 17956-17967.

[53] Puts, Catheleyne F and Holthuis, Joost C M (2009): Mechanism and significance of P4 ATPase-catalyzed lipid transport: lessons from a Na+/K+-pump., Biochimica et Biophysica Acta (vol. 1791), pp. 603-611.

[54] Liu, Ke; Surendhran, Kavitha; Nothwehr, S.F. and Graham, T.R. (2008): P4-ATPase requirement for AP-1/clathrin function in protein transport from the trans-Golgi network and early endosomes, Molecular biology of the cell (vol. 19), p. 3526.

[55] Pomorski, Thomas; Lombardi, Ruben; Riezman, Howard and PF (2003): Drs2p-related P-type ATPases Dnf1p and Dnf2p are required for phospholipid translocation across the yeast plasma membrane and serve a role in endocytosis, Molecular biology of the Cell (vol. 14), pp. 1240 -1254.

[56] Pérez-Victoria, F Javier; Gamarro, Francisco; Ouellette, Marc and Castanys, Santiago (2003): Functional cloning of the miltefosine transporter. A novel P-type phospholipid translocase from Leishmania involved in drug resistance., The Journal of biological chemistry (vol. 278), pp. 49965-71.

[57] Pérez-Victoria, F Javier; Sánchez-Cañete, María P; Castanys, Santiago and Gamarro, Francisco (2006): Phospholipid translocation and miltefosine potency require both L. donovani miltefosine transporter and the new protein LdRos3 in Leishmania parasites., The Journal of biological chemistry (vol. 281), pp. 23766-75.

[58] Moir, D; Stewart, S E; Osmond, B C and Botstein, D (1982): Cold-sensitive cell-division-cycle mutants of yeast: isolation, properties, and pseudoreversion studies., Genetics (vol. 100), pp. 547-563.

[59] Kato, Utako; Emoto, Kazuo; Fredriksson, Charlotta; Nakamura, Hidemitsu; Ohta, Akinori; Kobayashi, Toshihide; Murakami-Murofushi, Kimiko; Kobayashi, Tetsuyuki and Umeda, Masato (2002): A novel membrane protein, Ros3p, is required for phospholipid translocation across the plasma membrane in Saccharomyces cerevisiae, Journal of Biological Chemistry (vol. 277), pp. 37855-37862.

[60] Hanson, Pamela K; Malone, Lynn; Birchmore, Jennifer L and Nichols, J Wylie (2003): Lem3p is essential for the uptake and potency of alkylphosphocholine drugs, edelfosine and miltefosine., The Journal of Biological Chemistry (vol. 278), pp. 36041-36050.

[61] Saito, Koji; Fujimura-kamada, Konomi; Furuta, Nobumichi; Kato, Utako; Umeda, Masato and Tanaka, Kazuma (2004): Cdc50p , a Protein Required for Polarized Growth , Associates with the Drs2p P-Type ATPase Implicated in Phospholipid Translocation in Saccharomyces cerevisiae, Molecular Biology of the Cell (vol. 15), pp. 3418 -3432.

[62] Katoh, Yuriko and Katoh, Masaru (2004): Identification and characterization of CDC50A, CDC50B and CDC50C genes in silico., Oncology Reports (vol. 12), pp. 939-943.

[63] Poulsen, Lisbeth Rosager; López-Marqués, Rosa Laura; McDowell, Stephen C; Okkeri, Juha; Licht, Dirk; Schulz, Alexander; Pomorski, Thomas; Harper, Jeffrey F. and Palmgren, Michael Gjedde (2008): The Arabidopsis P4-ATPase ALA3 localizes to the golgi and requires a beta-subunit to function in lipid translocation and secretory vesicle formation., The Plant cell (vol. 20), pp. 658-76.

[64] van der Velden, Lieke M; Wichers, Catharina G K; van Breevoort, Adriana E D; Coleman, Jonathan A; Molday, Robert S; Berger, Ruud; Klomp, Leo W J and van De Graaf, Stan F J (2010): Heteromeric interactions required for abundance and subcellular localization of human CDC50 proteins and class 1 P4 ATPases., The Journal of biological chemistry.

[65] Bryde, Susanne; Hennrich, Hanka; Verhulst, Patricia M; Devaux, Philippe F; Lenoir, Guillaume and Holthuis, Joost C M (2010): CDC50 proteins are critical components of the human class-1 P4-ATPase transport machinery., The Journal of biological chemistry.

[66] Dean, M; Rzhetsky, A and Allikmets, R (2001): The human ATP-binding cassette (ABC) transporter superfamily., Genome Research (vol. 11), pp. 1156-1166.

[67] Procko, Erik; O'Mara, Megan L; Bennett, W F Drew; Tieleman, D Peter and Gaudet, Rachelle (2009): The mechanism of ABC transporters: general lessons from structural and functional studies of an antigenic peptide transporter., The FASEB journal official publication of the Federation of American Societies for Experimental Biology (vol. 23), pp. 1287-1302.

[68] Parodi-Talice, Adriana; Araújo, José María; Torres, Cristina; Pérez-Victoria, Jose María; Gamarro, Francisco and Castanys, Santiago (2003): The overexpression of a

new ABC transporter in Leishmania is related to phospholipid trafficking and reduced infectivity., Biochimica et Biophysica Acta (vol. 1612), pp. 195-207.

[69] Araújo-Santos, José María; Parodi-Talice, Adriana; Castanys, Santiago and Gamarro, Francisco (2005): The overexpression of an intracellular ABCA-like transporter alters phospholipid trafficking in Leishmania., Biochemical and Biophysical Research Communications (vol. 330), pp. 349-355.

[70] Castanys-Munoz, Esther; Alder-Baerens, Nele; Pomorski, Thomas; Gamarro, Francisco and Castanys, Santiago (2007): A novel ATP-binding cassette transporter from Leishmania is involved in transport of phosphatidylcholine analogues and resistance to alkyl-phospholipids., Molecular Microbiology (vol. 64), pp. 1141-1153.

[71] Castanys-Munoz, Esther; Pérez-Victoria, Jose María; Gamarro, Francisco and Castanys, Santiago (2008): Characterization of an ABCG-like transporter from the protozoan parasite Leishmania with a role in drug resistance and transbilayer lipid movement., Antimicrobial Agents Chemotherapy (vol. 52), pp. 3573-3579.

[72] Balasubramanian, Krishnakumar and Schroit, Alan J (2003): Aminophospholipid asymmetry: A matter of life and death., Annual review of physiology (vol. 65), pp. 701-34.

[73] Weinrauch, Y and Zychlinsky, A (1999): The induction of apoptosis by bacterial pathogens., Annual Review of Microbiology (vol. 53), pp. 155-187.

[74] Shen, Y and Shenk, T E (1995): Viruses and apoptosis., Current Opinion in Genetics & Development (vol. 5), pp. 105-111.

[75] Roulston, A; Marcellus, R C and Branton, P E (1999): Viruses and apoptosis., Annual Review of Microbiology (vol. 53), pp. 577-628.

[76] Duncan, R; Esmaili, A; Law, L M; Bertholet, S; Hough, C; Hobman, T C and Nakhasi, H L (2000): Rubella virus capsid protein induces apoptosis in transfected RK13 cells., Virology (vol. 275), pp. 20-29.

[77] DosReis, George A and Barcinski, M A (2001): Apoptosis and parasitism: from the parasite to the host immune response., Advances in Parasitology (vol. 49), pp. 133-161.

[78] Williams, G T (1991): Programmed cell death: apoptosis and oncogenesis., Cell (vol. 65), pp. 1097-1098.

[79] Rich, T; Allen, R L and Wyllie, A H (2000): Defying death after DNA damage., Nature (vol. 407), pp. 777-783.

[80] Bevers, Edouard M and Williamson, Patrick L (2010): Phospholipid scramblase: an update., FEBS letters (vol. 584), pp. 2724-30.

[81] Das, Manika; Mukherjee, SB and Shaha, Chandrima (2001): Hydrogen peroxide induces apoptosis-like death in Leishmania donovani promastigotes, Journal of Cell Science.

[82] Lee, N; Bertholet, S; Debrabant, A; Muller, J; Duncan, R and Nakhasi, H L (2002): Programmed cell death in the unicellular protozoan parasite Leishmania., Cell Death & Differ (vol. 9), pp. 53-64.

[83] Paris, Caroline; Loiseau, Philippe M and Bories, Christian (2004): Miltefosine Induces Apoptosis-Like Death in Leishmania donovani Promastigotes, Antimicrobial Agents and Chemotherapy (vol. 48), pp. 852-859.

[84] Verhoven, B; Schlegel, R A and Williamson, Patrick (1995): Mechanisms of phosphatidylserine exposure, a phagocyte recognition signal, on apoptotic T lymphocytes., The Journal of Experimental Medicine (vol. 182), pp. 1597-1601.

[85] Comfurius, Paul; Williamson, Patrick; Smeets, Edgar F and RA (1996): Reconstitution of Phospholipid Scramblase Activity from Human Blood Platelets†, Biochemistry (vol. 35), pp. 7631-7634.

[86] Bassé, F; Stout, J G; Sims, Peter J and Wiedmer, Therese (1996): Isolation of an erythrocyte membrane protein that mediates Ca2+-dependent transbilayer movement of phospholipid., Journal of Biological Chemistry (vol. 271), pp. 17205-17210.

[87] Williamson, Patrick; Christie, A; Kohlin, T; Schlegel, R A; Comfurius, Paul; Harmsma, M; Zwaal, Robert F A and Bevers, Edouard M (2001): Phospholipid scramblase activation pathways in lymphocytes., Biochemistry (vol. 40), pp. 8065-8072.

[88] Williamson, Patrick; van Den Eijnde, S and Schlegel, R A (2001): Phosphatidylserine exposure and phagocytosis of apoptotic cells., Methods in Cell Biology (vol. 66), pp. 339-364.

[89] Kamp, D; Sieberg, T and Haest, C W (2001): Inhibition and stimulation of phospholipid scrambling activity. Consequences for lipid asymmetry, echinocytosis, and microvesiculation of erythrocytes., Biochemistry (vol. 40), pp. 9438-46.

[90] Zhou, Quansheng; Zhao, Ji; Stout, James G; Luhm, Robert A; Wiedmer, Therese and Sims, Peter J (1997): Molecular cloning of human plasma membrane phospholipid scramblase. A protein mediating transbilayer movement of plasma membrane phospholipids., The Journal of biological chemistry (vol. 272), pp. 18240-4.

[91] Hamon, Y; Broccardo, C; Chambenoit, O; Luciani, M F; Toti, F; Chaslin, S; Freyssinet, J M; Devaux, P F; McNeish, J; Marguet, D and Chimini, G (2000): ABC1 promotes engulfment of apoptotic cells and transbilayer redistribution of phosphatidylserine, Nature Cell Biology (vol. 2), pp. 399-406.

[92] Züllig, Stephanie; Neukomm, Lukas J; Jovanovic, Marko; Charette, Steve J; Lyssenko, Nicholas N; Halleck, Margaret S; Reutelingsperger, Chris P M; Schlegel, Robert a and Hengartner, Michael O (2007): Aminophospholipid translocase TAT-1 promotes phosphatidylserine exposure during C. elegans apoptosis., Current biology : CB (vol. 17), pp. 994-9.

[93] Zhou, Quansheng; Zhao, Ji; Wiedmer, Therese and Sims, Peter J (2002): Normal hemostasis but defective hematopoietic response to growth factors in mice deficient in phospholipid scramblase 1., Blood (vol. 99), pp. 4030-8.

[94] Williamson, Patrick; Halleck, Margaret S; Malowitz, Jonathan; Ng, Susan; Fan, Xiaoxuan; Krahling, Stephen; Remaley, Alan T and Schlegel, Robert A (2007): Transbilayer phospholipid movements in ABCA1-deficient cells., PloS one (vol. 2), p. e729.

[95] Mirnikjoo, Banafsheh; Balasubramanian, Krishnakumar and Schroit, Alan J (2009): Suicidal membrane repair regulates phosphatidylserine externalization during apoptosis., The Journal of biological chemistry (vol. 284), pp. 22512-6.

[96] Contreras, F-Xabier; Sánchez-Magraner, Lissete; Alonso, Alicia and Goñi, Félix M (2010): Transbilayer (flip-flop) lipid motion and lipid scrambling in membranes., FEBS letters (vol. 584), pp. 1779-86.

[97] Smeets, Edgar F; Comfurius, Paul; Bevers, Edouard M and RFA (1994): Calcium-induced transbilayer scrambling of fluorescent phospholipid analogs in platelets and erythrocytes, Biochimica et Biophysica Acta (vol. 1195), pp. 281-286.

[98] Dekkers, David W C; Comfurius, Paul; Bevers, Edouard M and Zwaal, Robert F A (2002): Comparison between Ca2+-induced scrambling of various fluorescently labelled lipid analogues in red blood cells., Biochemical Journal (vol. 362), pp. 741-747.

[99] Henke, J; Engelmann, J; Kutscher, B; Nssner, G; Engel, J; Voegeli, R and Leibfritz, D (1999): Changes of intracellular calcium, fatty acids and phospholipids during miltefosine-induced apoptosis monitored by fluorescence- and 13C NMR-spectroscopy., Anticancer research (vol. 19), pp. 4027-4032.

[100] Lu Hg, Hong-Gang; Zhong, Li; Chang, Kwang-Po and Docampo, Roberto (1997): Intracellular Ca2+ pool content and signaling and expression of a calcium pump are linked to virulence in Leishmania mexicana amazonesis amastigotes., Journal of Biological Chemistry (vol. 272), pp. 9464-9473.

[101] Sarkar, Dhiman and Bhaduri, Amar (1995): Temperature-induced rapid increase in cytoplasmic free Ca2+ in pathogenic Leishmania donovani promastigotes., FEBS Letters (vol. 375), pp. 83-86.

[102] Prasad, A; Kaur, S; Malla, N; Ganguly, N K and Mahajan, R C (2001): Ca2+ signaling in the transformation of promastigotes to axenic amastigotes of Leishmania donovani., Molecular and Cellular Biochemistry (vol. 224), pp. 39-44.

[103] Hall, T A (1999): BioEdit: a user-friendly biological sequence alignment editor and analysis program for Windows 95/98/NT, Nucleic Acids Symposium Series (vol. 41), pp. 95-98.

[104] Ha, D. Sean; Schwarz, James K; Turco, Salvatore J and Beverley, Stephen M (1996): Use of the green fluorescent protein as a marker in transfected Leishmania, Molecular and Biochemical Parasitology (vol. 77), pp. 57-64.

[105] Kapler, Geoffrey M; Coburn, Cara M and Beverley, Stephen M (1990): Stable Transfection of the Human Parasite Leishmania major Delineates a 30-Kilobase Region Sufficient for Extrachromosomal Replication and Expression, Microbiology (vol. 10), pp. 1084-1094.

[106] Guenther, Ulf-Peter; Handoko, Lusy; Varon, Raymonda; Stephani, Ulrich; Tsao, Chang-Yong; Mendell, Jerry R; Lützkendorf, Susanne; Hübner, Christoph; von Au, Katja; Jablonka, Sibylle; Dittmar, Gunnar; Heinemann, Udo; Schuetz, Anja and Schuelke, Markus (2009): Clinical variability in distal spinal muscular atrophy type 1 (DSMA1): determination of steady-state IGHMBP2 protein levels in five patients with infantile and juvenile disease., Journal of Molecular Medicine (vol. 87), pp. 31-41.

[107] Bligh, E G and Dyer, W J (1959): A rapid method of total lipid extraction and purification., The Canadian journal of biochemistry and physiology (vol. 37), pp. 911-917.

[108] Hein, Eva-Maria; Blank, Lars M; Heyland, Jan; Baumbach, Jörg I; Schmid, Andreas and Hayen, Heiko (2009): Glycerophospholipid profiling by high-performance liquid chromatography/mass spectrometry using exact mass measurements and multi-stage mass spectrometric fragmentation experiments in parallel., Rapid Commun Mass Spectrom (vol. 23), pp. 1636-1646.

[109] Schiller, Jürgen; Arnhold, J; Benard, S; Müller, M; Reichl, S and Arnold, K (1999): Lipid analysis by matrix-assisted laser desorption and ionization mass spectrometry: A methodological approach., Analytical Biochemistry (vol. 267), pp. 46-56.

[110] Petković, M; Schiller, Jürgen; Müller, J; Müller, M; Arnold, K and Arnhold, J (2001): The signal-to-noise ratio as the measure for the quantification of lysophospholipids by matrix-assisted laser desorption/ionisation time-of-flight mass spectrometry., The Analyst (vol. 126), pp. 1042-1050.

[111] Fuchs, Beate; Schober, Celestina; Richter, Grit; Süss, Rosmarie and Schiller, Jürgen (2007): MALDI-TOF MS of phosphatidylethanolamines: different adducts cause different post source decay (PSD) fragment ion spectra., Journal of Biochemical and Biophysical Methods (vol. 70), pp. 689-692.

[112] van Meer, Gerrit; Voelker, DR and Feigenson, GW (2008): Membrane lipids: where they are and how they behave, Nature Reviews Molecular Cell Biology (vol. 9), pp. 112-124.

[113] Leventis, Peter A and Grinstein, Sergio (2010): The distribution and function of phosphatidylserine in cellular membranes., Annual review of biophysics (vol. 39), pp. 407-27.

[114] Parsons, Ainslie B; Lopez, Andres; Givoni, Inmar E; Williams, David E; Gray, Christopher A; Porter, Justin; Chua, Gordon; Sopko, Richelle; Brost, Renee L; Ho, Cheuk-Hei; Wang, Jiyi; Ketela, Troy; Brenner, Charles; Brill, Julie A; Fernandez, G Esteban; Lorenz, Todd C; Payne, Gregory S; Ishihara, Satoru; Ohya, Yoshikazu; Andrews, Brenda; Hughes, Timothy R; Frey, Brendan J; Graham, Todd R; Andersen, Raymond J and Boone, Charles (2006): Exploring the mode-of-action of bioactive compounds by chemical-genetic profiling in yeast., Cell (vol. 126), pp. 611-25.

[115] Emoto, Kazuo; Kobayashi, T; Yamaji, A; Aizawa, H; Yahara, I; Inoue, K and Umeda, M (1996): Redistribution of phosphatidylethanolamine at the cleavage furrow of dividing cells during cytokinesis., Proceedings of the National Academy of Sciences (vol. 93), pp. 12867-12872.

[116] Iwamoto, Kunihiko; Kobayashi, Shingo; Fukuda, Ryouichi; Umeda, Masato; Kobayashi, Toshihide and Ohta, Akinori (2004): Local exposure of phosphatidylethanolamine on the yeast plasma membrane is implicated in cell polarity., Genes Cells (vol. 9), pp. 891-903.

[117] Brajtburg, J; Powderly, W G; Kobayashi, G S and Medoff, G (1990): Amphotericin B: current understanding of mechanisms of action., Antimicrobial Agents Chemotherapy (vol. 34), pp. 183-188.

[118] De Freitas Balanco, J M; Moreira, M E; Bonomo, A; Bozza, P T; Amarante-Mendes, G; Pirmez, C and Barcinski, M A (2001): Apoptotic mimicry by an obligate intracellular parasite downregulates macrophage microbicidal activity., Current Biology (vol. 11), pp. 1870-1873.

[119] van Zandbergen, Ger; Bollinger, Annalena; Wenzel, Alexander; Kamhawi, Shaden; Voll, Reinhard; Klinger, Matthias; Müller, Antje; Hölscher, Christoph; Herrmann, Martin; Sacks, David; Solbach, Werner and Laskay, Tamás (2006): Leishmania disease development depends on the presence of apoptotic promastigotes in the virulent inoculum., Proceedings of the National Academy of Sciences of the United States of America (vol. 103), pp. 13837-42.

[120] Wanderley, João Luiz Mendes; Pinto Da Silva, Lucia Helena; Deolindo, Poliana; Soong, Lynn; Borges, Valéria Matos; Prates, Deboraci Brito; de Souza, Ana Paula Almeida; Barral, Aldina; Balanco, José Mario De Freitas; do Nascimento, Michelle

Tanny Cunha; Saraiva, Elvira Maria and Barcinski, Marcello André (2009): Cooperation between apoptotic and viable metacyclics enhances the pathogenesis of Leishmaniasis., PloS one (vol. 4), p. e5733.

[121] Anttila, H S; Reitamo, S; Ceska, M and Hurme, M (1992): Signal transduction pathways leading to the production of IL-8 by human monocytes are differentially regulated by dexamethasone., Clinical & Experimental Immunology (vol. 89), pp. 509-512.

[122] Dasgupta, B; Roychoudhury, K; Ganguly, S; Akbar, M A; Dasz, P and Roy, S (2003): Infection of Human Mononuclear Phagocytes and Macrophage-Like THP1 Cells with Leishmania donovani Results in Modulation of Expression of a Subset of Chemokines and a Chemokine Receptor, Scandinavian Journal of Immunology (vol. 1), pp. 366-374.

[123] Wurth, Georjeana A and Zweifach, Adam (2002): Evidence that cytosolic calcium increases are not sufficient to stimulate phospholipid scrambling in human T-lymphocytes., The Biochemical journal (vol. 362), pp. 701-708.

[124] Goodyear, Richard J; Gale, Jonathan E; Ranatunga, Kishani M; Kros, Corné J and Richardson, Guy P (2008): Aminoglycoside-induced phosphatidylserine externalization in sensory hair cells is regionally restricted, rapid, and reversible., Journal of Neuroscience (vol. 28), pp. 9939-9952.

[125] Wolfs, J L N; Comfurius, Paul; Bekers, O; Zwaal, Robert F A; Balasubramanian, Krishnakumar; Schroit, A J; Lindhout, T and Bevers, Edouard M (2009): Direct inhibition of phospholipid scrambling activity in erythrocytes by potassium ions., Cellular and molecular life sciences CMLS (vol. 66), pp. 314-323.

[126] Makino, Asami; Baba, Takeshi; Fujimoto, Kazushi; Iwamoto, Kunihiko; Yano, Yoshiaki; Terada, Nobuo; Ohno, Shinichi; Sato, Satoshi B; Ohta, Akinori; Umeda, Masato; Matsuzaki, Katsumi and Kobayashi, Toshihide (2003): Cinnamycin (Ro 09-0198) promotes cell binding and toxicity by inducing transbilayer lipid movement., The Journal of biological chemistry (vol. 278), pp. 3204-9.

[127] Andree, Harry A. M.; Reutelingsperger, C P; Hauptmann, R; Hemker, H C; Hermens, W T and Willems, G M (1990): Binding of vascular anticoagulant alpha (VAC alpha) to planar phospholipid bilayers., The Journal of Biological Chemistry (vol. 265), pp. 4923-4928.

[128] Brumatti, Gabriela; Sheridan, Clare and Martin, Seamus J. (2008): Expression and purification of recombinant annexin V for the detection of membrane alterations on apoptotic cells, Methods (vol. 44), pp. 235-240.

[129] Weingärtner, Adrien; Drobot, Björn; Herrmann, Andreas; Sánchez-Cañete, María P; Gamarro, Francisco; Castanys, Santiago and Günther-Pomorski, Thomas (2010): Disruption of the Lipid-Transporting LdMT-LdRos3 Complex in Leishmania donovani Affects Membrane Lipid Asymmetry but Not Host Cell Invasion, PLoS ONE (vol. 5), p. e12443.

[130] Wanderley, João Luiz Mendes; Moreira, Maria E C; Benjamin, Aline; Bonomo, Adriana C and Barcinski, Marcello A (2006): Mimicry of apoptotic cells by exposing phosphatidylserine participates in the establishment of amastigotes of Leishmania (L) amazonensis in mammalian hosts., The Journal of Immunology (vol. 176), pp. 1834-1839.

[131] Naderer, Thomas; Vince, James E and McConville, Malcolm J (2004): Surface determinants of Leishmania parasites and their role in infectivity in the mammalian host., Current molecular medicine (vol. 4), pp. 649-65.

[132] Sánchez-Cañete, María P; Carvalho, Luís; Pérez-Victoria, F Javier; Gamarro, Francisco and Castanys, Santiago (2009): Low plasma membrane expression of the miltefosine transport complex renders Leishmania braziliensis refractory to the drug., Antimicrobial Agents and Chemotherapy (vol. 53), pp. 1305-1313.

[133] Furuta, N.; Fujimura-Kamada, K.; Saito, K.; Yamamoto, T. and Tanaka, K. (2007): Endocytic recycling in yeast is regulated by putative phospholipid translocases and the Ypt31p/32p-Rcy1p pathway, Molecular biology of the cell (vol. 18), p. 295.

[134] Paulusma, Coen C; Folmer, Dineke E; Ho-Mok, Kam S; de Waart, D Rudi; Hilarius, Petra M; Verhoeven, Arthur J and Oude Elferink, Ronald P J (2008): ATP8B1 requires an accessory protein for endoplasmic reticulum exit and plasma membrane lipid flippase activity., Hepatology (Baltimore, Md.) (vol. 47), pp. 268-78.

[135] Araújo-Santos, José María; Gamarro, Francisco; Castanys, Santiago; Herrmann, Andreas and Pomorski, Thomas (2003): Rapid transport of phospholipids across the plasma membrane of Leishmania infantum., Biochemical and Biophysical Research Communications (vol. 306), pp. 250-255.

[136] Saxena, A; Lahav, T; Holland, N; Aggarwal, G; Anupama, A; Huang, Y; Volpin, H; Myler, P J and Zilberstein, D (2007): Analysis of the Leishmania donovani transcriptome reveals an ordered progression of transient and permanent changes in gene expression during differentiation, Biomedical Research (vol. 152), pp. 53-65.

[137] Naderer, Thomas and McConville, Malcolm J (2008): The Leishmania-macrophage interaction: a metabolic perspective., Cellular Microbiology (vol. 10), pp. 301-308.

[138] Seifert, Karin; Pérez-Victoria, F Javier; Stettler, Marianne; Sánchez-Cañete, María P; Castanys, Santiago; Gamarro, Francisco and Croft, Simon L (2007): Inactivation of the miltefosine transporter, LdMT, causes miltefosine resistance that is conferred to the amastigote stage of Leishmania donovani and persists in vivo., International Journal of Antimicrobial Agents (vol. 30), pp. 229-235.

[139] Aoki, Y; Uenaka, T; Aoki, J; Umeda, M and Inoue, K (1994): A novel peptide probe for studying the transbilayer movement of phosphatidylethanolamine., The Journal of Biochemistry (vol. 116), pp. 291-297.

[140] Emoto, Kazuo; Toyama-Sorimachi, Noriko; Karasuyama, Hajime; Inoue, Keizo and Umeda, Masato (1997): Exposure of Phosphatidylethanolamine on the Surface of Apoptotic Cells, EXPERIMENTAL CELL RESEARCH (vol. 232), pp. 430-434.

[141] Zhao, Ji; Zhou, Quansheng; Wiedmer, Therese and Sims, Peter J (1998): Palmitoylation of phospholipid scramblase is required for normal function in promoting Ca2+-activated transbilayer movement of membrane phospholipids., Biochemistry (vol. 37), pp. 6361-6366.

[142] Balasubramanian, Krishnakumar; Mirnikjoo, Banafsheh and Schroit, Alan J. (2007): Regulated externalization of phosphatidylserine at the cell surface: implications for apoptosis., The Journal of biological chemistry (vol. 282), pp. 18357-64.

[143] Wiedmer, Therese; Zhou, Quansheng; Kwoh, D Y and Sims, Peter J (2000): Identification of three new members of the phospholipid scramblase gene family., Biochimica et Biophysica Acta (vol. 1467), pp. 244-253.

[144] Suzuki, Jun; Umeda, Masato; Sims, Peter J. and Nagata, Shigekazu (2010): Calcium-dependent phospholipid scrambling by TMEM16F, Nature (vol. 468), pp. 834-838.

[145] Misra, Sujata; Naskar, Kshudiram; Sarkar, Dwijen and Ghosh, Dilip Kumar (1991): Role of Ca2+ ion on Leishmania-macrophage attachment., Molecular and Cellular Biochemistry (vol. 102), pp. 13-18.

[146] van den Eijnde, S M; Boshart, L; Baehrecke, E H; De Zeeuw, C I; Reutelingsperger, C P and Vermeij-Keers, C (1998): Cell surface exposure of phosphatidylserine during apoptosis is phylogenetically conserved., Apoptosis : an international journal on programmed cell death (vol. 3), pp. 9-16.

[147] Böse, Jens; Gruber, Achim D; Helming, Laura; Schiebe, Stefanie; Wegener, Ivonne; Hafner, Martin; Beales, Marianne; Köntgen, Frank and Lengeling, Andreas (2004): The phosphatidylserine receptor has essential functions during embryogenesis but not in apoptotic cell removal., Journal of biology (vol. 3), p. 15.

[148] van Engeland, M; Nieland, L J; Ramaekers, F C; Schutte, B and Reutelingsperger, C P (1998): Annexin V-affinity assay: a review on an apoptosis detection system based on phosphatidylserine exposure., Cytometry (vol. 31), pp. 1-9.

[149] Fan, Xiaoxuan; Krahling, Stephen; Smith, Douglas; Williamson, Patrick and Schlegel, Robert A (2004): Macrophage surface expression of annexins I and II in the phagocytosis of apoptotic lymphocytes., Molecular Biology of the Cell (vol. 15), pp. 2863-2872.

[150] Dasgupta, Swapan K; Guchhait, Prasenjit and Thiagarajan, Perumal (2006): Lactadherin binding and phosphatidylserine expression on cell surface-comparison with annexin A5., Translational research : the journal of laboratory and clinical medicine (vol. 148), pp. 19-25.

[151] Dasgupta, Swapan K; Abdel-Monem, Hanan; Guchhait, Prasenjit; Nagata, Shigekazu and Thiagarajan, Perumal (2008): Role of lactadherin in the clearance of phosphatidylserine-expressing red blood cells., Transfusion (vol. 48), pp. 2370-6.

[152] Wu, Yi; Tibrewal, Nitu and Birge, Raymond B. (2006): Phosphatidylserine recognition by phagocytes: a view to a kill, Trends in Cell Biology (vol. 16), pp. 189 - 197.

[153] Gregory, Christopher D and Devitt, Andrew (2004): The macrophage and the apoptotic cell: an innate immune interaction viewed simplistically?, Immunology (vol. 113), pp. 1-14.

[154] Mercer, Jason and Helenius, Ari (2008): Vaccinia virus uses macropinocytosis and apoptotic mimicry to enter host cells., Science (vol. 320), pp. 531-535.

[155] Fadok, Valerie A; A}, {de Cathelineau; Daleke, David L; Henson, P M and Bratton, Donna L (2001): Loss of phospholipid asymmetry and surface exposure of phosphatidylserine is required for phagocytosis of apoptotic cells by macrophages and fibroblasts., Journal of Biological Chemistry (vol. 276), pp. 1071-1077.

[156] Wanderley, João Luiz Mendes; Benjamin, A; Real, F; Bonomo, A; Moreira, M E C and Barcinski, M A (2005): Apoptotic mimicry: an altruistic behavior in host/Leishmania interplay., Brazilian journal of medical and biological research Revista brasileira de pesquisas medicas e biologicas Sociedade Brasileira de Biofisica et al (vol. 38), pp. 807-812.

[157] Yeung, Tony; Heit, Bryan; Dubuisson, JF; Fairn, GD and B (2009): Contribution of phosphatidylserine to membrane surface charge and protein targeting during phagosome maturation, The Journal of Cell Biology, pp. 917-928.

[158] Chen, Sophie; Wang, Jiyi; Muthusamy, Baby-Periyanayaki; Liu, Ke; Zare, Sara; Andersen, Raymond J and Graham, Todd R (2006): Roles for the Drs2p-Cdc50p complex in protein transport and phosphatidylserine asymmetry of the yeast plasma membrane., Traffic (Copenhagen, Denmark) (vol. 7), pp. 1503-17.

[159] Yu, Anan; Byers, David M; Ridgway, Neale D; Mcmaster, Christopher R and Cook, Harold W (2000): Preferential externalization of newly synthesized phosphatidylserine

in apoptotic U937 cells is dependent on caspase-mediated pathways., Biochimica et biophysica acta (vol. 1487), pp. 296-308.

[160] Yu, Anan; McMaster, Christopher R; Byers, David M; Ridgway, Neale D and Cook, Harold W (2003): Stimulation of phosphatidylserine biosynthesis and facilitation of UV-induced apoptosis in Chinese hamster ovary cells overexpressing phospholipid scramblase 1., The Journal of biological chemistry (vol. 278), pp. 9706-14.

[161] Nelson, G.J. (1967): Lipid composition of erythrocytes in various mammalian species, Biochimica et Biophysica Acta (BBA)-Lipids and Lipid Metabolism (vol. 144), pp. 221-232.

[162] Jain, S K (1985): In vivo externalization of phosphatidylserine and phosphatidylethanolamine in the membrane bilayer and hypercoagulability by the lipid peroxidation of erythrocytes in rats., THE JOURNAL OF CLINICAL INVESTIGATION (vol. 76), pp. 281-286.

[163] Balasubramanian, Krishnakumar and Schroit, Alan J. (1998): Characterization of Phosphatidylserine-dependent beta 2-Glycoprotein I Macrophage Interactions. IMPLICATIONS FOR APOPTOTIC CELL CLEARANCE BY PHAGOCYTES, The Journal of Biological Chemistry (vol. 273), pp. 29272-29277.

[164] Fischer, Karin; Voelkl, Simon; Berger, Jana; Andreesen, Reinhard; Pomorski, Thomas and Mackensen, Andreas (2006): Antigen recognition induces phosphatidylserine exposure on the cell surface of human CD8+ T cells., Blood (vol. 108), pp. 4094-4101.

[165] Emoto, K. (1996): Redistribution of phosphatidylethanolamine at the cleavage furrow of dividing cells during cytokinesis, Proceedings of the National Academy of Sciences (vol. 93), pp. 12867-12872.

[166] Nishibori, Ayako; Kusaka, Jin; Hara, Hiroshi; Umeda, Masato and Matsumoto, Kouji (2005): Phosphatidylethanolamine domains and localization of phospholipid synthases in Bacillus subtilis membranes., Journal of bacteriology (vol. 187), pp. 2163-74.

[167] Krogh, A; Larsson, B; Von Heijne, G and Sonnhammer, E L (2001): Predicting transmembrane protein topology with a hidden Markov model: application to complete genomes., Journal of Molecular Biology (vol. 305), pp. 567-580.

Addendum

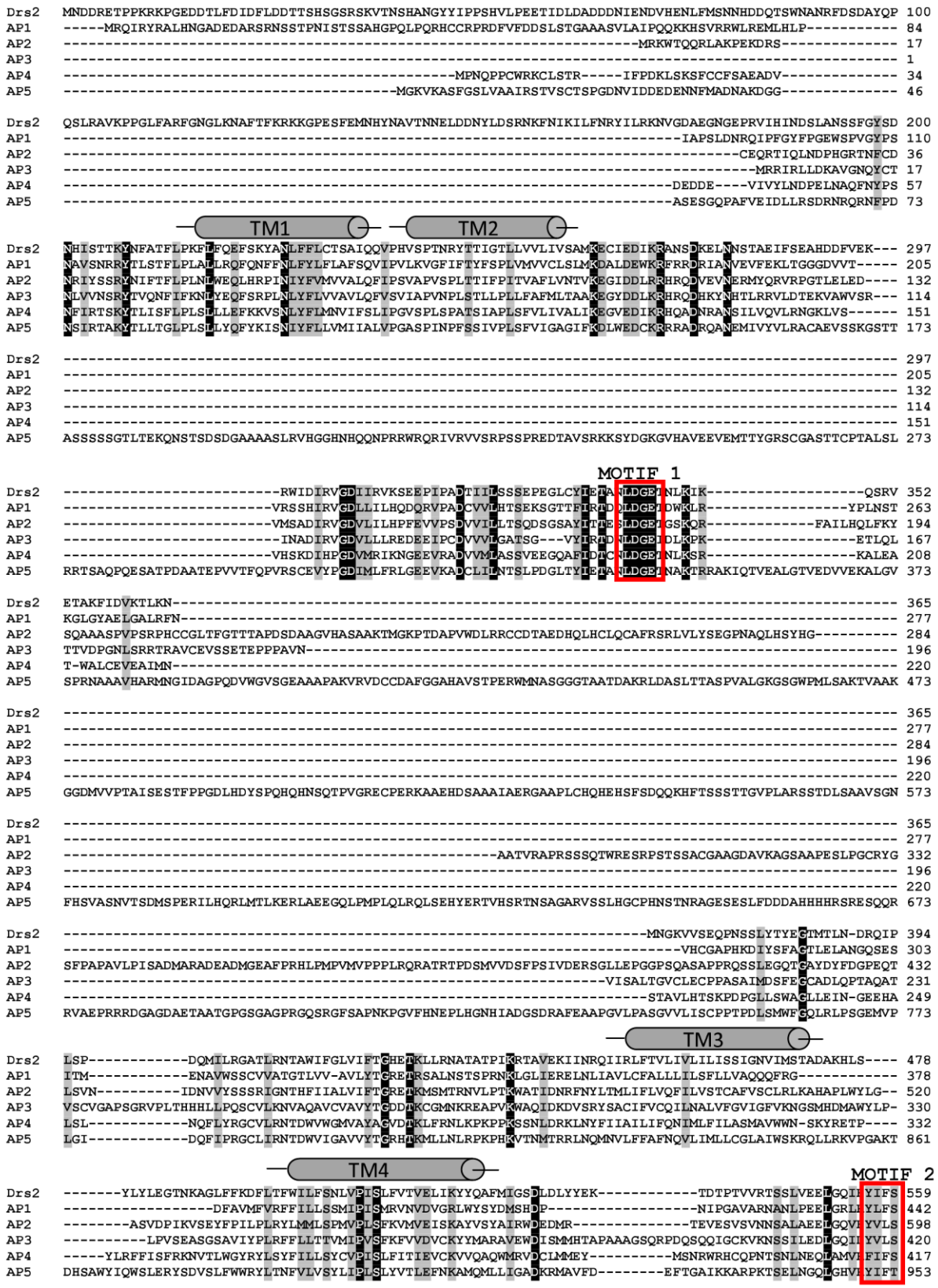

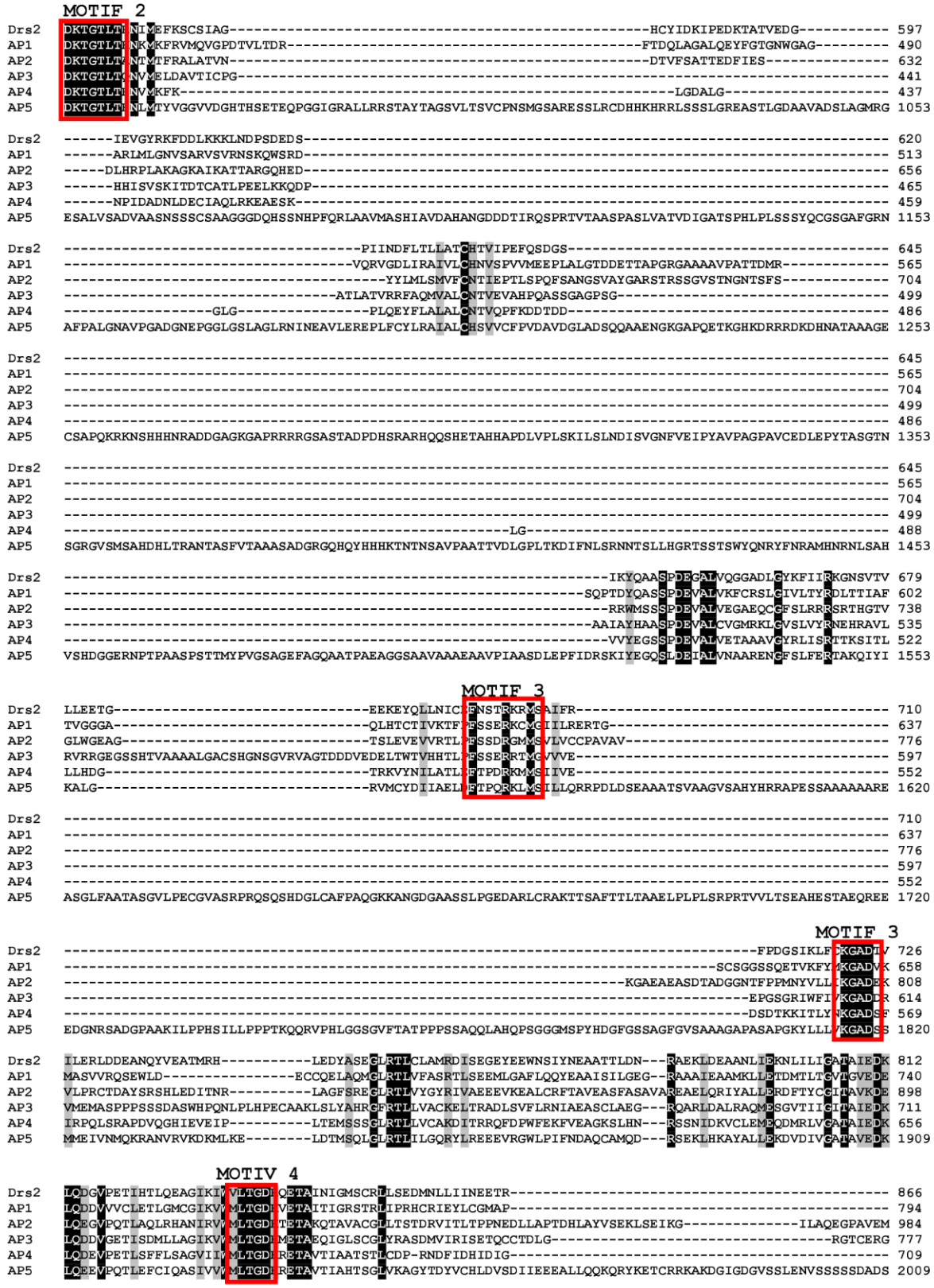
MOTIF 2
MOTIF 3
MOTIF 3
MOTIV 4

Figure 34: Sequence alignment of yeast Drs2p with putative P_4-ATPases identified in the *Leishmania infantum* genome.

Leishmania protein sequences were derived from *L. infantum* genome and aligned using ClustalW2 tool at the website of the European Bioinformatics Institute. The names AP1 to AP5 are given according to the similarity to the Drs2 while AP4 is identical to LdMT. Conserved motifs for P_4-ATPases as suggested by Lenoir at al. [51] are highlighted by red boxes. Transmembrane domains (1-10) as predicted with TMHMM tool developed by Krogh et al. [167] are indicated by barrels.

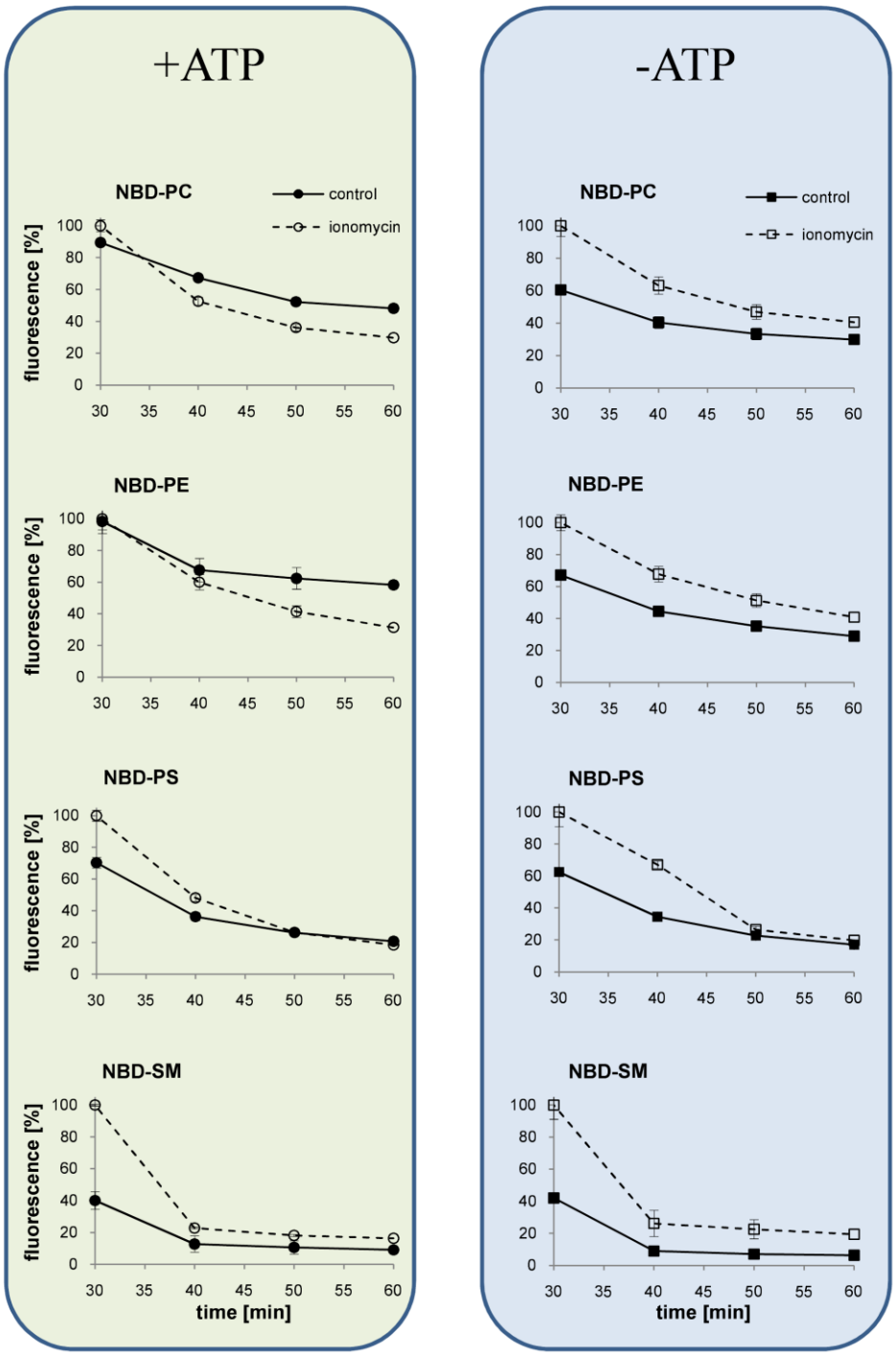

Figure 35: BSA extraction of NBD-lipids from *L. donovani* promastigotes untreated (control) or stimulated with ionomycin (ionomycin).

For this cells were ATP-depleted (-ATP) or not (+ATP) and loaded for 30 minutes on ice with 5 µM NBD-PC, -PE, -PS or –SM. Albumin was added to extract NBD-lipids which were not taken up. At indicated time points, aliquots were withdrawn and the fluorescence was measured by flow cytometry. Data are normalised for each lipid to ionomycin-treated samples and presented as mean ± SEM of five independent experiments.

Acknowledgement

This work was supported by many people, whom I would like to thank for their contribution.

First of all I would like to thank Prof. Thomas Günther-Pomorski for guiding me into the fascinating world of lipid flip-flop, for his fruitful discussions, his encouragement and constant motivation.

I also want to thank María Perez Sánchez-Cañete and all other collaborators from the Spanish groups of Francisco Gamarro Conde and Santiago Castanys who introduced me to the work with *Leishmania* and shared their experience with me.

I would like to express my gratitude to Prof. Andreas Herrmann for his support, his critical remarks and encouraging references.

Many thanks also to all members of the group of Molecular Biophysics for sharing equipment experience and coffee.

I am grateful for having had the opportunity to participate in the ZIBI Graduate School.

Special thanks go to Björn Drobot who excessively supported experiments in this work as a student research assistant.

Many thanks go also to to Frederic Mueller and Dr. Jürgen Schiller for support in lipid analysis.

I am much obliged to Hanka Hennrich for proof reading this manuscript.

Finally, I would like to thank my wife Claudia, our children and my parents for their love, constant support and patience.

Publications

Talks

2008 EU Flippase Meeting (2008) "Characterisation of P-type ATPases involved in lipid transport of *Leishmania donovani*", (Ascona, Switzerland)

2008 Zibi-Meeting 2008 "Lipid flip-flop in the membrane of *Leishmania*", (Meissen, Germany)

2008 EU Flippase Meeting Characterisation of Lipid transporting P-type ATPases in *Leishmania*", (Budapest, Hungary)

2006 GRAKO Retreat, "Characterisation of P-type ATPases involved in lipid transport of *Leishmania donovani*", (Berlin, Germany)

Poster

2008 Zibi-Meeting 2008 "Lipid flip-flop in the plasma membrane of *Leishmania donovani*", (Meissen, Germany)

2008 EU Flippase Meeting (2008) "Characterisation of P_4-ATPases of *Leishmania donovani*", (Ascona, Switzerland)

2006 FEBS Special Meeting "Characterisation of P-type ATPases involved in lipid transport of *Leishmania donovani*", (Noordwijkerhout, Netherlands)

Manuscripts

Weingärtner A, Drobot B, Herrmann A, Sánchez-Cañete MP, Gamarro F, Castanys S and Günther Pomorski T (2010) Disruption of the Lipid-Transporting LdMT-LdRos3 Complex in Leishmania donovani Affects Membrane Lipid Asymmetry but Not Host Cell Invasion. PLoS ONE 5(8): e12443. doi:10.1371/journal.pone.0012443

Vehring S, Pakkiri L, Schröer A, Alder-Baerens N, Herrmann A, Menon AK, and Pomorski T (2007) Flip-flop of fluorescently labeled phospholipids in proteoliposomes reconstituted with Saccharomyces cerevisiae microsomal proteins., Eukaryot Cell. 6 1625-1634.